Canada Alberta Northwest Territories

Northern River Basins Study






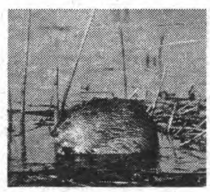



NORTHERN RIVER BASINS STUDY PROJECT REPORT NO. 103

HYDROMETEOROLOGICAL CONDITIONS CONTROLLING ICE-JAM FLOODS,

PEACE RIVER NEAR THE PEACE-ATHABASCA DELTA

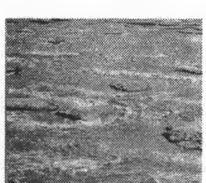



DATE DUE

Prepared for the
Northern River Basins Study
under Project 1422-C1

by

T. D. Prowse, M. Conly and V. Lalonde
National Hydrology Research Institute
Environment Canada

NORTHERN RIVER BASINS STUDY PROJECT REPORT NO. 103

HYDROMETEOROLOGICAL CONDITIONS CONTROLLING ICE-JAM FLOODS,

PEACE RIVER NEAR THE PEACE-ATHABASCA DELTA

Published by the
Northern River Basins Study
Edmonton, Alberta
February, 1996

CANADIAN CATALOGUING IN PUBLICATION DATA

Prowse, Terry Donald, 1952-

Hydrometeorological conditions controlling ice-jam
floods, Peace River near the Peace-Athabasca Delta

(Northern River Basins Study project report,
ISSN 1192-3571 ; no. 103)
Includes bibliographical references.
ISBN 0-662-24620-9
Cat. no. R71-49/3-103E

1. Floods -- Alberta -- Peace-Athabasca Delta.
2. Ice on rivers, lakes, etc. -- Alberta --
Peace-Athabasca Delta.
3. Peace River (B.C. and Alta) -- Regulation --
Environmental aspects.
I. Conly, M. (Malcolm)
II. Lalonde, V.
III. Northern River Basins Study (Canada)
IV. Title.
V. Series.

GB1398.5C3P76 1996 551.48'9'0971232 C96-980206-4

PREFACE:

The Northern River Basins Study was initiated through the "Canada-Alberta-Northwest Territories Agreement Respecting the Peace-Athabasca-Slave River Basin Study, Phase II - Technical Studies" which was signed September 27, 1991. The purpose of the Study is to understand and characterize the cumulative effects of development on the water and aquatic environment of the Study Area by coordinating with existing programs and undertaking appropriate new technical studies.

This publication reports the method and findings of particular work conducted as part of the Northern River Basins Study. As such, the work was governed by a specific terms of reference and is expected to contribute information about the Study Area within the context of the overall study as described by the Study Final Report. This report has been reviewed by the Study Science Advisory Committee in regards to scientific content and has been approved by the Study Board of Directors for public release.

It is explicit in the objectives of the Study to report the results of technical work regularly to the public. This objective is served by distributing project reports to an extensive network of libraries, agencies, organizations and interested individuals and by granting universal permission to reproduce the material.

This report contains referenced data obtained from sources external to the Northern River Basins Study. Individuals interested in using external data must obtain permission to do so from the donor agency.

NORTHERN RIVER BASINS STUDY
PROJECT REPORT RELEASE FORM

This publication may be cited as:

Prowse, T. D., Conly, M. and Lalonde, V. 1996. *Northern River Basins Study Project Report No. 103, Hydrometeorological Conditions Controlling Ice-Jam Floods, Peace River Near the Peace-Athabasca Delta*. Northern River Basins Study, Edmonton, Alberta.

Whereas the above publication is the result of a project conducted under the Northern River Basins Study and the terms of reference for that project are deemed to be fulfilled,
IT IS THEREFORE REQUESTED BY THE STUDY OFFICE THAT;
this publication be subjected to proper and responsible review and be considered for release to the public.

F. J. Wrona — 22 Apr 96
(Dr. Fred J. Wrona, Science Director) — (Date)

Whereas it is an explicit term of reference of the Science Advisory Committee "to review, for scientific content, material for publication by the Board",
IT IS HERE ADVISED BY THE SCIENCE ADVISORY COMMITTEE THAT;
this publication has been reviewed for scientific content and that the scientific practices represented in the report are acceptable given the specific purposes of the project and subject to the field conditions encountered.
SUPPLEMENTAL COMMENTARY HAS BEEN ADDED TO THIS PUBLICATION: [ ] Yes [ ] No

P. A. Larkin — April 23/96
(Dr. P. A. Larkin, Ph.D., Chair) — (Date)

Whereas the Study Board is satisfied that this publication has been reviewed for scientific content and for immediate health implications,
IT IS HERE APPROVED BY THE BOARD OF DIRECTORS THAT;
this publication be released to the public, and that this publication be designated for: **[ ] STANDARD AVAILABILITY [ ] EXPANDED AVAILABILITY**

Lucille Partington — April 23/96
(Lucille Partington, Co-chair) — (Date)

R. McLeod — 30/04/96
(Robert McLeod, Co-chair) — (Date)

HYDROMETEOROLOGICAL CONDITIONS CONTROLLING ICE-JAM FLOODS, PEACE RIVER NEAR THE PEACE-ATHABASCA DELTA

STUDY PERSPECTIVE

> ***Related Study Questions***
>
> *10. How does and how could river flow regulation impact the aquatic ecosystem?*

The Northern River Basins Study Board requested scientists to assess the effects of flow regulation on the aquatic/riparian ecosystem. Special emphasis was placed on the Peace River and the Peace-Athabasca Delta (PAD). Previous studies into the effects of the Bennet Dam on the river and delta were not sufficiently detailed to address potential remedies. Yet the changing conditions of the river and delta were an ongoing concern to residents living within or near these waters. Within PAD, isolated perched basins require over bank flooding to periodically replenish water levels. At full supply, there is approximately 19,000 km. of shoreline within the PAD that contributes to its important role as a staging and rearing area for migratory waterfowl. It also supports a diverse and abundant fish community.

Since the Bennett Dam there were two commonly held perceptions to explain for the lack of flooding in the delta. One view held that the dam had restricted flow volumes and thus reduced the frequency of open water floods sufficient to flood the perched basins. The other was that reduced spring flows were responsible for the decline in severe ice jams in the delta area.

Examination of flow and weather records showed that the historically high open water floods of 1990 did not flood the higher elevations in the PAD. This new evidence suggested that open water floods could not produce high enough water elevations, frequently enough, to sustain the perched basins. Backwater effects from ice jams developed during the 1974 breakup were the last documented significant flooding events in the PAD.

Records revealed that these ice jam floods were associated with large runoff events in the tributaries, especially the Smoky River. These large runoff events were also associated with large spring snow packs and run-off. Snow packs in the Smoky basin since the mid 1970's have been lower than average, which also coincides with the absence of PAD floods.

The main effect of flow regulation is its influence on the increased freeze-up elevations of river channel ice due to higher flows being maintained in the fall. With higher winter flows, the ice cover forms higher off the bed of the river. This creates more channel area under the ice for flows to pass without causing the ice sheet to breakup. Under flow regulation, the production of spring ice jams is more dependent on downstream tributary run-off. It appears construction of the Bennett Dam was also coincident with snow packs that have been smaller resulting in reduced tributary flows during spring run-off. This has resulted in fewer breakup ice jams and associated flooding.

Results from this project are being integrated with other hydrology investigations. This project work was a joint venture with a companion study, "Peace Athabasca Delta Technical Study". Information gained from projects carried out under both studies" will be used to produce a synthesis report on the impacts of flow regulation on the Peace and Slave rivers, and their deltas.

REPORT SUMMARY

This study stemmed from the concerns raised regarding the long term trying trends affecting the Peace Athabasca Delta (PAD), one of the world's largest freshwater deltas. A common perception during the 1970's and 1980's was that lower flows on the Peace River due to regulation by the W.A.C. Bennett Dam, minimized the probability of large open water flood events capable of inundating the perched basins of the PAD adjacent to the Peace River. Local traditional knowledge and other anecdotal information suggested that ice jams also played a role in some flood events.

Analysis of hydrometric data in conjunction with various historical and local-knowledge sources confirms that open-water floods have been ineffective in producing high-elevation floods along the Peace River adjacent to the Peace-Athabasca Delta. Even the historically high flow event of 1990 did not produce a flood of sufficient magnitude to flood high-elevation portions of the delta. Over the period of hydrometric record, backwater produced during river-ice breakup has exceeded that of the 1990 open-water event on several occasions. It was breakup backwater, in 1974, that resulted in the last major flooding of the elevated perched basin within the PAD.

In the lower portions of the Peace River, flow regulation seems to have produced minor changes in factors, such as ice thickness and strength, that could significantly affect the severity of breakup and related ice-jam flooding. Temporal analysis of these factors, however, also detected a weak climate signal suggesting that since approximately the mid-1970's the period of ice cover may have become slightly warmer and the pre-breakup melt period may have become more intense and/or more protracted.

A common perception was that reduced flows due to regulation were responsible for the decline in severe ice jams. Flow contributions from the point of regulation, however, are higher, on average, at the time of breakup near the PAD in the post-regulation period than prior to regulation. The major ice-jam floods that occurred in the 1960's prior to regulation and in the early 1970's after regulation have been associated with large runoff events from downstream

tributaries, especially the Smoky River. These large tributary flow events also appear to be correlated with large spring snowpacks and associated snowmelt runoff. A preliminary evaluation of temporal trends in the size of the snowpack on the Smoky River suggests that there has been a shift in the mid-1970's to values lower than the long-term average. A similar trend in snowpack accumulation has been identified in British Columbia.

The major effect of regulation on the occurrence of breakup ice jamming near the Peace-Athabasca Delta is related to higher winter flows and increased freeze-up elevations. In general, the higher a freeze-up cover, the greater the flows it can pass without breaking. Two runoff sources combine to generate spring flows that can exceed the freeze-up level:: the upstream flow from above the point of regulation and the downstream tributary flow. Under regulated conditions, a major increase in upstream flows (above the point of regulation) is unlikely at the time of breakup near the Peace River Delta due to the operational transition to lower summer releases. Furthermore, if the amount of regulated flow at the time of breakup is declining, tributary flow will have to account for this "loss" to the main-stem discharge, before having an affect on the ice cover. Under the current regulated regime, production of severe breakups has become more dependent on tributary inflow, particularly from the Smoky River. Large spring runoff from the tributaries have been effective since regulation in producing large breakup floods (e.g., 1972 and 1974) but the apparent decline in spring snowpacks has reduced their subsequent effectiveness. Thus the absence of a large-order event since 1974 seems to be related to a combined effect of flow regulation and the vagaries of climate.

ACKNOWLEDGEMENTS

The authors wish to acknowledge the extensive support in data compilation/verification, computer modelling, and graphics production provided by the following: R. Keller (University of Saskatchewan), M. Jones (Environment Canada, Fort Smith), D. Bucilla (NHRI), G. Stryanko, M. Hey and the late Barbara Miller. Editorial and scientific reviews by L. Watson (NHRI) and L. Hamlin (University of Waterloo) are also gratefully acknowledged. Additional thanks are due to J. Choles (Alberta Environmental Protection/NRBS Study Office) for contract administration support.

TABLE OF CONTENTS

LIST OF FIGURES

Ordered by Figure number following the text.

LIST OF TABLES

Ordered by Table number following Figures

1.0 INTRODUCTION

This report is the result of work conducted for the Northern Rivers Basin Study (NRBS), the Peace-Athabasca Delta Technical Studies (PADTS) and the National Hydrology Research Institute (NHRI). The project evolved from a concern expressed by the NRBS and PADTS regarding a long term drying trend that has affected the Peace Athabasca Delta, one of the world's largest freshwater deltas. Flooding is critical to the ecosystem health of river-delta environments, particularly to perched-ponds and lakes that are vertically separated from the open-water flow system. Unfortunately, the PAD has not experienced a major flood since 1974. As a result, significant drying has occurred in the higher-elevation portions of the PAD landscape. This is believed to have lead to significant changes in, for example, the vegetation regime and the related small-mammal habitat. The PADTS is currently completing a companion study of the significance of drying/flooding to the vegetation regime of the PAD.

Beginning in 1968, the Peace River became regulated with the construction of the W.A.C. Bennett Dam in its headwater reaches within the province of British Columbia. Initial filling of the dam caused major reductions in water levels within the PAD and resulted in the construction of rock-filled weirs in an attempt to restore levels to pre-regulation conditions. Unfortunately, this has only been successful for the large lake and channel systems directly connected by the main flow system of the Athabasca, Peace and Slave rivers. Drying has continued in the higher elevation perched basins because of the lack of large overbank floods.

A common perception during the late 1970's and 1980's was that lower flows on the Peace River resulting from regulation precluded the generation of flood levels that would inundate the perched basins, especially in the northern areas of the PAD near the Peace River. However, there were numerous anecdotal references within the PAD literature and opinions expressed by local inhabitants that ice jams also played a role in some flood events. No analysis had been completed, however, to determine whether such events were more or less important to flooding than open-water floods. This formed the initial objective of this study, i.e., to determine the relative role of ice jams in flooding the PAD. Assuming ice jams to be a significant factor, a second objective was to determine the hydrometeorological conditions that lead to their generation near the PAD and thirdly to determine what role flow regulation has had on their formation.

The remainder of this report is divided into seven major sections: 1) a general site description of the PAD relative to the major controlling river reaches, 2) a review of the changes that have occurred in the flow-regime as a result of flow regulation, 3) an analysis of hydrometric records to determine the relative significance of open-water and ice-induced flood peaks to flooding of the PAD, 4) a temporal evaluation of changes to the timing and duration of the ice regime on the Peace River, 5) an analysis of the hydrometeorological conditions that control the driving and resistance forces associated with breakup, 6) a discussion of the relative importance of the various factors that have led to a decline in ice-jam frequency, and 7) some final conclusions and recommendations for future work.

2.0 SITE DESCRIPTION

2.1 Peace River

The Peace River originates in the alpine regions of northeastern British Columbia (Figure 2.1). Many of these alpine basins are glacial fed and ultimately feed into the large Williston Reservoir behind the W.A.C. Bennett dam. Immediately below the dam, in the foothills, the basin is mostly forest and has little capacity for basin storage. The river is incised more than 200 m into the Alberta Plateau as far downstream as the town of Peace River. It decreases in slope from approximately 0.00049 near the dam to 0.00028 near the town of Peace River (Kellerhals *et al.*, 1972). The channel is predominantly straight with occasional islands and minor gravel bars, and is approximately 450-500 m in width. Closer to the town of Peace River, the channel becomes progressively more sinuous, still with occasional islands and bar features.

The Smoky River, the main tributary to the Peace, enters a short distance upstream of the town of Peace River. It drains the front ranges of the Rocky Mountains and has an area of approximately 50,300 km^2 representing 27% of the Peace River basin at this point. From the confluence of the Smoky River, the river trends northward, switching to the north east in the vicinity of Fort Vermilion. This reach of the Peace River primarily drains the Peace River Lowlands although the headwaters of some tributaries extend onto the Alberta Plateau.

The river is incised into the surrounding plain, decreasing from 200 m at Peace River to about 30 m in the vicinity of Fort Vermilion. The reach between Peace River and Fort Vermilion can be characterized as partly entrenched and confined, with irregular meanders. The river widens from approximately 500 m at Peace River to around 650 m at Fort Vermilion. As in the upper reaches of the Peace River, intermittent islands and bar complexes exist in the channel, although the alluvial material along this reaches is finer than upstream.

No major tributary contributions occur between the town of Peace River and Fort Vermilion. The contributing area along this reach of the river represents only 16.5% of the basin area at Fort Vermilion and only 12.5% of the basin area at Peace Point. In terms of the non-regulated basin area, this section represents 24% and 16.5% at Fort Vermilion and Peace Point respectively. The basin is dominated by forested terrain with intermittent muskeg.

From Fort Vermilion to Peace Point the river, which is in the vicinity of the upstream boundary of the PAD, is in distinct contrast to the upper reaches. The landscape of the lower Peace River valley is no more than 20-25 m deep, incised into the old lake bed of Glacial Lake McConnell (Craig, 1965). As the river cut into these lacustrine deposits it wandered away from its preglacial course in several places and subsequently began to cut into bedrock. These locations coincide with the small waterfalls and rapids existing along this reach (eg. Vermilion Chutes and Boyer Rapids). Kellerhals *et al*. (1972) report the channel slope between Fort Vermilion and Peace Point as being 0.00008, excluding Vermilion Chutes. The Vermilion Chutes, approximately 80 km downstream of Fort Vermilion, results in a 10 m drop in bed elevation over a few kilometres. The channel downstream of the Chutes increases dramatically in width, exceeding 1500 m at some locations. The channel pattern is weakly sinuous with split channels and island complexes. Further downstream the channel narrows (approximately 700 m at Peace Point) and has an irregular meandering channel pattern with only occasional islands and bar complexes.

The only significant tributary draining into the Peace River below Fort Vermilion is the Wabasca River which drains the southern portions of the Birch Mountains and surrounding plains. This basin has an area of approximately 35,800 km^2 representing 51% of the drainage between Fort Vermilion and Peace Point and 12% of the entire basin at Peace

Point. The overall drainage area between Fort Vermilion accounts for 24% of the entire Peace River basin and 31% of the unregulated basin area at Peace Point. Unlike the upper areas of the Peace river catchment, this portion of the basin is dominated by a forested muskeg terrain.

After some 1100 km, the Peace River finally reaches the northern edge of the PAD. Total drainage area to this point is 293,000 km^2.

2.2 Peace-Athabasca Delta

The Peace-Athabasca Delta (PAD) is formed by the Peace, Athabasca and Birch Rivers at the western end of Lake Athabasca in the province of Alberta (Figure 2.1). Delta development began following recession of the Pleistocene ice sheet, with these rivers draining into a much larger Lake Athabasca. Initially, the Peace Delta had a rapid rate of growth, but as levees attained sufficient height, most of the flow and sediment were carried directly to the Slave River; thus, the Peace River Delta can be considered inactive (Bayrock and Root, 1973). In contrast, the Athabasca and Birch River deltas are still actively depositing sediment, although the Birch River only contributes a fraction of the sediment to the total delta complex compared to the Athabasca.

As the PAD continued to grow, many water bodies became separated from Lake Athabasca. Three large shallow lakes (Figure 2.1; Claire, Mamawi and Baril; <1 to 3 m deep) currently occupy a large proportion of the 3900 km^2 delta area, and are connected to Lake Athabasca and other small basins by a myriad of active and inactive channels. The PAD and Lake Athabasca are connected to the northward-flowing Peace and Slave rivers by three major channels, Rivière des Rochers, Revillon Coupé, and Chenal des Quatre Fourche (Figure 2.2). Although flow is normally northward, it can reverse when the Peace River is higher than the level of Lake Athabasca. Discharge in these channels is proportional to the difference in water levels of the lake systems and the Peace River; reversing flows in the PAD are not uncommon. Water levels experience a peak on the Peace and Athabasca rivers during the spring breakup period (late April-early May) and a few weeks later (June) during a period of sustained high flow produced by runoff from the Rocky Mountain headwaters. It is during these two periods that high water levels on the Peace River can obstruct the northward flow of water. As a result, lake-water levels are typically highest in the PAD and on Lake Athabasca during the spring and summer, but then recede during fall and winter when the outflow to the Slave River is greater than inflow to the PAD. Weirs have been installed within the PAD (see below) affect lake water levels by restricting the northward flow of water out of the PAD.

Depending on the elevation of lake and river water levels, water can also feed into the adjacent landscape, and fill the shallow perched basins. Topographic relief seldom exceeds 1m above the surface of the major Delta lakes, except for the levees and islands of Canadian Shield outcrops located primarily in the north-east. Perched basins have been classified according to the degree of their connection with the lake and channel flow system as open-drainage, restricted-drainage, and isolated (Peace-Athabasca Delta Project Group, 1973). These classifications roughly correspond to the general mapping of drainage types noted on Figure 2.2, i.e., open, restricted and severely restricted drainage (Jaques, 1989; Prowse and Demuth, 1996).

In the case of isolated perched basins (severely restricted drainage), water can only enter the basin through overbank flooding, and water-level decreases are almost exclusively controlled by evapotranspiration. Average annual small-pond evaporation for this region is approximately 450 mm (Fisheries and Environment Canada, 1978) while the recorded average annual precipitation is 381 mm (Atmospheric Environment Service, 1993), thereby yielding an annual water deficit of 80 mm. Given that groundwater flow through the levees is negligible (Nielsen, 1972), periodic flooding of these perched basins is essential for their survival. When full, such basins account for over 19,000 km of shoreline within the delta (Townsend, 1984).

One of the principal factors controlling the rich wildlife productivity of these basins (see below) is that early successional forms of vegetation support the largest number of wildlife. Muskrat, for example, survive best in relatively shallow marshes (e.g., ~1 m) having an abundance of emergent and submergent aquatic vegetation. Their numbers were estimated to be in the range of 200,000 to 300,000 in the mid-1960's (Peace-Athabasca Delta Project Group, 1973). Similarly, bison prefer sedge and grasses (*Calmagrostis canadensis* and *Carex atherodes*) common to these flooded marsh environments. Sustaining these types of vegetation requires either a permanent shallow depth of water or periodic flooding, as is the case for perched basins. Since the vertical range of most delta plant communities is quite small, only minor changes in water levels can lead to the advance or retreat of plant succession over large areas.

The shallow perched basins scattered across the PAD grasslands also provide ideal habitat for nesting waterfowl. Such habitat has made the Delta a central node in four North American flyways and an important refuge for duck populations forced to migrate northward during drought years on the more southerly prairies. Over 600,000 young waterfowl have been raised in the Delta during years of optimum water-level conditions (Townsend, 1984).

3.0 CHANGES TO THE PEACE RIVER FLOW REGIME

Filling of the Williston Lake behind the W.A.C. Bennett Dam in 1968 marked the beginning of lower than average flows on the Peace River. During the four years, 1968-1971, there was a net storage behind the dam of 41 X 10^9 m^3 of water (Muzik, 1985). As a result, Peace River flows were reduced by as much as 5600 $m^3 s^{-1}$ and associated water levels by as much as 3 to 4 m (see subsequent discussion). Over this filling period, the perched-basin shoreline was reduced by approximately 36% and the water-surface area by 38%, exposing some 500 km^2 of mudflats that were quickly seeded by new meadow and willow communities. Over the period 1966 to 1972, muskrat harvest fell from 144,000 to less than 2,000 (Townsend, 1975). As well as reducing water levels on the connected system of lakes and channels, lower peak flows on the Peace River were believed to eliminate the potential for flooding of higher perched-lake environments (Peace-Athabasca Delta Project Group, 1973).

In response to the ecological impacts to the Delta, fixed crest weirs were constructed on the Rivière des Rochers and Revillon Coupé in 1976 (Figure 2.2). Although the control structures served to restore water levels at lower elevations of the Delta (Aitken and Sapach, 1993), perched basins along the Peace River and at higher elevations in the Delta have continued to dry. To date, these basins have not been flooded since 1974. The lack of annual flooding has killed sedge meadows and allowed the invasion of more persistent shrub communities such as willow and poplar.

4.0 FLOOD RECORDS-Hydrometric Record Analysis

4.1 Open-Water Flow Peaks

A commonly held perception has been that lower flows on the Peace River have precluded flooding of the perched-basin environment of the Peace-Athabasca Delta. Past analysis of peak water levels, however, has focussed primarily on water levels recorded in the main Delta lakes and channels (e.g., Aitken and Sapach, 1993; Muzik, 1985). Such analysis is relevant to assessing the flooding probability of open-drainage/restricted-drainage basins, but not of high-elevation isolated basins, particularly near the Peace River. The following analysis, therefore, focusses on water levels recorded on the Peace River at Peace Point. This is the closest (approximately 70 km upstream of the main Delta area) hydrometric station to the Peace-Athabasca with a pre-regulation record.

The direct effects of flow regulation can best be realized at the Hudson Hope hydrometric station, located just downstream of the dam. Figure 4.1 shows the pre- and post-regulation monthly hydrographs for this site. Following regulation, there has been an obvious flattening of the annual hydrograph, with much of the summer flows being stored and released during the winter period. The relative influence of this regulation on locations as far downstream as the Peace-Athabasca (approximately 1100 km) is complicated by two primary factors: a) climatic variability and its effect on the flow regime, both upstream and downstream of the dam, and b) the large contributing area downstream of the dam, much of which is ungauged. The ratio of catchment areas between Hudson Hope and Peace Point (223 x 10^3 km^2) and upstream of Hudson Hope (69 x 10^3 km^2) is over 3:1. The effect of regulated flows on downstream hydrographs is currently the focus of a major flow modelling study by a government water-resources agency, Alberta Environmental Protection.

Regardless of the reasons, there have also been major changes in mean and peak flows near the Peace-Athabasca Delta. Figure 4.2 shows the mean, maximum and minimum monthly flows recorded at Peace Point for the pre- and post-regulation periods. Unfortunately, the pre-regulation record extends back only to 1959/60. As shown in Figure 4.2, the pre-regulation peak-monthly flows typically occurred in June ranging from a low of 5,950 $m^3 s^{-1}$ to a maximum of 9,790 $m^3 s^{-1}$ and averaged 7,482 $m^3 s^{-1}$. With the seasonal adjustment to flow, these figures all decreased by some 3,500 $m^3 s^{-1}$. This translates into a decrease of open-water levels ranging from approximately 1.75 m at the higher maximum mean-monthly flows, to 3.25 for the minimum mean-monthly flows (-2.56 m for the change in mean-monthly flows). More specifically, Figure 4.3 shows the peak-annual water levels achieved under open-water flow conditions before and after regulation. For the eight-year, pre-regulation period, peaks averaged 217.5 m, whereas the post-regulation period averaged 215.4 m. This 2.1 m decline in instantaneous peaks is comparable to that for the mean-monthly values.

Notably, the post-regulation data include the largest flow event on record for the Peace River. In 1990, the Peace River discharge reached 12,600 $m^3 s^{-1}$, 700 $m^3 s^{-1}$ greater than the previous high recorded in 1964 prior to regulation. Significantly, however, even this historically-high, open-water flood failed to recharge the high-elevation perched basins. It is estimated that an open-water flow in the order of 14,000 $m^3 s^{-1}$ is required to overtop the Peace River banks near the Delta (i.e., at Sweetgrass Landing near the Claire River, Figure 2.1; Peace-Athabasca Delta Project Group, 1973). The major conclusion of this analysis is that open-water floods have not been responsible for the overbank flooding of the high-elevation perched-basin regime. The other obvious source of potential flooding is that produced by ice-jam backwater.

4.2 Ice-induced Backwater Peaks

In early hydrologic assessments of the Peace-Athabasca, the role of ice jams in flooding perched-basins was mentioned periodically. With large-scale drying of the Delta beginning in the 1970's, however, attention was focused, almost exclusively, on open-water conditions and engineering structures (weirs) for restoring water levels within the large lake system. Following the failure of the historically-high, open-water event of 1990 to flood the perched basins, the focus shifted to the role of ice jams. The logic for such a change in focus was strengthened by Jaques (1990) who found the weirs largely ineffective in halting vegetation changes within the perched basins. Specifically, he noted that between 1976 and 1989, there had been an estimated 47% reduction in the aquatically-productive vegetation community that (78%) existed primarily above the elevation-zone influenced by the weirs and the mean-peak, summer water level (post-regulation period).

The main hydrometric station on the Peace River near the PAD is located at Peace Point. Records from this site are used to provide a general index of ice breakup severity and hence expected ice-jam severity. This is considered a reasonable assumption given that the river reach near Peace Point is similar in character to most of the Peace River near the Peace River Delta. Furthermore, as reviewed by Gray and Prowse (1993), the severity of ice jamming is usually in direct relation to the breakup severity; dynamic or mechanical breakups produce the largest ice jam floods and thermal breakups the most ineffective jams.

Peak-instantaneous, water level data for spring breakup were extracted directly from original hydrometric chart recordings for the period, 1962-1992 (although chart records of breakup are only available as of 1962, published flow records exist from 1959). Recorded survey checks and a review of the data by Water Survey of Canada field staff (M. Jones, Fort Smith, Canada) were used to ensure that the most accurate estimate of breakup water levels could be obtained from the charts. The data represent the peak water levels measured during the breakup periods. These levels could result from the effects of a breakup front moving past the site or could be due to backwater from downstream ice jamming.

Figure 4.4 shows these data and the open-water rating curve for the Peace Point station. Notably, peak breakup water levels for seven breakup years exceed that produced by the 1990 open-water event - some by as much as 2 m. Furthermore, these levels were produced by Peace River spring flows of a 1/3 to a 1/2 that which produced the 1990 open-water event. Three of the large breakup events occurred biennially during the 6-year record preceding regulation and four within the subsequent 25-year period. Note, however, that some missing records during breakup mean that some water levels could be underestimates (indicated by arrows in Figure 4.4). Although the Peace Point levels cannot be directly extrapolated to the main Delta area, they do indicate that much higher levels are produced by ice-induced backwater and at much lower flows.

4.3 Historical Knowledge

Because of the significance of flooding to the Peace-Athabasca Delta, there have been attempts to construct flood histories from local residents and historical archives (e.g., Peterson, 1992; 1994; Thomson, 1993; Thorpe, 1986). The lack of true elevation data meant that such analyses had to rely on simple magnitude classifications of the various disparate data. The summary by Peterson (1994) notes that ice jams have been a critical factor in flooding of the PAD and account for over 70% of the highest magnitude floods. Summer floods have been less common and less effective, the 1990 event again cited as having produced the highest water level recorded since the 1930's but being of insufficient magnitude to flood the high-elevation perched-basins of the delta. This report also notes that since 1803 there have been at least 13 years of major ice jam floods on the Peace River, the most recent including 1958, 1962, 1965 and 1974 (Peterson, 1994). An earlier report by Peterson (1992), acknowledged that some confusion existed in local accounts about the actual year of the "1962" flood which was also reported as 1961 and 1963. Subsequent archival research has uncovered early correspondence regarding an aerial surveillance of the flood conducted as part of a forestry impact assessment (Jackson, 1963). This document confirms that 1963 was a major ice-jam flood year as also indicated by the Peace-Point hydrometric record (Figure 4.4). This data set also indicated that 1972 was probably a major event but the Peterson (1992) report assigns a "zero" magnitude to this year. Again, however, other documentary evidence (Smith, 1972) has been unearthed that describes a bankfull flood produced by an ice jam on the Peace River near the PAD.

In general, some problems exist with attempting to use local knowledge in accurately quantifying the significance of ice-jam floods on the Peace River, probably related to the high spatial variability in local residents source information [i.e., the data are representative of conditions observed from various portions of the delta and should not reflect identical flood-level conditions because of variations in proximity to the ice-jam location] For example, Peterson (1992) notes that the 1974 flood was observed to affect a relatively remote site near Dog Camp (major flow node in the PAD) but was not recorded by residents living in the major community of Fort Chipewyan, a distance of approximately 8 km to the east. Despite the disparate nature of the historical data, the early summaries by Peterson (1992, 1994) and the subsequent additional archive information (Jackson, 1963; Smith, 1972) corroborate the occurrence of most of the major floods observed at the Peace Point hydrometric station and validates its use as an indicator of flood events that affect the Peace-Athabasca Delta. Furthermore, local information has also permitted the identification of two critical ice jam sites: a sharp bend in the Peace River at Rocky Point, located just downstream of the Quatre Fourches channel, and the entrance to the Slave River (Figure 2.1; Peterson, 1992).

4.4 Summary of Flood Peaks

In summary, the hydrometric analysis of the Peace Point hydrometric record in conjunction with various historical and local-knowledge data confirms that open-water floods have been ineffective in producing high-elevation floods along the Peace River adjacent to the Delta. Even the historically high flow event of 12,600 $m^3 s^{-1}$ did not produce a flood of sufficient magnitude to flood the PAD. Over the period of hydrometric record, backwater produced during river-ice breakup has resulted in water levels that often exceed those produced by the 1990 historically-high open-water event. Based on data from the Peace Point hydrometric station, this occurred on a biennial basis in the 1960's prior to regulation (1968) of the Peace River, but only three times since.

5.0 TIMING AND DURATION OF PEACE RIVER ICE REGIME

In general, the occurrence of breakup ice jamming is dependent on the timing and nature of upstream ice conditions. Although not originally a component of this study, requests were made to summarize the general change in the ice season along the Peace River as background information for the analysis of the breakup regime near the PAD. The following details the results of this work.

Since regulation of the Peace River, considerable information has accumulated about changes to the timing and duration of the ice season along the Peace River. Extensive work had to be conducted, however, to consolidate and standardize the available information. The main sources of information are the observer notes that form part of the standard hydrometric measurement procedure conducted by Environment Canada personnel and the recorder charts that continuously record water levels at the various hydrometric stations. Ancillary information was obtained from local sources such as newspapers and records from municipal "breakup date" lotteries.

Table 5.1 lists the hydrometric stations along the Peace River and the dates of available record. Locations of the stations are noted on Figure 2.1. Copies of all recording charts were obtained and analyzed on an hour by hour basis throughout the ice-season periods for all years of available record. The data were checked and rechecked by staff at the National Hydrology Research Institute and by M. Jones of the Water Survey of Canada who was involved in the original recording of much of this data. Data were extracted from the recorder chart according to techniques outlined in Beltaos *et al.* (1990). In general, the dates of freeze-up and breakup are identified on the charts by the large and pronounced fluctuations in water levels resulting from the hydraulic disturbance produced by these two periods of dynamic ice motion. Other forms of data were used to augment or replace the water-level records whenever this primary information source was deficient or unavailable. Figures 5.1 to 5.5 summarize the records of ice coverage for the stations listed in Table 5.1.

Unfortunately, not all stations have the same period of available record and only one site (*Peace River at Hudson Hope*) has a lengthy pre-regulation record (Table 5.1). Fortunately, however, the stations with the longest periods of record (*Hudson Hope, town of Peace River, and Peace Point*) are dispersed well along the full length of the Peace River, thus permitting an evaluation of temporal and spatial trends in the ice regime data. Table 5.2 provides the summary statistics regarding the mean and standard deviation of freeze-up and breakup dates, and duration of the seasonal ice regime, for the pre-regulation and post-regulation periods. Note that the years 1968 to 1972 have been excluded from this data summary because they are representative of a highly anomalous flow regime that prevailed only during the filling of the reservoir. As evident in Figures 5.1 to 5.5, however, they do appear to have caused major disruptions to the ice regime. Also provided in Table 5.2 are the results of statistical tests to evaluate whether the mean dates or season duration significantly differ. This could not be assessed for some stations simply because the general winter conditions changed from ice-covered to open-water or intermittent ice cover, with the introduction of the regulated regime. This is most prevalent in the upper reaches of the Peace River closest to the point of regulation.

The ice-regime record for the Peace River at Hudson Hope (uppermost station) includes an interval from 1917 to 1922 but the most recent continuous record did not begin until 1949. Prior to regulation, the main freeze-up cover was in place by mid to late November. Records indicate that the winter ice cover was often intermittent with the latest indications of ice occurring by late April to early May. Since regulation, however, this station has not reported any significant ice effects. The pre-regulation record for the Peace River at Taylor is also reasonably good, and with dates reasonably similar to those for Hudson Hope. Following regulation, this site has only experienced an intermittent (space and time) ice cover.

In an in-depth analysis of Peace River freeze-up conditions, also conducted as part of the NRBS hydrologic-research program, Andres (1995) reported on similar delays in freeze-up, the most significant changes being evident in the upper reaches of the river and ascribed to the supply of warm hypolimnetic water from the Williston reservoir. This effect is believed to have a significant impact on freeze-up dates to as far downstream as approximately the town of Peace River. The data in Table 5.2 and Figure 5.6 confirm this. Overall, there has been a significant decrease in the average length of the ice-covered period at the town of Peace River, decreasing from 124 days in the pre-regulation period (averaged from 1958 to 1967) to approximately 97 days following regulation. The modifier "*approximately*" is used in this case simply because of problems identifying a true freeze-over (establishment of complete ice cover) date in many of the years following regulation. It appears that this site can experience a number of short-duration ice covers before establishing a complete cover that will remain intact until the spring breakup. The advancing front of a freeze-up cover is often characterized by a cycling between freeze-up and breakup conditions (see paragraph below). The recording of such conditions near the town of Peace River may simply indicate that this station now occupies a position in the post-regulation ice regime near the uppermost point of complete freeze-up conditions. It may also be due, in part, to the greater emphasis placed on the observation of ice conditions since regulation of the river. In either case, there has been a significant change in the occurrence of freeze-up conditions near the town of Peace River and this, more than the change in the date of spring breakup, accounts for a shortening in the overall ice season. The mean date of spring breakup at the town of Peace River has not significantly changed but the data shown in Figure 5.6 suggest that it might be more variable since regulation. A significance test on the coefficient of variation does not confirm this, however, although the lack of significance could be a function of the small sample size.

An added point to be stressed about the breakup dates for the town of Peace River shown in Figure 5.6 is that they refer to the spring breakup. Significant mid-winter breakups have also occurred at the town of Peace River: the most notable being in February, 1992 (Fonstad, 1992). In such a breakup, there is limited temporal distinction between the times of freeze-up and breakup. Historically (pre-regulation), this site experienced a fall freeze-up but, with regulation, the arrival of the freeze-up has been delayed until much later in the fall or into the main winter period. With an intense period of warming in the winter, such as occurred in 1992, a breakup event can be precipitated almost concomitant with the initial establishment of the freeze-up cover. The potential hazards, responsibilities and design of safe operating procedures associated with such events are currently the focus of internal-agency reviews and a joint British Columbia-Alberta Task Force (British Columbia-Alberta Task Force, 1992).

Further downstream, some records exist for Fort Vermilion but are of insufficient length or quality to permit any valid assessment of temporal or spatial data trends. Thus, the only remaining data are available for the site of interest, Peace Point, near the Peace-Athabasca Delta. While this is a remote site, it has an excellent record of ice conditions. As the data in Figure 5.7 and Table 5.2 indicate, however, this site has not experienced any significant change in the timing of freeze-up or breakup, and thus the overall ice season.

In summary, regulation appears to have significantly altered the timing and duration of the ice regime upstream of the town of Peace River. Closest to the dam, the ice season has been virtually eliminated. Further downstream, only an intermittent ice cover develops and at the town of Peace River, there has been a significant delay in the initiation of freeze-up and the overall ice season. At the downstream extremity of the Peace River, regulation does not appear to have affected the timing or duration of the main ice season. As demonstrated in the previous section, however, there appears to have been a dramatic change in the severity of breakup conditions at Peace Point since approximately 1974. The role of other factors, beyond the simple timing of ice events, are considered in subsequent sections.

6.0 HYDROMETEOROLOGICAL CONDITIONS AFFECTING BREAKUP

6.1 Breakup Classifications

Breakup severity is a function of the hydrometeorological conditions preceding the period when the cover is finally dislodged from its "overwintering" position. Breakup activity are usually classified into two types: thermal or overmature, and dynamic or pre-mature [the latter also often referred to as mechanical]. Mature breakups are similar to those that occur on a lake where the forces exerted by water flow are at a minimum. The hydrometeorological conditions that produce a mature breakup on a river include low spring runoff, usually the result of a small winter snowpack or protracted melt, and extensive decay of ice thickness and strength. Ultimately, the remnant ice cover is so thermally weakened it can be dislodged by discharge comparable to the low-flow winter period. Quite an opposite set of hydrometeorological conditions characterize dynamic breakup events. They usually include the generation of a large spring flood-wave produced by the rapid melt of a large winter snowpack. Such conditions offer little possibility for the thermal decay of the river ice cover. Thus the advancing flood-wave must push into a reasonably competent ice sheet, one that can only be dislodged by large upstream forces such as created by large ice-jam surges.

In general, river ice breakup results when the force imparted by the upstream ice and flow conditions exceed the factors operating to keep the cover in place and intact, i.e., the resistance force. The severity of breakup is a function of the relative importance of these two forces. Furthermore, as earlier noted, the severity of ice jamming is usually in direct relation to the breakup severity; dynamic or mechanical breakups producing the largest ice jam floods and thermal breakups, the most ineffective jams. As described in a study of the Liard River (Prowse, 1986), ice jams produced by thermal breakups producing only minimal rises in stage. The lack of strong upstream forces combined with weak downstream resistance offered by a thermally weakened ice sheet does not favour the formation of thick ice masses, typical of equilibrium ice jams (e.g., see Beltaos, 1983; 1995) that create maximum backwater levels. Changes to either the upstream or resistance forces could explain why there appears to have been temporal changes to the severity of Peace River breakup events affecting the Peace-Athabasca Delta.

6.2 Resisting Forces

6.2.1 Background

The resistance of a river-ice cover to breakup is principally determined by its thickness, attachment to the bed and banks, and mechanical strength. Unfortunately, except for ice thickness, no regular measurements of these variables are undertaken. Since changes to all these resistance factors are controlled by atmospheric and hydrothermal heat fluxes, however, inter-annual variations of their condition can be estimated through modelling of meteorological heat exchanges and approximations of flow-related heat fluxes. The following sections evaluate any significant temporal variations in the resistance factors, and whether these can be demonstrably linked to the timing or nature of flow alteration.

6.2.2 Winter Ice Growth

6.2.2.1 *Potential Sources of Change*

One measure of ice-sheet resistance is the thickness of the cover at the time of breakup. Inter-annual variations in thickness could result from changes in hydrometeorological conditions, produced by climate and/or flow conditions. In the case of a regulated system, a number of factors could affect ice growth and final thickness. These include changes in ice cover duration, initial ice thickness, and hydrothermal heat fluxes.

In general, the shortening of the ice season, because of a delayed freeze-up or advanced breakup, would translate into a thinner ice cover. In the lower regions of the Peace River, however, the duration of the ice season has not been noticeably affected by regulation; hence, the potential for ice growth has equally not been affected.

The winter thickness of an ice cover can also be strongly influenced by its initial freeze-up thickness as dictated by the prevailing hydraulic conditions (i.e., slope, velocity, flow depth, ice type and geometry). Although higher velocities associated with increased regulated flow during freeze-up are likely to produce enhanced cover thickness in the steeper upstream reaches of the Peace River, this is not the case in the lower slope reaches that characterize the lower portions of the Peace River near the Delta (Andres, 1995).

Ice thickness can also be significantly affected by the introduction of warm water to a river system. As earlier noted, inputs of warm hypolimnetic water from the Williston

Reservoir are responsible for the delay in freeze-up of the ice cover in the upstream reaches of the Peace River and are probably also responsible for some retardation of ice growth near the advancing freeze-up front. During the course of NRBS the question of whether or not such heat could affect winter ice thicknesses near the PAD has been posed. Such an effect would not be present because of the rapidity of the water to ice heat flux. Under the turbulent flow conditions experienced on the Peace River, flow temperatures would be rapidly reduced to 0°C within a relatively short distance (i.e., ~ < several hundred metres) of the freeze-up front (i.e., interface between the upstream open-water and downstream ice cover). Hence, any direct thermal effect of regulation would only be experienced in the upstream reaches of the Peace River and not downstream where the ice season is relatively unaffected.

Increases in flow can also mean an increase in heat flux to the ice cover because of increased fluid friction, ϕ_f, as defined by:

[1] $$\phi_f = \rho_w g S V h$$

where ρ_w is the density of water (kg/m^3)

g is the acceleration due to gravity (m/s^2)

S is the energy slope

V is the mean flow velocity (m/s)

h is the flow depth (m).

The heat produced by fluid friction can either retard ice growth during the winter period, when the overall energy balance is negative (positive net flux to the atmosphere), or accelerate ice ablation during the spring, when the energy balance is positive (positive net flux from the atmosphere). A general understanding of the potential increases in fluid friction that might result from increased winter flow can be gained from Table 6.1, which shows the average pre- and post-monthly flows for the Peace Point hydrometric station and the related heat flux associated with fluid friction. Assuming a similar slope of .00011 and river width of 700 m (Hicks and McKay, 1995) for both scenarios, the enhanced flow would result in an approximate three-fold increase in ϕ_f, from an average of less than 1 W/m^2 for the pre-regulation flows to approximately 2.4 W/m^2 for the post-regulation winter period. Such values are small, however, compared to the winter atmospheric heat fluxes promoting ice growth. A common, simplified approach for estimating the latter fluxes is to use a product of the surface to atmosphere temperature difference and a generalized heat transfer coefficient:

[2] $\phi_* = C_o\,(T_s - T_a)$

where ϕ_* = the total atmospheric heat flux (W m^{-2}),

C_o = the heat transfer coefficient (W m^{-2} °C^{-1}), and

T_a, T_s = the air and surface temperatures (°C), respectively.

Various methods exist for calculating suitable values of C_o from meterological information (see for example Dingman and Assur, 1969) but, in the absence of such data, C_o is often approximated with typical values in the range of 15 to 25 W m^{-2} °C^{-1}. Hence, with an air temperature of -20°C and assuming a coefficient of 20 W m^{-2} °C^{-1}, the total loss of heat from, for example, a 0°C water or ice surface would be 400 W m^{-2}, or more than two orders of magnitude greater than that of the increase in the heat due to fluid friction noted above.

Although ϕ_f is normally small relative to the atmospheric fluxes, it can accumulate to a substantial total over the entire winter period. The total increase in the fluid friction heat flux over the four main months of winter ice growth (December to March) can be converted into a "melt-equivalent" of ice from:

[3] $t_m = \Sigma\phi_f /(\lambda_i\, \rho_i)$

where t_m = the total "melt equivalent" of ice (m)

$\Sigma\phi_f$ = the accumulated heat due to fluid friction (J/m^2)

λ_i = the latent heat of fusion for ice (J/kg)

ρ_i = the density of ice (kg/m^3).

Assuming all such heat is transferred to the overlying ice cover, this would result into a melt-equivalent of approximately 56 mm for the four-month winter period. The significance of this to overall peak ice thickness on the Peace River is discussed below.

6.2.2.2 *Observed Peak Ice Thickness*

To evaluate whether there has been any temporal trend in late-season ice thickness for Peace Point, data were compiled from the Water Survey of Canada (WSC) hydrometric station at Peace Point. During winter measurements of discharge, measurements are made of the ice thickness from the top of the water column to the base of the ice sheet at a number of points across the ice sheet transverse to the flow direction (e.g., Terzi, 1981). Data were extracted for the Peace Point gauge from all late-season hydrometric measurements. The timing of measurements varies considerably from year to year and, in some years, no measurements were conducted several months prior to breakup. To obtain consistency in the data for comparative purposes, only those measurements conducted between March 14 (Julain Day 73) and the beginning of the spring melt period were used. Determination of this latter date is described in the subsequent section that focusses on ice ablation. Where more than one measurement survey was conducted in a given year within this time frame, the maximum value was used. Table 6.2 summarizes the resultant, mean ice thickness values. The pre-breakup peak ice thickness averaged 0.86 m (σ = 0.08; n = 9) while that for the post-regulation period was 3 cm greater at 0.89 m (σ = 0.13; n = 15). The difference is not statistically significant (α = 0.5).

As shown in Table 6.2, the data span a period of approximately one month (i.e., March 14 to April 16). Although rates of ice growth are likely to be low at this time of year (due to insulation effects and more moderate pre-breakup weather conditions), a one month difference does introduce error into this inter-annual comparison. Moreover, two additional factors make the WSC data difficult to compare. Firstly, the cross-section surveys during the winter period are not necessarily conducted at the same site each year because of the quality of the measurement section as determined by such factors as congestion by frazil ice. The presence or absence of such ice is known to significantly affect growth rates of the "thermal" ice cover (e.g., Calkins, 1979) and could account for some inter-annual variability in the reported ice thicknesses. Unfortunately, insufficient data exist in the WSC field notes to eliminate the variability introduced by the presence of frazil.

The second problem relates to the nature of the actual measurement itself and the effect of snow loading (Adams and Prowse, 1986). Measuring from the top of the water to the base of the ice sheet does not permit the determination of a real total ice thickness. To obtain this, an additional measurement from the water surface to the top of the ice cover is necessary. Assuming a snow-free, free-floating ice cover with a density of 910 kg/m^3, the WSC measurement would underestimate the total ice thickness by 9%. Any snow load on the surface of the ice depresses the ice sheet relative to the hydrostatic water level and effectively increases the snow-free *WSC ice measurement.* Although WSC data could be adjusted to account for snow loading effects and derive a true ice-thickness value, no requisite snow depth or density measurements are conducted by WSC.

6.2.2.3 *Modelled Peak Ice Thickness*

Given the potential errors in measurement, variations in snow-load effects and variations in timing of the measurements relative to the precise peak-growth time period, it was decided to model the peak ice thickness for each year. Although the most accurate estimates would be obtained by an energy-balance modelling approach (e.g., Ashton, 1986; Gray and Prowse, 1993), insufficient hydrometeorological data required that a simplified degree-day model (Michel, 1971) be used. Although somewhat inaccurate in the early stages of ice growth, this approach has been proven to provide reliable results when varied to account for different growth environments. Thickness at any given time can be estimated according to:

[4] $$t_i = \kappa D_f^{0.5}$$

where: t_i = ice thickness (mm),

κ = a coefficient varied to account for conditions of exposure and surface insulation ($mm/°C^{1/2}d^{1/2}$)

D_f = accumulated degree-days above freezing, (°C d).

To test the applicability of this approach to the Peace River at Peace Point, all ice thickness measurements were assembled from the WSC records and plotted according to their respective value of D_f. Degree-days were accumulated from the date of freeze-up as determined from the original hydrometric records for each year. Air temperature data were obtained from the AES station at Fort Chipewyan. The results are shown in Figure 6.1.

As suggested by Michel (1971), values of 0.14 to 0.17 appear to be representative of conditions on an "average river with snow". Statistically, the most suitable value of κ for the Peace Point data was found to be 0.18 with an r^2 of 0.61. Using this value in equation [4], peak ice thickness values were then modelled. Unfortunately, air temperature data does not exist on a continuous basis for the Fort Chipewyan station until 1963 which leaves only a very small pre-regulation period to model.

In modelling ice thickness, the date of "peak ice thickness" was assumed to be the date of first significant spring melt as described in the subsequent section on ice ablation. The results are shown in Figure 6.2. Overall, the data suggest there may be some form of decreasing trend with time, but this would appear to occur in the mid-1970's and not at the point of regulation. The mean peak thicknesses were 0.96 m (σ = 0.033; n = 5) for the period 1963 to 1967 (pre-regulation) and 0.94 m (σ = 0.061; n = 21) for the longer post-regulation period (1972 to 1992). As was the case for the measured values, these two mean values are not statistically different.

The apparent decrease of modelled thicknesses in approximately the mid-1970's suggests that the "coldness" of the main ice growing season (date of freeze-up to date of first significant spring melt) may have changed. Although beyond the scope of this report, it is recommended that further climatic analysis be conducted of the winter weather affecting this region to explain this potential shift in climate.

6.2.3 Ice Ablation

The thickness of the pre-breakup ice cover and its associated attachment to the banks and bed can decrease because of atmospheric and/or hydrothermal melt. Unless there is a significant input of warm water from groundwater or tributary flow, bottom melt of an intact ice cover by the hydrothermal flux is relatively small. The main ablation results from surface melt, first usually involving the surface snowpack and then the underlying ice sheet. Unfortunately, little data are ever collected about rates of river-ice ablation because of the logistic and safety problems associated with obtaining such information. To determine whether there have been any temporal trends in seasonal ice-ablation, the controlling heat fluxes and pre-breakup ice thicknesses were modelled for the period 1959 to 1992. The modelling period and method of modelling depended on the availability and type of meteorologic data. The two methods were a detailed energy balance approach and a simplified degree-day approach.

6.2.3.1 *Energy Balance Model*

The following describes the energy balance approach for analyzing the melt of the ice cover by applying the law of conservation of energy to a control volume of ice. The upper and lower boundaries of the control volume are the ice-air interface and ice-water interfaces, respectively. Horizontal transfers of energy are assumed to be negligible. (See Gray and Prowse, 1993 for further details of the energy-balance volume approach). Thus the major heat fluxes to an ice cover can be expressed as:

[5] $$Q_m = Q^* + Q_h + Q_e + Q_p + Q_w - \Delta U/\Delta t$$

where: Q_m = total energy available for melt (W/m^2);

Q^* = net radiation, heat flux (energy per unit cross-sectional area per unit time) of energy at the surface due to the exchange of radiation (W/m^2);

Q_h = sensible energy, the turbulent flux of energy exchanged at the ice surface due to a difference in temperature between the ice surface and overlying air (W/m^2);

Q_e = latent energy, the turbulent flux of energy exchanged at the ice surface due to vapour movement as a result of a vapour pressure difference between the ice surface and the overlying air; evaporation represents a loss and condensation a gain (W/m^2);

Q_p = advected energy, energy derived from external sources, such as precipitation, that is added to the volume (W/m^2);

Q_w = hydrothermal energy, the turbulent flux of energy exchanged at the ice bottom due to a difference in temperature between the ice bottom and the underlying water; this term is comprised of heat due to fluid friction, geothermal heat and bed-sediment heat (W/m^2);

$\Delta U/\Delta t$ = rate of change of internal energy in the volume per unit surface area per unit time (W/m^2).

The net radiation flux can be further broken down to its principal components according to:

$$[6] \qquad Q^* = S\downarrow (1 - \alpha_s) + (L\downarrow + L\uparrow)$$

where $S\downarrow$ = global (short-wave) radiation (W/m^2)

α_s = albedo of the surface layer

$L\downarrow$ = atmospheric long-wave radiation (W/m^2)

$L\uparrow$ = terrestrial long-wave radiation (W/m^2).

The sensible and latent heat fluxes were modelled using bulk aerodynamic formulae that have been proven in many snow and ice ablation studies to provide good daily results (e.g., Moore, 1983). Sensible heat transfer can be written as:

$$[7] \qquad Q_h = \rho_a C_p D_h (T_a - T_i)$$

where ρ_a = air density (kg/m^3)

C_p = specific heat of air at constant pressure (J/kg/°C)

D_h = the exchange coefficient for sensible heat (J/m^3)

T_a = the air temperature (°C) at height z (m), and

T_i = the snow/ice surface temperature (°C).

Latent heat is expressed in a similar manner:

$$[8] \qquad Q_e = \rho_a \lambda_v D_e \gamma (e_a - e_i)/P$$

where λ_v = the latent heat of vaporization for water (J/kg; at 0°C)

D_e = the exchange coefficient for latent heat (J/m^3)

γ = the ratio of molecular weight of water and air, and

e_a and e_i = the vapour pressures above the ice and at the ice surface (mb), and

P = atmospheric pressure (mb).

D_h and D_e are assumed equal to that of momentum (D_m) so that under neutral conditions:

[9] $D_h = D_e = D_m = (k^2 u)/[\ln(z/z_o)]^2$

where k = von Karman's constant (0.4)

u = the wind velocity (m/s) at height z,

and z_o is the roughness length (m).

For situations where temperature and relative humidity are measured at a different height than that of the wind velocity, Sverdrup (1936) suggests:

[10] $D_h = D_e = D_m = (k^2 u)/[\ln(z/z_o)^* \ln(z_l/z_o)]$

where z_l = the height (m) of temperature and relative humidity instruments.

To account for non neutral conditions, a stability factor (Ω) must be applied (Price and Dunne, 1976):

[11] $\Omega = 1/(1+\sigma R_i)$

for stable conditions, and

[12] $\Omega = 1 - \sigma\, Ri$

for unstable conditions, where

σ = a constant approximately equal to 10 (Webb 1970), and

Ri = a bulk form of the Richardson number:

[13] $Ri = g\, z\, \Delta T_a / (T_a(\Delta u)^{2)}$

where g = the acceleration due to gravity (m/s^2)

ΔT_a and Δu = the air temperature (°K) and wind speed differences (m/s) between the surface and height z (m).

All forms of precipitation with a temperature greater than that of the snow/ice on which it falls will transfer heat to the surface. In the case of an isothermal ice cover, only rain at temperatures greater than 0°C is a potential heat source. Snow, sleet or super-cooled rain can act only as a heat sink. The amount of heat that may be transferred from rain to an isothermal ice sheet is a function of the rain volume and temperature:

[14] $Q_p = \rho_w C_w P_i (T_p - T_s)$

where ρ_w = density of water (kg/m^3)

C_w = specific heat of water (J/kg/°C)

P_i = precipitation intensity (m/s)

T_p = temperature of the precipitate (°C)

T_s = temperature of the snow/ice surface, respectively (°C).

Where T_p is not available, it is often approximated by the wet bulb air temperature. This was the approach used in the following analysis. These values were calculated from the records of humidity and temperature for each rain event.

If a heat deficit remains in the ice cover, a second and much larger heat flux may be generated by rainfall. Rain, in the presence of a large enough heat deficit, will freeze and release latent heat to the surrounding snow and ice. In this study, periods of melt were selected (see below) during which it was assumed that the ice cover had reached an isothermal state. Hence, this additional heat flux is not considered.

The importance of the hydrothermal heat flux, Q_w, and the storage term, $\Delta U/\Delta t$, are discussed in the results sections below.

6.2.3.2 *Degree-Day Model*

Calculation of the above can provide a good estimate of the rate and total melt of the ice sheet prior to breakup. In cases where there is insufficient data to adopt an energy-balance approach, a simplified temperature-index approach has been known to provide reasonable results (Bilello, 1980). Reductions in ice thickness are estimated according to:

[15] $\Delta h_i = \tau T_{\Sigma M}$

where τ = an empirical coefficient (m/°C/d)

$T_{\Sigma M}$ = accumulated thawing degree days (°C/d) with a base of -5°C.

Bilello (1980) found τ to vary from approximately 0.004 to 0.01 for northern (i.e., > 60°N) Canadian and Alaskan rivers, and Prowse et al. (1989) found the lower value to be suitable for a temperate river in eastern Canada.

6.2.3.3 *Data/Model Requirements for Calculations of Ice Ablation*

The site of interest is a relatively remote location but has one meteorological station at nearby Fort Chipewyan at which basic recordings of temperature, wind speed, relative humidity, barometric pressure, snow cover, and some sky conditions (e.g., cloud height, type and opacity) are made. The next closest station is located at Fort Smith, N.W.T (Figure 2.1), approximately 150 km to the northwest. Hourly data are available for Fort Chipewyan for the period 1963-1979 but only daily data since 1979. These data were sufficient for the degree-day model and to calculate the convective fluxes in the energy balance model, but no direct measurements were available for solar radiation. Since short-wave radiation is often such a dominant heat flux and because it is also important to the decay of ice strength (see subsequent section), it was decided to model radiation.

Guided by the results of Task IX of the International Energy's Solar Heating and Cooling Programme in which 12 solar irradiance models were evaluated (Davies and McKay, 1989), a cloud layer model for estimating $S\downarrow$ was utilized in this study. These models are of the general form:

[16] $G\downarrow_c = G\downarrow \psi_c \ f(\alpha)$

where $G\downarrow_c$= incident global irradiation under cloudy sky conditions

$G\downarrow$ = incident global irradiation under clear sky conditions

ψ_c = the cloud field transmittance for global irradiation

$f(\alpha)$= a function of ground albedo α which includes multiple reflections between the ground and atmosphere.

As outlined by Davies *et al.* (1984), equation [16] can be expanded into a geometric series:

[17] $G{\downarrow}_c = G{\downarrow}\ \psi_c\ (1 + \alpha\beta + \alpha^2\beta^2 + \ldots \alpha^{n-1}\beta^{n-1})$

where β = an atmospheric backscattering coefficient which accounts for molecular scattering (for cloudless portion of the sky), scattering by aerosols below the cloud base, and the albedo of the cloud base (Davies and McKay, 1982).

With:

[18] $\psi_c = (1 - C + tC)$

where C = cloud cover amount

t = an empirically derived cloud transmittance (Monteith, 1962),

it becomes:

[19] $G{\downarrow}_c = G{\downarrow}\ (1 - C + tC)(1 - \alpha\beta)^{-1}$

This then allows for transmission through clear skies (1 - C) and to account for multiple reflections.

A model based on the above and entitled "McMaster Model" or MAC was obtained from Dr. J.A. Davies, Department of Geography, McMaster University. It was subsequently modified for application in the study area. Since the study area should not experience significant effects of aerosol attenuation (i.e., non-urban) an aerosol transmission value of 1.0 was employed. A single scattering albedo value of 0.75 was also used in β (Davies, 1994, pers. comm.)

Specific data required for the revised version of the model (noted by Atmospheric Environment Service, Digital Archive of Canadian Climatological Data-Surface, names and [assigned element numbers]) include: ceiling [71], visibility [72], sea level pressure [73], dew point temperature [74], wind speed [76], station pressure [77], dry bulb temperature [78], wet bulb temperature [79], relative humidity [80], total cloud opacity [81], total cloud amount [82], weather [83], snow [91], lowest cloud opacity [107], lowest cloud amount [108], lowest cloud amount [109], lowest cloud type [110], second cloud layer opacity [111], second cloud layer amount [112], second cloud layer type [113], and second cloud layer height [114].

Although measurements of global radiation were unavailable for Fort Chipewyan, such data were available for nearby Fort Smith, N.W.T. over the period 1972 to 1978 (i.e., RF1-global solar radiation [61]). These data were used to validate the model at this latitude and time of year. Experience running the model indicated that it was most appropriate to use only the first layer of cloud data as it provided the most consistent results. In validating the model, two simulated runs (one with calculated α, the other with $\alpha = 0.5$) were compared with the measured values (Figures 6.3 to 6.9). A value of 0.5 for α was considered to be best representative of melting snow and ice-covered conditions (e.g., Gray and Prowse, 1993) that would have dominated during the calibration period of April-May. The mean bias error (MBE), root mean square error (RMSE), and correlation coefficient (r^2) for each run are noted in Table 6.3. Given the similarity in results for the two modelled runs and potential difficulties in calculating α for the final Fort Chipewyan application, it was decided to run the model with α set at 0.5. Following final validation, the modified MAC model was used to predict hourly global radiation data using Fort Chipewyan data for the spring breakup periods in the years 1963 to 1979.

The absence of long-wave radiation data for Fort Chipewyan also meant that $L\downarrow$ and $L\uparrow$ had to be modelled. Following Brutsaert (1982), $L\uparrow$ was determined according to:

[20] $L\uparrow = \varepsilon_s \sigma T_s^4$

where ε_s = the emissivity of the surface,

σ = the Stephen-Boltzman constant, and

T_s = the surface temperature (°K).

The emissivity of the melting ice and snow was taken to be a constant of 0.98. Since surface temperatures were unavailable, the river-ice surface was assumed to be at 0°C if the air temperature was above 0°C. Otherwise the surface temperature was assumed to be equal to the near-surface air temperature.

The atmospheric long-wave radiation under clear skies was calculated as:

[21] $L\downarrow = \varepsilon_a \sigma T_a^4$

where ε_a = the atmospheric emissivity under clear skies, and

T_a = the near-surface air temperature (°K).

Atmospheric emissivity was determined from:

[22] $\varepsilon_a = 1.24(e_a/T_a)^{1/7}$

As this formulation was derived for sea level conditions it had to be corrected for barometric pressure and temperature differences with elevation. According to Marks (1979):

[23] $\varepsilon_a = 1.24\ (e_a'/T_a')^{1/7}(P/1013)$

where T_a' = the adjusted sea level temperature (°C), and

e_a' = the adjusted sea level vapour pressure (mb).

Corrected air temperature and vapour pressure are obtained by:

[24] $T_a' = T_a + (0.0065z')$

[25] $e_a' = (e_T/e_s)e_s'$

where z' = elevation of the study site,

e_T = saturation vapour pressure at temperature T_a, and

e_T' = saturation vapour pressure at temperature T_a'.

Values for clear sky $L\downarrow$ were adjusted to account for the effect of clouds by:

[24] $L\downarrow_c = L\downarrow\ (1 + am_c^b)$

where $L\downarrow_c$ = atmospheric long-wave radiation under cloudy skies (W/m^2),

a = a constant based on cloud type with b = 2, and

m_c = the fraction of cloud cover

In determining the latent and sensible heat components, some assumptions had to be made about the ice-surface temperature, roughness length, and stability factor limits. An ice surface temperature of 0°C was used considering that this study focussed only on periods of active melt as outlined below. Considering that determination of sensible and latent heat is not highly sensitive to changes in the roughness height, especially over a smooth flat surface consisting of snow and ice, Sverdrup's (1936) value of 2.5×10^{-3} was assumed. In applying the model it was found that as the Richardson's number approached -0.01 or less the heat flux under stable conditions became unrealistically high. To avoid these anomalous conditions, limits where placed on the stability factor. These were rare occurrences and not believed to significantly affect the overall heat calculations or, more specifically, the comparison of inter-annual variations in total heat inputs.

Sufficient air temperature data existed for Fort Chipewyan to use the thawing-degree day approach from 1963 on.

6.2.3.4 *Period of Ice Ablation*

Unless there is a large hydrothermal flux, ice ablation does not usually commence until melt of the surface snowcover has begun. At this point, melt may occur at the ice surface due to atmospheric exchanges and at the base because of terrestrial runoff, groundwater, and radiative heating. Calculation of the various heat fluxes required knowledge of the cover during its melt state, so that proper assumptions could be made about surface conditions, such as temperature and vapour pressure. A procedure was developed, therefore, to identify the period of active melt, i.e., the melt period spanning from the initiation of pronounced spring melt to the day of breakup. The length of this interval and the accumulated heat flux that occurs within it are indicative of the intensity of the pre-breakup melt period, as earlier discussed regarding types of breakup.

Since no annual records of surface snow temperature were available, three criteria were employed in combination to define the date of ablation initiation. These included:

a) daily snow depth

b) daily maximum and minimum air temperature

c) small index stream runoff

Daily snow depth records were assembled from both the Fort Chipewyan and Fort Smith climate stations. Note that these are single point measurements and not the results of snow surveys. The objective in this analysis, however, was not to define representative water equivalents but rather to define the point of pronounced snowmelt initiation. The daily snow depth records were reviewed, therefore, to identify the point associated with pronounced melt. In interpreting the records, it was recognized that snow depths will decrease in the early spring simply as result of settling associated with metamorphic processes before it actually becomes ripened and begins to melt.

Daily maximum and minimum air temperatures were also assembled from the Fort Chipewyan climate station. These were analyzed for the point when air temperatures began to rise and remain above 0°C.

Daily streamflow records were assembled for a number of nearby small streams: ones that would rapidly show the effects of snowmelt runoff and hence be good indicators of melt initiation. These streams include the Beaver, Bench, Birch, Fire Bag, Jack Pine and Ponton and Richardson. Table 6.4 provides the basic statistics for these basins. All basins were less than 10,000 km^2 in size and primarily located within 250 km of the Peace Point hydrometric station. It was reasoned that when these basins began to produce spring flow, the ablation period had begun and the ice cover would also be in a state of ablation. Due to varying record length and availability, different stations had to be employed for differing years.

Plots of all three variables were assembled and compared in combination. Scientific judgement was then used to determine the date of ablation initiation for each year. Figure 6.10 shows an example of the combination plots and Table 6.5 the ablation period for each year.

6.2.3.5 *Results of Energy-Balance Ice Ablation Calculations*

In evaluating the terms of equation [5], the storage term was treated as zero since it was assumed that the snow/ice was always in a melting state. It was recognized that this would not be the case for all days, such as during cooling phases when Q_h and/or Q_e could offset the positive Q*; it was reasoned, however, that these would be only for brief periods and not significantly affect the overall summary heat calculations. As a further measure to reduce error in any interpretation associated with the inability to consider re-freezing periods, summaries and comparison were also made of only the daily positive heat fluxes. In calculating Q_a, the hydrothermal heat flux was not included, simply because of the lack of data to permit its calculation. Moreover, this is likely to be a very small term relative to the large atmospheric heat fluxes during the pre-breakup period. For example, Marsh and Prowse (1987) found from direct field measurements of an ablating river-ice cover that Q_w was only approximately 10 W/m^2 in the active melt period one week prior to breakup. Only once the active breakup period commenced did this term rise to significant value relative to the atmospheric terms.

Summaries of the daily heat fluxes (Q*, Q_h, Q_e, Q_p and Q_a which is the sum of the four atmospheric heat fluxes) appear in Figures 6.11a to 6.11q for the pre-breakup melt period of each year from 1963 to 1979 (i.e., the years in which hourly data were available to model the various fluxes). Although this record length is insufficient to analyze for significant changes in the time series of the heat components, it does contain a good combination of breakup event types as measured by the magnitude of the peak breakup water level. For example, it contains six of the seven breakup events that produced water levels exceeding that resulting from the historic high-flow event of 1990. It also includes numerous lower-order events that occurred in the intervening years of the 1960's and 1970's. The following reviews the heat fluxes that tend to dominate breakup conditions in the Peace Point area and evaluates whether the severity of the breakup event (as indexed by water levels) has any relationship to the magnitude or type of atmospheric heat fluxes.

The total net and positive heat flux values for each year are presented in Figures 6.12 and 6.13 and as a percentage of their respective Q_a in Figures 6.14 and 6.15. As revealed by the net and positive heat flux results, most events have been primarily high-radiation melt events. On average, Q* accounted for approximately 69% of the total heat atmospheric heat flux during the pre-breakup melt periods. As to be expected for such clear sky melt periods, Q_e tended to be negative and contribute only to evaporation of the ice/snow mass, as opposed to additional melt through latent heat associated with condensation. Although the convective transport of sensible heat averaged only 25% of the net Q_a (30% of positive Q_a), it was significant in some years often reaching in the 20's (MJ/m^2) and in 1964, as high as 52 (MJ/m^2). Overall, however, most melt periods were dominated by the radiative component. This was due to the dominance of the short-wave component as shown in Figure 6.16, which separates the annual values of Q* into its two components S* and L*. Net short-wave radiation exceeds the combined total heat flux (net or positive) in all years, including 1964 when significant contributions of sensible heat were added. As discussed, it is the solar radiation component that contributes not only to thickness decreases but also to internal melt and mechanical strength decreases. The implications of this are considered in a subsequent section.

As identified earlier, the years 1963, 1965, 1967, 1972, 1974 and 1979 (those within the available record length for heat flux calculations) were ones associated with significant (> the 1990 open-water flood) breakup water levels. The composition of the major heat fluxes associated with these specific years was evaluated to see if there were any characteristics that differentiated from those of years of less severe breakup (i.e., as defined by lower water levels). Again similar conclusions result from comparison of the net and positive heat flux results. On average, the large breakup years were characterized by a melt period of lower total Q_a (average net Q_a = 41 MJ/m^2) than those of other years (55 MJ/m^2; excluding years of major reservoir filling, winter 1969 to 1971, although complete final filling did not occur until June 1972). 1972 was, however, an exception with Q_a = 61 MJ/m^2. Part of the reason for the generally lower overall heat flux is that the period of melt tended to be shorter, averaging 9 days (range = 7 to 15; standard deviation = 2.9) for the large breakup years and 11 days (range = 6 to 19; standard deviation = 3.9) days for the other non-fill years. Such differences, however, are dependent on the degree of error involved with the original selection of the melt-initiation date. Considering such differences in melt duration, the more severe years of breakup were actually characterized by a marginally lower rate of melt 4.9 MJ/m^2/d compared to 5.7 MJ/m^2/d. Again, it is unfortunate that the record length was not longer so that a clearer pattern could emerge regarding the character of the melt periods and any significant differences in the time series.

As a further attempt to explore whether there was a relationship between breakup water levels and the magnitude of pre-breakup melt, yearly values of Q_a (net and positive totals) were regressed against the breakup backwater level, Δh . The latter was obtained by first calculating the water level that would result from the discharge on the day of peak water level under open-water conditions, h_o and subtracting this value from the measured peak water level, h_m:

[27] $\Delta h = h_m - h_o$

The established open-water rating curve for the Peace Point hydrometric station and the published daily flow records were used for determining h_o The resulting data are presented in Table 6.6 and the results of the two comparisons in Figures 6.17 and 6.18. Although there appears to be some trend to the data, r^2 in both cases was <0.07, the net heat flux provided the superior value. Within the data set for the net heat flux results, there appears to be one strong outlier. This point is produced by 1972 which had an exceptionally high Δh of 5.8 m but also, as mentioned above, an anomalously high Q_a of 61 MJ/m^2. Excluding this value raises the linear regression for the net heat flux to r^2 = 0.14. Recognizing that anomalous conditions might apply to all the filling years, the years 1968 to 1971 were also excluded resulting in a dramatic increase in r^2 to 0.37 (net Q_a).
The nature of this relationship - decreasing backwater with increasing pre-breakup melt - makes practical sense in terms of the broad classification of breakup events defined earlier. Events plotting to the right-hand side of Figure 6.17 would fall into the category of thermal breakups, ones associated with extensive melt (high heat input). Those to the left would more probably refer to the dynamic type of events when pre-breakup thermal inputs are at a minimum.

One problem underlies the above interpretation of breakup severity. In calculating Δh, it is assumed that the measurement site (Peace Point hydrometric station) experiences equally the effects of breakup from one year to the next. This, however, need not be the case, primarily because of the spatial variability in ice jamming. For example, in one year, an ice jam might form just downstream of Peace Point so that the hydrometric station records the maximum effect (e.g., located within the *equilibrium* reach of the jam; see for example Beltaos (1983;1985) for theoretical discussion of maximum water levels due to breakup ice jams) of ice-jam backwater. In another year of equivalent flow, however, the jam might occur some distance downstream and only minor backwater levels are felt at the gauge. Although it is believed that there are some recurrent ice jam sites along the lower portions of the Peace River, no specific field observations are available to evaluate potential errors in using Δh as an index of ice-jam flood severity. Given this, the results of Figure 6.18 could be considered more useful. It is unfortunate that the available data set for such analysis restricted the extent of this analysis. In an attempt to further evaluate the time series portion of this analysis, the degree-day index results are considered next.

6.2.3.6 *Results of Degree-Day Ice Ablation Calculations*

It should be recognized that melting-degree-day approaches, commonly employed in snow/ice studies, only provide a crude index of heat available for melt. Moreover, such indices are known to be poorest at representing melt conditions where short-wave radiation dominates the total heat flux (e.g., see Gray and Prowse, 1993), such as in the above analysis. They are much more reliable for indexing melt conditions where the solar component is converted into other heat fluxes more closely indexed by temperature. This is the case for snowmelt under forested conditions where incoming short-wave radiation is converted into long-wave radiation within the forest canopy.

The major reason for the use of degree-day indices is that temperature is the most readily available *weather* parameter. In this study, standard temperature data were available to calculate $T_{\Sigma M}$ for a thirty year period from 1963 to 1992. From this lengthy record, it was possible to evaluate, more fully, the relationship between heat input and breakup severity (i.e., Δh) and to analyze any temporal trend in pre-breakup melt conditions.

In the first series of degree-day calculations, attempts were made to define a suitable β coefficient for use in equation [15]. Unfortunately, insufficient reliable data about spring decreases in ice thickness were available to establish a realistic β coefficient. However, ice thickness is simply a linear function of $T_{\Sigma M}$, it was decided to perform the inter-annual comparison directly with the degree-day values.

In calculating $T_{\Sigma M}$, a base reference temperature of -5°C was used because of its previous validation in ice-ablation studies (e.g., Bilello, 1980; Prowse et al., 1989). Two values of $T_{\Sigma M}$ were calculated for each study year (1963-1992). The first summed melting degree days from April 01 of each year to the time of breakup ($T^1_{\Sigma M}$) and the second, from the day of first melt initiation ($T^2_{\Sigma M}$) to breakup, as described above. The results of each are plotted in Figure 6.19. Again, the lack of data before 1963 makes it difficult to compare pre-and post-regulation conditions. Although there is no significant difference for the $T_{\Sigma M}$ values associated with these two periods, there does appear to be a tendency to higher values after the mid-1970's. The major breakup events prior to regulation (1963, 1965 and 1967) and the three since regulation (1972, 1974 and 1979) occurred with $T^2_{\Sigma M}$ values (base of -5°C) less than 131 and no year prior to 1974 exceeded 134. In the period since, however, over half the years equalled or exceeded this value. This could suggest that there has been a tendency to more intense and/or protracted melt periods since the mid- to late- 1970's. Such enhanced heating would lead to increased thinning of the ice cover and, all other factors being equal, a lower ice thickness at the time of breakup. Notably, however, there have also been years during the 1980's with $T_{\Sigma M}$ values equal to or less than those associated with the large breakups of the 1960's and early 1970's.

In comparing the $T_{\Sigma M}$ values with those for Δh, it was found, as in the heat-flux analysis, that the data corresponding with the defined melt period (i.e., $T^2_{\Sigma M}$) provided a better explanation of the variations in Δh (Figures 6.20 and 6.21). Furthermore, removal of the filling years increased the r^2 for a linear-regression analysis from 0.09 to 0.14. Although the overall explanation was lower than that for the heat flux approach, the data again suggest there may be a similar, albeit weaker, trend of decreasing-Δh with increasing heat input (Figure 6.21).

A longer duration record also permitted some basic trend analysis to be performed on the degree-day data. Recognizing that the $T^2_{\Sigma M}$ results provided the best explanation of variations in breakup severity, these values were normalized and plotted in Figure 6.22. The data suggest there may be a difference in conditions prevailing before and after approximately the late 1970's.

In an attempt to identify, more readily, any potential temporal trend in the data, they were analyzed by means of residual mass curves, a method commonly used in the analysis of hydrometeorological data (e.g., Buishand, 1982; Hirst *et al.*, 1987; Church, 1995). Unlike simple analyses such as running-means that smooth variability in temporal records, this method focusses more on identifying persistent trends in a time series. The method is based on the formula:

[28] $\Psi_i = 100\, \Sigma\, [\, x_i / \bar{x} \; - \; 1\,]$

where Ψ_i = cumulative percentage departure after i years,

x_i = value for year i, and

$\bar{x}$ = mean for the period of record,

n = number of years of record.

A negative slope between two datums indicates that the second value is less than average, while a positive slope indicates the opposite. The $T^2_{\Sigma M}$ data were used in equation [26] and are plotted in Figure 6.23. Again, the data point to a shift in the late 1970's (specifically 1979); one in which the pre-breakup melt period is characterized by higher values of $T^2_{\Sigma M}$. A number of methods were used to test for homogeneity within the time series including the von Neumann ratio and Q and R values as outlined by Buishand (1982). To calculate the latter values, the cumulative deviations from the mean were first rescaled by dividing by the sample standard deviation instead of the mean as outlined in equation [28]. None of these tests suggested a strong shift in the mean within the time series. A t-test for a shift in the mean at 1979 (Salas, 1993), however, (based on two time series on either side of this apparent break point) resulted in a rejection of $\bar{x}_1 = \bar{x}_2$, thereby indicating that there is a significant shift in the data at this point. Tests on other subseries within the record length showed no significant difference in sub-series means.

If there is a shift to years of higher degree days after 1979, the implications are increased melt prior to breakup and, if a relationship does exist between pre-breakup melt and breakup severity, a tendency to lower stage increases as a result of breakup. Aspects of this apparent shift in pre-breakup melt conditions are discussed more fully in a later section.

6.2.4 Changes to Ice Strength

The most dynamic type of breakup is more likely to occur when the downstream ice cover is competent and has retained most of its mechanical strength. This poses the strongest resistance to the downward progression of a breakup front and maximizes the probability of the formation of a severe ice jam and related flooding. If, however, the ice cover loses much of its internal strength during the pre-breakup melt period, it will pose minimal resistance to the downstream progression of a breakup front and be less likely to form a significant ice jam or related flooding. No regular measurements of ice strength are made in hydrometric programs and even research studies of ice strength are relatively rare. There are, however, some basic relationships that have been established relating ice strength to changes produced by internal melt of the ice matrix. Again, calculation of such melt requires knowledge of heat fluxes to the ice cover, particulary radiation. As this is rarely available, the heat fluxes also must be modelled. Given the extensive level of modelling required to evaluate conditions for a remote location like the Peace River, it was decided that even if a coarse index of ice strength could be determined, it might be useful for interpreting the temporal trends that have occurred in breakup ice jamming. The following describes the theoretical background to ice strength determination; the methods employed to arrive at an index of pre-breakup strength; and the relationship of the index values to ice jam occurrence.

6.2.4.1 *Theoretical Relationships between Ice Strength and Solar Radiation*

Radiative heating (short- and long-wave) and the transfers of sensible and latent heat by convection and conduction are all important to the ripening (warming to 0°C) and ablation of a river-ice cover. Warming of an ice cover can also change its strength. Under rapid melt conditions or as a result of a sudden regulated release of flow, breakup could be initiated while a river-ice cover was still relatively cold. Under natural breakup conditions (natural *vis-à-vis* timing), however, such as experienced in the lower portions of the Peace River, the main ice temperature (excluding diurnal surface temperature fluctuations due to long-wave radiation effects) likely rises close to 0°C well before the actual breakup occurs. Hence, any inter-annual variations in strength would result from changes after the ice cover had warmed to 0°C. Such changes occur primarily from the absorption of solar radiation.

The amount of radiation received by an ice cover during the pre-breakup period depends on the available short-wave radiation, the degree of reflective insulation provided by surface snow and ice, and the duration of the pre-breakup period. During the early stages of melt, radiation input is consumed largely by surface melt and warming of the ice cover. Significant internal melt does not occur until the ice has reached 0°C, usually after the surface snow has ablated. For snow-free ice, the ice-cover radiation balance is described by:

[29] $S_a = S{\downarrow} (1 - \alpha_s) - S_x = S_o - S_x$

where S_a = short-wave radiation (W/m^2) absorbed within an ice thickness of x (m),

$S{\downarrow}$= total incoming short-wave radiation (in this case also $G{\downarrow}_{c_i}$ W/m^2), and

S_x = short-wave radiation (W/m^2) reaching depth x.

S_o = short-wave radiation after losses due to surface reflection (W/m^2).

The quantity of radiation reaching any depth x can be expressed as:

[30] $S_x = S_o\, e^{-\eta x}$

where η = a bulk extinction coefficient.

Attenuation, however, is also known to be spectrally selective and η is therefore dependent on depth. To account for this spectral variation η was fitted by Ashton (1985) with a power law dependence on depth using data from Grenfell and Maykut (1977) for first-year blue ice:

[31] $\eta = 0.68x^{-0.5}$

where x = depth (m)

η = the bulk extinction coefficient (m^{-1}).

Substituting equation [31] into [32] and reintegrating permits definition of the radiation at any depth:

[32] $S_x = S_o\, e^{-1.36x^{\wedge}0.5}$

Radiation absorption within an ice sheet occurs preferentially at grain boundaries because of a concentration of impurities deposited as part of the freeze-out process. If the rate of heat removal by internal conduction is less than the rate of internal warming from radiation attenuation, localised melt will occur forming melt pores. Once an ice cover reaches a 0°C isothermal condition, all radiative energy is used to produce internal melt. For an isothermal 0°C ice sheet, the melt fraction or porosity (Φ_i) produced by internal radiative melt is calculated by integration of:

[33] $d\Phi_i/dt = S_a/(\rho_i\lambda_i)$

where all terms have been previously defined.

Grain geometry controls the pore arrangement within the ice matrix and, hence, the reduction in grain contact area and, ultimately, the load bearing- and deformation-behaviour of the ice sheet while resisting downstream forces.

In general, most available data from theoretical (Ashton, 1985), laboratory (Bulatov, 1970; Shishokin, 1965) and field (lake-ice beam tests: Prowse *et al.*, 1990b; river-ice borehole jack tests: Prowse *et al.,* 1988; Prowse and Demuth, 1992) studies dealing with changes in strength due to radiation decay can be described in a general strength-porosity relationship of the form:

[34] $\theta/\theta_o = 1 - c\,\Phi^k$

where θ/θ_o = ratio of strength at any porosity development to original strength value at 0°C,

c and k = constants defining the strength reduction, the latter term determined by the geometry and distribution of voids with respect to the ice structure.

As shown by Prowse and Demuth (1992), most field-derived data closely track the theoretical relationships to a value of approximately $\Phi = 0.1$. In the case of sea ice, this is the point at which flexural strength is not significantly affected by porosity (brine volume; Weeks and Assur, 1972). Moreover, this has been suggested as the upper limit with respect to initiation of river ice breakup (Prowse *et al.*, 1988) based on direct field measurements of river-ice strength and atmospheric fluxes obtained during this period. Approximate values for c and k in equation [34] to describe this decay range are 2.8 and 0.5, respectively.

6.2.4.2 *Modelled Changes in Ice Strength at Breakup*

Insufficient data exist to calculate accurately the internal strength of the river-ice cover for the different years of breakup on the Peace River. It is possible, however, to use the above theoretical background with some generalized values for specific parameters to obtain a 1st-order approximation of relative differences in ice strength. This was accomplished by first calculating $S\downarrow$ as described earlier and verified with data from Fort Smith. The point of initial calculation was the same day as identified for the overall heat calculations, i.e., the day when rapid ablation first started as indicated by stream runoff response, snow-depth decreases, and air-temperature increases (see Table 6.5).

The $S\downarrow$ values were then input to equation [29] to calculate the total absorbed radiation. A value of α_s had to be assumed for the calculation of S_o since observations of surface snow/ice type are not part of the hydrometric data collection program. Field observations conducted as part of this study, however, suggest that the freeze-up conditions in the reach from Peace Point to the Slave River are likely to favour the formation of a surface stratum of white ice. This type of ice normally has a small grained polycrystalline structure and is comprised of either dynamic ice forms produced at freeze-up (i.e., of frazil origin) or snow-ice forms that develop from the slushing and freezing of surface snow. In some, usually localised cases, a river-ice cover might have a surface black ice stratum formed by highly tranquil freeze-up conditions (Prowse and Demuth, 1993) but this was considered unlikely in this reach which is fed by turbulent flow from the Boyer Rapids (just upstream of the hydrometric station at Peace Point). It should be further noted that the albedo of decaying black-ice surfaces is not too dissimilar from that of white ice. For example, although the albedo of clear, cold black ice can be as low as 0.1 (Bolsenga, 1969), acicular melt processes affecting the surface grains can quickly raise it. Prowse *et al.* (1990a), for example, reported from field experiments on black ice that this process produced a black ice albedo in the general range of 0.2 to 0.4. Similarly, Prowse and Marsh (1989) reported a range from 0.17 to as high as 0.52, with a value of 0.39 in a "candled" state. Hence, based on the above, a value of $\alpha_s = 0.4$ was considered suitable as a first-order estimate in calculating S_o. The value of x was set to an approximate average ice thickness of 0.95 m.

The resultant radiation values were then used to derive S_a, Φ_i, and finally θ/θ_o. Results from the first set of calculations indicated extremely rapid changes in ice strength. Without direct field data, it is impossible to know whether these results are real or due to some inaccuracies in the current theoretical assumptions, or related to the use of a bulk porosity/strength value for the entire cover. As the objective of this section was to compare inter-annual differences in an index of ice-cover strength at breakup, it was decided to employ a slightly different index approach, but one still based on the established exponential decay of strength with porosity. This second approach involved first calculating values of S_a for the middle 50% of the ice sheet using equation [32] and then a strength index from equations [33]and [34].

6.2.4.3 *Results*

The resultant daily changes in ice strength are plotted in Figure 6.24 for the years 1963 to 1979, and the final values at breakup compared in Figure 6.25. As evident in Figure 6.25, there is no significant trend in the ice strength data for the short period that permitted its calculation. Note that in one year, 1968, the strength ratio become slightly negative. Although this is indicative of further problems in calculating precise values for the heat fluxes and θ/θ_o, it does not hinder inter-annual comparisons of their relative magnitudes. A residual mass curve of the data is presented in Figure 6.26, but again no clear trend is apparent. Comparing the final strength ratios to those of breakup severity (Δh), reveals no clear association of high strength years with those of high Δh, as might have been intuitively expected. Any linear or logical exponential relationship applied to the data produces an r^2 of no more than approximately 0.04. Years of very high Δh are characterized by final strength ratios comparable to those for years of very low Δh. In general, there does not appear to be any significant relationship between Δh and θ/θ_o values at breakup. Notably, however, this does not mean that such strength values would not be suitable for predicting the timing of breakup; it simply means that the breakup severity is not significantly related to the strength of the ice cover at the time of breakup. Moreover, even this is not certain given the small number of years for which it was possible to calculate the relevant values.

6.3 Driving Forces to Breakup

6.3.1 Flow Contributions at Breakup

As noted in Section 4.3, breakup water levels are strongly related to spring discharge. In the case of ice jams, the magnitude of the jam is very much a function of the flow at the time of jam formation. In response to a commonly-held hypothesis that reduced flows have been responsible for reduced ice-jam activity, an analysis was completed of spring flows that have contributed to breakup events on the Peace River near the PAD.

As a first step, mean spring hydrographs were generated from the Water Survey of Canada records for three major long-term stations along the Peace River. These included stations near: Hudson Hope, the town of Peace River, and Peace Point. The analyzed period brackets the time of breakup at Peace Point, i.e., approximately mid-April (beginning of intense melt) to mid-May (conclusion of ice effects). The mean daily hydrographs +/- one standard deviation for the pre-dam and post-dam periods are shown in Figures 6.27 and 6.28. Note again that the pre-regulation records are relatively short compared to those post-regulation.

The effects of regulation are quite evident for the Hudson Hope station in which a previously slow-rising hydrograph has been replaced by an almost flat, and then slightly declining, flow. In general, lower flows prevailed prior to May 03 (Julian Day 123) before regulation, but these have now been raised with the increased flow that generally prevails throughout the winter period, as a result of regulation. On April 15 (Julian Day 105), for example, average flow prior to regulation was approximately 400 m^3/s, but this has increased, after regulation, by approximately three-fold to about 1200 m^3/s. This difference declines to zero at the point of crossover of the two mean hydrographs on about May 04 (Julian Day 124).

At the downstream end of the Peace River, at Peace Point, the increase in the early stage of the hydrograph is also readily apparent, with the mean pre- and post-regulation flows for April 15 (Julian Day 105) rising by a factor of over two times from approximately 800 m^3/s to 1800 m^3/s. Again this difference steadily declines until May, after which the pre-regulation values become greater. Notably, a majority of all breakups and the recordings of peak breakup water levels have occurred at the Peace Point site before May 05 (Julian Day 125) (see Table 6.5).

As Figures 6.27 to 6.28 only represent mean flows and the pre-regulation record for Peace Point is very short, it is prudent to evaluate flow conditions for specific years. Figure 6.29 and 6.30 show the hydrographs for the 3 major Peace River stations for the spring breakups of 1965 and 1974 - major events before and after regulation with good hydrometric records. More importantly, these are also two years known to be years of very large ice-jam flooding of the Peace-Athabasca Delta (see Section 4.3).

To evaluate the magnitude of flow, occurring at specific reaches along the Peace River or originating from a tributary, that contributed to the discharge causing breakup conditions at Peace Point, it was necessary to lag the upstream flows according to documented flow travel times. This exercise was undertaken only to identify the relative significance of flow sources contributing to breakup at Peace Point. It does not assume that breakup advanced down to the Peace River at the assumed flow travel times. Although breakup advance is usually characterized by highly transient flow conditions, these were not considered to be a source of significant error in the interpretation of relative flow contributions since the comparisons were to be made at a one-day time step.

Approximate one-day lag times were obtained along the Peace River by using output from the one-dimensional flow model developed as a companion study to the Hydrology Component of the Northern Rivers Basin Study (Hicks and McKay, 1995). Figure 6.31 shows the estimated time of travel (+/- 6-12 hours) for flows in the order of 5,000-6,000 m^3s^{-1} and 10,000 to 12,000 $m^3\ s^{-1}$. On a daily basis, there is approximately a 2-day lag in flow between Hudson Hope and Peace River Town and an additional 5-day lag to Peace Point. This compares favourably with the results of Fonstad (1992) based on data provided by the Alberta River Forecast Centre for the reach from Hudson Hope to Peace River Town.

Employing the above 2 day and 5 day lags, the corresponding days of Peace Point breakup have been annotated on the hydrographs shown in Figure 6.29 and 6.30. Two points are annotated: a) the day associated with the initial breakup of the ice cover as determined from inspection of the original hydrometric charts and observers' notes (h_b), and b) the day of peak water level during breakup (h_m), (i.e., the values summarized in Section 4.2. In the following discussion of upstream flow conditions (main stem or tributary), the flows on the days of h_b and h_m (occurring at Peace Point) are the average 3-day lagged flow bracketing the respective breakup date. This was done to minimize the effects of any potential errors in flow travel times and, for some years of poor quality records, precise dates of breakup.

In both example years (1965 and 1974) of major breakups, the Peace River at Peace River Town experiences major spring-flow events whereas the hydrograph at Hudson Hope remains relatively flat. A slight rise in flow does occur several days later in 1965 but this is insignificant relative to the large flow driving breakup or as recorded at Peace River Town.

To assess the origin of the spring flows that appeared to be driving breakup in these two sample years, the spring hydrographs for the major gauged catchments entering the Peace River between Hudson Hope and Peace Point were also analyzed. Their river drainage area, percentage of the total Peace River catchment area above Peace Point, and approximate flow travel time to Peace Point are listed in Table 6.7. Figures 6.32 to 6.33 depict their long-term pre- and post-regulation hydrographs and, earlier figures 6.34 to 6.35, their 1965 and 1974 hydrographs. Clearly in both these years, many of the tributaries were experiencing abnormally-high (relative to long-term mean values) spring runoff that would significantly contribute to the Peace Point breakup. This is particularly the case for the Smoky River in both years and for the Wabasca River at least in 1974. Unfortunately, no pre-regulation record is available for this other major tributary.

Smoky River, which enters just upstream of the gauge at Peace River Town (Figure 2.1), drains almost one quarter (23%) of the total Peace River catchment between Hudson Hope and Peace Point, an area equivalent to 72% of that above the point of regulation (above Hudson Hope). Significantly, it was found to have contributed (all percentages based on lagged and averaged flows) 18% (1965) and 13% (1974) of the total Peace River flow at this site on the day of breakup initiation at Peace Point and appreciably more, (67%, 1965; 39%;

1974), on the day of maximum breakup water levels. By contrast, the flow contributions from above Hudson Hope were relatively small. In 1965, the flow on the day of maximum breakup water levels was only 13% of that produced by the Smoky River, although the Hudson Hope hydrograph was just beginning to show a slight rise. The higher winter flows from regulation in 1974 result in flow at Hudson Hope being considerably higher, but even then it is only approximately 50% of that contributed by the Smoky River or approximately 70% of the Wabasca River flow. Notably, however, Hudson Hope comprised almost 50% of the flow in 1974 at the time of breakup initiation.

Together the Wabasca and Smoky River comprise 38% of the catchment area between Hudson Hope and Peace Point. Virtually all of the Wabasca River lies below approximately 600 m and a significant portion of the Smoky below 900 m. In general, their response can be considered representative of the smaller downstream tributaries that drain the foothill and plains regions. For example, the Notikewin River, a smaller plains tributary was also experiencing a similar large spring freshet in 1965 and 1974. A less clear situation exists for tributaries farther upstream, such as the Beaton, Halfway and Pine Rivers, which drain generally higher elevation zones (Table 6.7 and Figure 2.1). Although they generally exhibit some degree of rise in spring flow, their contributions at the time of Peace Point breakup are relatively small compared to the downstream tributaries. Their major flow contributions for these sample years are supplied to the Peace River after the major breakup period.

Extending the above hydrograph analysis to all breakup years, the flow at each of the mainstem nodes and tributaries was analyzed for the two breakup dates (h_b and h_m at Peace Point). Figures 6.36 to 6.39 depict their flows and relative contributions at the time of h_b and Figures 6.40 to 6.43 at the time of h_m for the years 1962 to 1992. While these figures do not permit an assessment of the overall nature of the spring hydrograph (e.g., rate of rise or decline in their respective hydrographs) for each reach or tributary, as provided in the above detailed descriptions for 1965 and 1974, they do indicate the relative contributions of the various flow sources at two critical times (i.e., h_b and h_m).

Between the two periods, 1962-67 and 1972-1992 there has been no significant change in the flow that caused peak breakup water levels at Peace Point (averaging 4128 m^3/s and 3771 m^3/s, respectively) although the average flow that has initiated breakup have increased (averaging 3050 m^3/s and 3418 m^3/s, respectively). The latter is largely a product of the higher flows that are sustained throughout the winter period. There has also been a significant change in the average contribution provided by headwater and downstream flows. From 1962-1967, the average flow recorded at Hudson Hope (7 days prior) was only 19% (range of 12 to 29%) of that which caused breakup at Peace Point whereas the flow from the Smoky River, only one downstream tributary, contributed more flow at an average 24% (range 9 to 43%). In terms of the peak breakup water levels, the upstream flow was again smaller at only 17% (range 9 to 29%), but the Smoky River contributed almost twice as much averaging 28% (range 8 to 67%). In general, the Smoky River alone was on average slightly more important than the upstream flow in initiating breakup and significantly more important in producing the peak breakup water levels. As shown in Figure 6.39 and 6.43, the greater importance of this one tributary over the upstream flow holds true for the large breakup years of 1963, 1965 (previously discussed in detail) and 1967. The larger importance of flow contributed from the downstream portion of the basin (below the point of regulation) compared to the upstream becomes more apparent if all the downstream tributary flow is combined: see Figures 6.32 and 6.33, although the Smoky River still dominates. Note that the Wabasca River is not available for this pre-regulation period.

Since 1972, the percentage of the flow upstream of Hudson Hope has on average become relatively more important to Peace Point breakup conditions. The average percentage flow from this site contributing to h_b increased from 19 to 36% (range of 15 to 63%), and to h_m increased from 17 to 33% (range 8 to 63%). As the hydrographs of Figure 4.1 suggest, this reflects the change to sustained higher flows throughout the winter period. Notably, the contribution during the breakup of 1974 was high at breakup initiation (49%) but declined to only 18% at the time of h_m. This dramatic change in percentage contribution was due simply to a rapid increase in the contributing flow from the downstream tributaries. The flow at Hudson Hope, in fact, remained relatively constant rising from 1070 to 1180 m^3/s (3-day average lagged flow values) between the nine days separating h_b and h_m.

Mean flow of the Smoky River between the two periods has declined and its average contribution to h_b decreased from 24 to 14 % (range 6 to 33%), and to h_m decreased from 28 to 15% (range of 5 to 39%; the latter value from the 1974 event). In summary, the average relative contribution of the flow at Hudson Hope has increased while the average contribution from the downstream tributaries (as indexed by the Smoky River) has decreased. Some of the extreme events in both the pre- and post-regulation periods (e.g., 1965 and 1974), however, appear to be associated with abnormally high spring flows in the tributaries, especially the Smoky River.

In assessing the flow contributions at breakup, attempts were made to determine the rate of discharge increase because this factor is also known to influence breakup severity. Unfortunately, it was found that the flow records during the breakup period lacked the suitable accuracy and time resolution to determine such rates. Modelling of breakup flows was not possible either, since no reliable models exist that would permit downstream routing of upstream and tributary flow during the highly transient flow period that characterizes breakup. It is recognized, however, that the most rapid rates of change would be associated with years of large and rapid runoff from the downstream tributary basins such as the Smoky and Wabasca, as occurred in 1965 and 1974. The flow records suggest that such rapid events have not been as frequent in more recent years. The reasons for this are explored in the next section.

6.3.2 Snowmelt as the source of Spring Flow

The relatively small flow contribution of the Peace River upstream of Hudson's Hope during the pre-regulation period is consistent with the hypsometry of the Peace River basin: the headwaters being largely within high-elevation alpine regions of the Rocky Mountains. Spring runoff from the higher-elation zones does not usually occur until June, well after breakup has occurred in the lower-elevation downstream portions of the Peace River. The significant rise in downstream flows on the Peace River, and particularly as they affect breakup in the Peace-Athabasca Delta, are more dependent on flow contributions from the lowland areas such as those drained by the Smoky and Wabasca Rivers. There appears, however, to have been significant inter-annual variability in the magnitude of these flows, possibly related to the magnitude and rate of spring snowmelt.

To explore this aspect further, the snowpack records for the lower portions of the Peace River were collected and summarized. Unfortunately, very few stations record snow survey information with sufficient detail for such an analysis, and most records do not begin until approximately 1963. For the period of interest, the stations include: Fort St. John (ten-point snow course conducted monthly by the British Columbia, Ministry of the Environment; airport station at 690 m amsl), Fort Vermilion (ten-point snow course conducted by Agriculture Canada at their station, 280 m amsl), Grande Prairie (668 m amsl), and Peace River (570 m amsl; the latter two both being 5-point snow courses conducted by the Atmospheric Environment Service, Environment Canada at airport locations). The most complete record is available for Grande Prairie which stretches from 1947 to the present. The high quality of this station within the Smoky River catchment is valuable because of the demonstrated significance of the Smoky River spring runoff to spring breakup of the Peace River breakup. The water-equivalent data for the maximum spring snowpacks for all four stations are shown in Figure 6.44. All the major breakup events occurred with the peak snowpack (water equivalent) at Grand Prairie exceeding approximately 110 mm; the 1974 event also being the year of the long-term maximum-peak snow water equivalent. Notably, other years of less severe breakup (h_m) also occurred with large spring snowpacks (e.g., 1966, 1971, and 1982). It should be remembered, however, that such snowpacks are only an indication that there is potential for large spring snowmelt. Numerous other factors, such as rate of melt and antecedent moisture conditions, control whether the large spring snowpack will be transferred into a major runoff event. As earlier noted in Section 6.3.1, a year like 1974 was characterized by a pronounced above-normal spring runoff response in the Smoky River catchment, one most probably linked with intense melt of the above normal snowpack. By contrast, it was revealed that the 1982 event was characterized by only a gradual rise in spring discharge resulting from a protracted melt of the above-normal snowpack. Although beyond the scope of this report, it is recommended that a simple snowmelt model be applied to the major tributaries, especially the Smoky River. This would better facilitate analysis of the nature of past events and would also permit forecasting of the potential of future large events. Such information would be valuable to the proper design of downstream remedial measures, such as the artificial ice-dams being employed by the Peace-Athabasca Delta Technical Studies to enhance flooding of the Peace-Athabasca Delta (e.g., Prowse *et al.*, 1995; Prowse and Demuth, 1996).

The downstream station at Fort Vermilion might be a good surrogate for the Wabasca River, but no data exist prior to 1968. The two breakup years of 1972 and 1974 show up as peak values for the 1970's, although some equally high events also occurred in the 1980's.

Given the apparent importance of the Grande Prairie station to runoff of the Smoky River, a longer-term winter-precipitation record was also assembled and analyzed for this site. Figure 6.45 shows the winter accumulated precipitation, from November 1 to March 31, for each year from 1947 to 1992. Also shown is a 7-year running mean through this data set. The plotted data suggest there may have been a general shift to below normal snowpacks beginning in the mid-1970's; only the 1982 event is significantly above the long-term normal.

To explore further the potential existence of a trend in the snowpack records for Grande Prairie, the data were converted to residual mass curves (as outlined earlier in this report). The cumulative percentage departure from the mean are shown in Figure 6.46 for the accumulated winter precipitation (1947-1992) and the spring maximum snow-survey values (1963-1992). In both cases, there appears to be a downward trend in the data beginning after 1974. This apparent mid-1970 shift in peak snowpack values has also been observed in adjacent British Columbia. Moore and McKendry (1996) note that from 1966 to 1976 snowpack conditions were dominated by two regimes: one of heavy snowpacks over most of British Columbia to one where heavier snowpacks developed in the south than in the north. This situation reversed after 1976 (1977-1992) to two patterns where snowpacks were generally light over the whole province or were heavier in the north than in the south. Changes in the frequencies of snow-producing weather types appear to be consistent with documented shifts in sea surface temperatures and atmospheric circulation patterns over the North Pacific (e.g., Trenberth, 1990). Although the strength of the North Pacific circulation patterns diminishes inland and their shapes become increasingly distorted by the mountainous relief, the apparent step-like shift in the snowpack records for Grand Prairie strongly suggests some degree of tele-connection with the intensity of the Pacific North American (PNA) circulation pattern. The relationships are less clear for the other Alberta stations. It is expected that distinct spatial patterns in spring snowpack records may exist for the lower portions of the Peace River just as found by Moore and McKendry (1996) for British

Columbia. There is already some suggestion that there is a north-south separation in the patterns (Both, 1995, pers. comm.).

Given the importance of spring runoff from the downstream tributaries of the Peace River to downstream flood events, and the apparent climatic signal in the snowpack record, the National Hydrology Research Institute has now undertaken a project to examine temporal anomalies in spring snowpack records. These are being related to atmospheric circulation and synoptic climatic variations through a frequency analysis of winter weather types. Some preliminary results of this study should be available before completion of the Northern Rivers Basin Study.

6.4 Freeze-up Effects

It is generally believed that there is a relationship between freeze-up stage, h_f, on a river and the stage at breakup initiation, h_b (e.g., Beltaos *et al.,* 1990). Essentially, breakup normally is not initiated until h_f has been exceeded. As shown in Figure 6.47, there is a generally good relationship between h_f and h_b for the Peace Point hydrometric station. (Data were extracted from copies of the original hydrometric charts following the methods outlined in Beltaos *et al.* (1990). As in the previous analysis, Water Survey of Canada personnel assisted in the extraction and rechecking of the data to minimize errors. Note: Andres (1995) also extracted a more limited data base of h_f in an evaluation of freeze-up processes; average values proved to be comparable-see below).

The data in Figure 6.47 are categorized temporally according to the phase of regulation. The post-regulation data tend to be skewed to the higher freeze-up levels. All h_f values are plotted in an annual time series in Figure 6.48. Although data could not be extracted for some years, and despite the very short record prior to regulation, there has been a significant increase (1.2 m) in levels from before, to after regulation (i.e., from approximately 212.5 to 213.7 m amsl). Based on a smaller data set, but following a similar data extraction method, Andres (1995) found that this site has experienced a comparable 1.4 m (212.7 to 214.0 m amsl) increase in h_f as a result of regulation. Such increases can be the result of two factors: increased autumn flows and greater staging potential [for a review of freeze-up formation by hydraulic control see, e.g., Ashton (1986); Gray and Prowse (1993);

Beltaos (1995)]. As modelled by Andres (1995), however, the relatively low slope reaches of the lower Peace River do not favour freeze-up formation by consolidation processes (thicker covers that promote increased freeze-up staging) even under highly elevated discharge values. Instead, the freeze-up cover tends to form by the simple juxtaposition of ice floes (thinner initial ice cover with less freeze-up staging). Hence, the increases in h_f at Peace Point (and in the lower portions of the Peace River, in general) are primarily the result of increased flows.

Figures 4.1 and 4.2 illustrate the mean monthly flows and their relative increase along the Peace River over the winter months for three stations: Taylor, Town of Peace River, and Peace Point. Elevated winter discharge at the time of freeze-up is quite evident for Peace Point where the ratio of average November flow (main month of freeze-over at Peace Point) for post to pre-regulation conditions is 1.4. (This ratio subsequently increases to an average of 3.3 for the main winter months, December to March).

Higher freeze-up levels may be related not only to the breakup initiation level (as shown in Figure 6.47) but also to overall breakup severity. Although an attempt was made to relate values of h_f to a simple index of breakup severity, such as the maximum breakup water level ($h_{b'}$), there was no obvious correlation [$r^2 = 0.16$]. This is not unreasonable given the large number of other variables controlling $h_{b'}$, such as ice jamming and relative location to the hydrometric station, ice strength and thickness, melt conditions, etc. An improvement in r^2 might occur, for example, if a distinction was made between thermal and mechanical events; an objective beyond the scope of this initial project but one worth further scientific study. Despite the apparent difficulty in quantifying a relationship between freeze-up levels and breakup severity, there are some strong arguments that can be made as to why one should exist. The basis for these arguments stems from two sources: a) resiliency of elevated ice covers to "breakup" discharge, and b) the decreasing effect of tributary inflow with increasing main-stem discharge.

Firstly, considerable knowledge about the resiliency of ice covers to pre-mature breakup has been gained through operating schemes employed by hydro-electric facilities during the freeze-up period. Operation schemes employed by Canadian hydro-electric plants to establish such a cover are reviewed by Wigle *et al.* (1990). Schemes vary from decreasing flow velocities to temporarily increasing flows, such as practised in the upstream portions of the Peace River to avoid flooding of the Town of Peace River (British Columbia-Alberta Task Force, 1992). Once established, the plants can increase their flow significantly because the river can accept much higher flows without causing the cover to break. In the case of the International Section of the St. Lawrence River, for example, flows can be increased by up to 30% (Wigle *et al.*, 1990, p. 16 and 69).

Summarizing the above into the simplest terms, the higher a freeze-up cover is stabilized, the greater the flows it can withstand without breaking. If this general rule-of-thumb has been demonstrated by numerous hydro-operating schemes to apply to the freeze-up and winter period, it logically applies also to the spring breakup period. Thus, elevating an ice cover during the winter period through regulation of flow, means that the river will be able to pass greater discharge in the spring without rupturing the ice cover, all other factors remaining constant.

The ability to pass greater discharge could also mean that the river is somewhat more resistant to breakup jamming. This is because the higher velocities associated with the greater discharge may be able to move more fragmented ice under the elevated ice sheet at the breakup front, thereby reducing the chances of jamming. A similar theory was offered by Andres (1975; 1978) in reviews of the major factors affecting breakup water levels at the Town of Peace River. Such an effect is likely to be less pronounced in the lower slope reaches of the downstream reaches of the Peace River where it has already been noted for the freeze-up period that velocities are generally insufficient to underturn ice floes (i.e., in the creation of a "consolidated" ice cover). Elevated ice levels do not mean, however, that the river will be immune to large spring breakups. If the spring flow significantly exceeds that associated with the elevated freeze-up stage, a severe breakup could still be produced. It can be argued, however, that the probability of such events is lowered because of b) the decreasing effect of tributary inflow with increasing main-stem discharge.

As shown in the specific analysis of ice jam events, it is tributary inflow that is the traditional driving force behind the flows that control peak breakup water levels. At the outset of breakup, the main-stem discharge must exceed h_f by some factor (e.g., 30%) to initiate a dynamic breakup. Otherwise, the cover will simply continue to deteriorate *in situ* until it is so thermally weakened that a low magnitude flow is able to move it downstream, a situation more akin to a thermal breakup and much less likely to produce a significant ice-jam flood (see earlier discussion of the hydro-climatic definitions of breakup types). Furthermore, extensive melt would also reduce the ice volume available for ice-jam formation, possibly even to the point where an *equilibrium* jam (see e.g., Beltaos, 1995) and associated maximum backwater flooding could not develop.

The amount that the spring flows exceed a freeze-up level depends on two contributing sources: the upstream flow from above the point of regulation plus the downstream tributary flow. Under regulated conditions, a major increase in upstream (above the point of regulation) is unlikely at the time of breakup near the Peace River Delta because of the operational strategy of the W.A.C. Bennett dam. Although the earlier analysis of breakup events has shown that more flow is received from the headwater areas after regulation than before, on an intra-annual scale, the amount of regulated flow contributed to the system tends to be on a decline during the breakup period. The months of April and May are the transition period for regulated flow from elevated levels during the winter to decreased levels during the summer. This is evident in the seasonal hydrograph of Figure 4.1 where the ratio of post to pre-regulation flows decreases from 2.0 in April to less than 1.0 (0.8) in May.

Thus, to exceed the winter regulated flow (or h_f) significant contributions must come from tributaries downstream of the point of regulation. Furthermore, if the amount of regulated flow at the time of breakup is declining from higher winter values, tributary flow must also account for this "loss" to the main-stem discharge.

It is clear from the analysis of flow contributions at breakup that examples exist, before and after regulation, where large tributary flow has been highly effective in dislodging the cover and producing large breakup flooding. It is less clear, however, whether there has been a decrease in the effectiveness or potency of middle-to-lower tributary flow events in other years. Prior to regulation, a middle-order spring runoff event from the Smoky or Wabasca Rivers of say 500 m^3/s might have acted as a significant trigger to the lower Peace River flowing at 1000 m^3/s in late April. However, with an elevation of the pre-breakup levels and flows to say 1500 m^3/s, the tributary flow must be much less effective. The overall effect is that one would expect more thermal-type events to occur after regulation simply because the potency of the tributary effect has been reduced. Again, this does not mean a total elimination of large, dynamic breakups but simply a reduction in the probability of their formation. Evidence that the Peace River catchment is still capable of creating large floods near Peace Point is provided by the two post-regulation events of 1972 and 1974.

Hence, in summary, freeze-up water levels probably play a role in controlling the dynamics of breakup because of a) the increased resiliency of elevated ice covers to "breakup" discharge, and the decreased potency of tributary inflow relative to the higher freeze-up and winter discharge produced by regulation: the latter factor becoming even more important if regulated flows are decreased during the breakup period.

7.0 SUMMARY DISCUSSION AND RECOMMENDATIONS

Hydrometric analysis in conjunction with various historical and local-knowledge data confirms that open-water floods have been ineffective in producing high-elevation floods along the Peace River adjacent to the Peace-Athabasca Delta. Even the historically high flow event of 1990 did not produce a flood of sufficient magnitude to flood high-elevation portions of the delta. Over the period of hydrometric record, backwater produced during river-ice breakup has exceeded that of the 1990 open-water event. Based on data from the Peace Point hydrometric station, such events occurred on a biennial basis in the 1960's prior to regulation but only three times since. It is breakup backwater, therefore, that historically inundated the hydraulically-isolated perched basins, especially those nearest the Peace River that have not experienced a major flood since 1974.

In the lower portions of the Peace River, flow regulation seems to have produced minor changes in factors, such as ice thickness and strength, that could significantly affect the severity of breakup and related ice-jam flooding. Temporal analysis of these factors, however, also detected a weak climate signal suggesting that since approximately the mid-1970's the period of ice cover may have become slightly warmer and the pre-breakup melt period may have become more intense and/or more protracted. Although this needs to be explored more thoroughly, if it proves to be the case, such factors could also favour the development of thermal over dynamic breakups, and hence reduce the probability of severe ice-induced flooding.

A common perception was that reduced flows due to regulation were responsible for the decline in severe ice jams. Results show, however, that flow contributed from above the dam is higher on average at the time of breakup near the Peace-Athabasca Delta in the post-regulation period than it was prior to regulation. The major ice-jam floods that occurred in the 1960's prior to regulation and in the early 1970's after regulation have been associated with large runoff events from downstream tributaries, especially the Smoky River. The flow contributed by tributaries at the time of breakup far exceeds that contributed by headwaters above the point of regulation. These large tributary flow events also appear to be correlated with large spring snowpacks and associated snowmelt runoff. A preliminary evaluation of temporal trends in the size of the snowpack on the Smoky River suggests that there has been a shift in the mid-1970's to values lower than the long-term average. A similar trend has been identified in British Columbia and appears to be responsible for decreased spring runoff on some rivers.

The major effect of regulation on the occurrence of breakup ice jamming near the Peace-Athabasca Delta is related to the higher winter flows and freeze-up elevations. In general, the higher a freeze-up cover is stabilized, the greater the flows it can pass without breaking. The amount the spring flows exceed a freeze-up level depends on two contributing sources: the upstream flow from above the point of regulation and the downstream tributary flow. Under regulated conditions, a major increase in upstream flows (above the point of regulation) is unlikely at the time of breakup near the Peace River Delta under the standard operational strategy of the W.A.C. Bennett dam: i.e., at the time of transition to lower summer releases. Furthermore, if the amount of regulated flow at the time of breakup is also declining, additions from tributary flow will also have to account for this "loss" to the main-stem discharge. Thus under the current regulated regime, production of severe breakups has become more dependent on tributary inflow, particularly from the Smoky River. Large spring runoff from the tributaries have been effective since regulation in producing large breakup floods (e.g., 1972 and 1974) but the apparent decline in spring snowpacks has reduced their subsequent effectiveness.

RECOMMENDATION [1]: Given the importance of spring runoff from the downstream tributaries of the Peace River to ice-jam flooding, and the apparent climatic signal in the snowpack record, it is recommended that a future project be undertaken to examine temporal anomalies in spring snowpack records. These should be related to atmospheric circulation and synoptic climatic variations through a frequency analysis of winter weather types. A regional analysis that encompasses all major tributary catchments is required.

RECOMMENDATION [2]: A climatic analysis should be conducted to examine more closely the temporal trends in atmospheric conditions that control a) the growth of winter ice and b) the pre-breakup thinning and mechanical weakening of the ice cover. The latter period should specifically include an analysis of changes in the major atmospheric heat fluxes including solar radiation.

RECOMMENDATION [3]: It is further recommended that a snowmelt model of the major tributaries be used to predict flow that could contribute to downstream ice jamming near the Peace-Athabasca Delta. This would better facilitate detailed analysis of the nature of past events and would permit forecasting of the potential of future large events. This information would be valuable to the proper design of downstream remedial measures, such as the artificial ice-dams being employed by the PADTS to enhance flooding of the Peace-Athabasca Delta.

RECOMMENDATION [4]: The one-dimensional flow model of the Peace-Athabasca Delta should be integrated with ice-jam models currently being developed for the reach of the Peace River that controls spring flooding of the Peace-Athabasca Delta.

RECOMMENDATION [5]: Although breakup modelling and forecasting is still in a state of infancy, it is recommended that some consideration be given to modifying the current regulated regime to increase the chances of creating a breakup jam near the Peace-Athabasca Delta. Relying solely on the reservoir to produce a major breakup near the Peace-Athabasca Delta would require an enormous release of water from the Williston reservoir. Notably, this could also lead to unpredictable ice-related backwater flooding at other upstream and downstream locations. Some success might be achieved, however, if minor adjustments are made to the regulation strategy in years where tributary inflow is forecast to be large. In some years, the only modification might be a delay in the retarding of spring flows. Current ice jam modelling by the PADTS should provide an idea of the size of combined flow needed to initiate flooding of the Peace-Athabasca Delta. Furthermore, PADTS water-balance modelling will provide guidance on how frequently such intervention might be required.

RECOMMENDATION [6]: To facilitate the implementation of some of the above recommendations (i.e., model calibration, prediction and validation), a regular field observation and data collection program on ice breakup and ice jamming should be established on the lower Peace River near the Peace Athabasca Delta.

8.0 REFERENCES

Adams, W.P. and Prowse, T.D, 1986; with M.A. Bilello, E. Eliassen, S. Freysteinsson, O. Laasanen, T. Pangburn, B. Raab, E. Tesaker and A. Tvede. Techniques for measurement of snow and ice on freshwater in Nordic countries. In - Proceedings of the Sixth Northern Research Basins Symposium, Houghton, Michigan, pp. 133-182.

Aitken, B. and R. Sapach, 1993. Natural and modified flow modelling of the Peace-Athabasca Delta. Report prepared for the Northern River Basins Study by the Water Planning and Management Branch, Environment Canada, Regina, Saskatchewan, 44 pp.

Andres, D.D, 1975. Ice break-up observations and mitigation at the Town of Peace River, April, 1975. Technical Services Division, Environmental Engineering Support Services, Alberta Department of the Environment, October 1975.

Andres, D.D, 1978. Effects of the Dunvegan Dam on the ice regime of the Peace River at the Town of Peace River. Technical Services Division, Environmental Engineering Support Services, Alberta Department of the Environment, July 1978, 34 pp. + figs.

Andres, D.D., 1995. The freeze-up regime of the Peace River, Taylor to the Slave River. Draft report prepared for the Northern River Basins Study and Alberta Research Council by Trillium Engineering and Hydrographics Inc.

Ashton, G.D., 1985. Deterioration of floating ice covers. Journal of Energy Resources Technology, 107, 177-182.

Ashton, G.D. (Editor), 1986. River and lake ice engineering. Water Resources Publications, Littleton, Colorado, 485 pp.

Atmospheric Environment Service, 1993. Canadian climate normals 1961-90. Environment Canada, Atmospheric Environment Service, Minister of Supply and Services Canada.

Bayrock, L. and J.D. Root, 1973. Geology of the Peace-Athabasca Delta. In - The Peace-Athabasca Delta Project, Technical Appendices Volume 1: Hydrology Investigations.

Beltaos, S., 1983. River ice jams: Theory, case studies and applications. American Society of Civil Engineering, Journal of Hydraulic Engineering, 109(10), 1338-1359.

Beltaos, S., 1985. Initial fracture patterns of river ice cover. National Water Research Institute contribution # 85-139, Burlington, Ontario..

Beltaos, S., 1995. Monograph on river ice jams. Water Resources Publications, Littleton, Colorado, 390 pp.

Beltaos, S., R. Gerard, S. Petryk and T.D. Prowse, 1990. Working group on river ice jams: Field studies and research needs. NHRI Science Report No.2, National Hydrology Research Institute, Environment Canada, Saskatoon, Saskatchewan, 121 pp.

Bilello, M.A., 1980. Maximum thickness and subsequent decay of lake, river and fast sea ice in Canada and Alaska. U.S. Army Corp of Engineers, Cold Regions Research and Engineering Laboratory, CRREL Report 80-6.

Bolsenga, S.J., 1969. Total albedo of Great Lakes ice. Water Resources Research 5(5), 1132-1133.

British Columbia-Alberta Task Force, 1992. Operating procedures for influencing freezeup and break-up of the Peace River at the Town of Peace River, Dunvegan and Taylor. Unpublished draft report.

Brutsaert, W., 1982. Evaporation into the Atmosphere. D. Reidel, London, 299 pp.

Buishand, T.A., 1982. Some methods for testing the homogeneity of rainfall records. Journal of Hydrology, 58, 11-27.

Bulatov, S.N., 1970. Calculating the strength of thawing ice cover and the beginning of wind-activated drift. Trudy Vypysk 74, Gidrometeorologisheskoye Izdatel'stvo, Leningrad. Translation by U.S. Army Corps of Engineers, CRREL, IR 799, 120 pp.

Calkins, D.J., 1979. Accelerated ice growth in rivers. U.S. Army Corps of Engineers, Cold Regions Research and Engineering Laboratory, CRREL Report 79-14, 4 pp.

Church, M., 1995. Environmental change and rivers in Cordilleran Canada. Unpublished manuscript.

Craig, B.G., 1965. Glacial lake McConnell, and the surficial geology of parts of the Slave River and Redstone River map areas, District of Mackenzie. Geological Survey of Canada, Bulletin 122, pp. 12-33.

Davies, J.A. and D.C. McKay, 1982. Estimating solar irradiance and components. Solar Energy, 29(1), 55-64.

Davies, J.A. and D.C. McKay, 1989. Evaluation of selected models for estimating solar radiation on horizontal surfaces. Solar Energy, 43(3), 153-168.

Davies, J.A., M. Abdel-Wahab and D.C. McKay, 1984. Estimating solar irradiation on horizontal surfaces. Interantional Journal of Solar Energy, 2:405-424.

Dingman, S.L. and A. Assur, 1969. The effects of thermal pollution on river ice conditions, part.II: A simplified method of calculation. U.S. Army Corps of Engineers, Cold Regions Research and Engineering Laboratory, CRREL Research Report No. 206, Part II, 10pp.

Fisheries and Environment Canada, 1978. Hydrological atlas of Canada. Minister of Supply and Services Canada, 34 plates.

Fonstad, G.D., 1992. Final report, Peace River ice jam flooding, February 28, 1992. Alberta Environment, River Engineering Branch, June 1992, 18 pp. + figs.

Gray, D.M. and T.D. Prowse, 1993. Snow and floating ice, Chapter 7. In - Handbook of Hydrology, D. Maidment, (Editor), McGraw-Hill, New York, pp. 7.1 - 7.58.

Grenfell, T.C. and G.A. Maykut, 1977. The optical properties of ice and snow in the Arctic Basin. Journal of Glaciology, 18(80), 445-463.

Hicks, F.E. and K. McKay, 1995. Peace/Slave River flow modelling. Water Resources Engineering Report 95-H3, Northern River Basins Project 1154-D1, December 1995, 18 pp. + figures + appendices.

Hirst, S.M., M. Miles, S.P. Blachut, L.A. Goulet and R.E. Taylor, 1987. Quantitative synthesis of the Mackenzie Delta ecosystems. Appendix C: Analysis of historical variations in discharge regimes in the Mackenzie Basin. Inland Waters Directorate, Environment Canada, Contract Report No. 62SS, December 1987.

Jackson, G.M., 1963. Unpublished correspondence between G.M. Jackson and R.H. Kendall, Superintendent of Forestry, Fort Smith, N.W.T., entitled "Inspection Peace River flood area". May 8, 1963, Fort Smith, N.W.T., 2 pp.

Jaques, D.R., 1989. Topographic mapping and drying trends in the Peace-Athabasca Delta, Alberta, using LANDSAT MSS imagery. Prepared by Ecosat Geobotanical Surveys Inc. for Parks Canada, Wood Buffalo National Park, 52 pp.

Jaques, D.R., 1990. Vegetation habitat types of the Peace-Athabasca Delta: 1976-1989. Prepared by Ecosat Geobotanical Surveys Inc. for Parks Canada, Wood Buffalo National Park, 46 pp.

Kellerhals, R., C.R. Neill and D.I. Bray, 1972. Hydraulic and geomorphic characteristics of rivers in Alberta. Research Council of Alberta, River Engineering and Surface Hydrology, Report 72-1, 52 pp.

Marks, D., 1979. An atmospheric radiation model for general alpine application. In - Proceedings of the Conference on Modelling of Snow Cover Runoff, S.C. Colbeck and M. Ray (Editors), Hanover, New Hampshire, 1978, pp. 167-178.

Marsh, P. and T.D. Prowse, 1987. Water temperature and heat flux to the base of river ice covers. Cold Regions Science and Technology, 14, 33-50.

Michel, B., 1971. Winter regime of rivers and lakes. U.S. Army Corps of Engineers, Cold Regions Research and Engineering Laboratory, Monograph III-B1a, 139 pp.

Monteith, J.L., 1962. Attenuation of solar radiation: A climatological study. Quarterly Journal of the Royal Meteorological Society, 88, 508-521.

Moore, R.D., 1983. On the use of bulk aerodynamic formulae over melting snow. Nordic Hydrology, 14(4), 193-206.

Moore, R.D. and I.G. McKendry, 1996. Spring snowpack anomaly patterns and winter climatic variability, British Columbia, Canada. Water Resources Research (in press).

Muzik, I., 1985. Recent hydrological changes of the Peace-Athabasca Delta. Zeitschrift fur Gletscherkunde und Glazialgeologie, 21, 175-182.

Nielsen, G., 1972. Groundwater investigation, Peace-Athabasca Delta, section J. In - Peace-Athabasca Delta Project, Technical Report and Appendices: Volume 1, Hydrological Investigations, 1973, 36 pp.

Peace-Athabasca Delta Project Group, 1973. Peace-Athabasca Delta project, technical report and appendices: volume 1, hydrological investigations; volume 2, ecological investigations.

Peterson, M., 1992. Flood history study, Peace-Athabasca Delta, Wood Buffalo National Park. Data Report 92-14/WB, 24 pp.

Peterson, M., 1994. Flood history study. Task F.1 Peace-Athabasca Delta ecosystem management plan technical study. Wood Buffalo National Park, Fort Chipewyan, Alberta, 15 pp. + appendix.

Price, A.G and T. Dunne, 1976. Energy balance computations of snowmelt in a subarctic area. Water Resources Research, 12, 686-694.

Prowse, T.D., 1986. Ice jam characteristics, Liard-Mackenzie River confluence. Canadian Journal of Civil Engineering, 13(6), 653-665.

Prowse, T.D. and M.N. Demuth, 1992. Application of the borehole jack indentor in river ice break-up research. In - Proceedings of the International Association for Hydraulic Research, Ice Symposium, Banff, Alberta, 15-19 June 1992, pp. 787-801.

Prowse, T.D. and M.N. Demuth, 1993. Strength variability of major river-ice types. Nordic Hydrology, 24(3), 169-182.

Prowse, T.D. and M.N. Demuth, 1996. Using ice to flood the Peace-Athabasca Delta, Canada. Regulated Rivers: Research and Management (in press).

Prowse, T.D. and P. Marsh, 1989. Thermal budget of river ice covers during break-up. Canadian Journal of Civil Engineering, 16(1), 62-71.

Prowse, T.D., M.N. Demuth and C.R. Onclin, 1988. Using the borehole jack to determine changes in river ice strength. In - Proceedings of the Fifth Workshop on Hydraulics of River Ice/Ice Jams, Winnipeg, 21-24 June 1988, pp. 283-303.

Prowse, T.D., S. Beltaos, B. Burrell, P. Tang and J. Dublin, 1989. Breakup of the Nashwaak River, New Brunswick. Proceedings of the Forty-sixth Eastern Snow Conference, Quebec City, Quebec, June 1989, pp. 142-155.

Prowse, T.D., M.N. Demuth and C.R. Chew, 1990a. Changes in the flexural strength of ice under radiation decay. Nordic Hydrology, 21, pp. 341-354.

Prowse, T.D., M.N. Demuth and C.R. Chew, 1990b. The deterioration of freshwater ice due to radiation decay. Journal of Hydraulic Research, 28(6), pp. 685-697.

Prowse, T.D., B. Aitken, M.N. Demuth and M. Peterson, 1996. Strategies for restoring spring flooding to a drying northern delta. Regulated Rivers: Research and Management (in press).

Salas, J.D., 1993. Analysis and modelling of hydrologic time series, Chapter 19. In - Handbook of Hydrology, D. Maidment (Editor), McGraw-Hill, New York, pp. 19.1 - 19.72.

Shishokin, S.A., 1965. Ice deterioration under the influence of solar radiation. Environment Canada Translation 00ENV-2608: Trudy Koordinatskionnykh Soveshchanii Po Gidrotekhnike, Transactions of the Coordination Meetings on Hydraulic Engineering, 23, pp. 137-143.

Smith, T.W., 1972. Unpublished correspondence between T.W. Smith, Superintendent, Wood Buffalo National Park and G. Rogers, Regional Director, entitled "Flooding - Swanson Lumber Company". June 21, 1972, Fort Smith, N.W.T., 1 p.

Sverdrup, H.U., 1936. The eddy conductivity of the air over a smooth snow field. Geofysiske Publikasjoner, 11(7), 1-69.

Terzi, R.A., 1981. Hydrometric field manual - measurement of stream flow. Water Resources Branch, Environment Canada, Ottawa, 37 pp.

Thomson, S., 1993. Peace-Athabasca flood history. Historical Services, Parks Canada, Winnipeg. Unpublished Technical Report, Wood Buffalo National Park, Fort Chipewyan, Alberta, 23 pp.

Thorpe, W., 1986. Review of the literature and miscellaneous other parameters relating to water levels in the Peace-Athabasca Delta particularly with respect to the effects on muskrat numbers. Parks Canada, Wood Buffalo National park, 9 pp.

Townsend, G.H., 1975. Impact of the Bennett Dam on the Peace-Athabasca Delta. Journal of the Fisheries Research Board of Canada, 32, 171-176.

Townsend, G.H., 1984. Wildlife resources of the Slave River and Peace-Athabasca Delta. Journal of the National and Provincial Parks Association of Canada, 20(2), 5-7.

APPENDIX A: TERMS OF REFERENCE

APPENDIX A: TERMS OF REFERENCE

NORTHERN RIVER BASINS STUDY

Project 1422-C1: Hydrometeorological conditions controlling ice-jam floods on the Peace River.

I. OBJECTIVE

The overall objective of this planned two-year project is to quantify the general flow and meteorological conditions that have controlled the generation of ice-jam floods on the Peace River. The rationale for this study stems from NRBS Question #10 "How does and how could river flow regulation impact the aquatic ecosystem". Major ecosystem impacts on the Peace-Athabasca Delta and, more recently, on the main Peace River channel, have been linked to changes in the ice-jam flood regime of the river. Although it is believed that such changes are controlled by changes to the flow regime, it is less clear whether such changes are only the result of upstream regulation. Other factors such as downstream snowmelt runoff from tributary streams and natural variations in meterological and ice conditions could also have affected the observed changes in the flow regime and spring floods. This study is designed to quantify the relative importance of the controlling natural and regulated factors. Achieving this understanding is a prerequisite to addressing the issue of ecosystem impacts resulting from flow regulation.

The first year objective of this two-year study will be to -compile discharge, water level, remote-sensing information, and relevant meteorologic and snow-ice data available for pre- and post-regulation ice jam periods on the Peace River. A summary data report on the above will be produced by March 31, 1994

The final objective of this study is to produce an interpretative report on the above data sets from which the effects of flow regulation on the ice-flood regime can be separated from those due to natural variations in hydrometeorological conditions. This report will subsequently be used as a component for an NRBS synthesis report of the effects of flow regulation on the aquatic ecosystem.

II. REQUIREMENTS

1. Obtain hydrometric station data related to spring ice jam floods along the Peace River for years of available record. Interpret such records based on accepted techniques for deriving critical flow and water levels associated with break-up ice jamming (ref: NHRI Science Report No. 2, 1990)

2. Quantify hydrometeorological conditions that control the resistance of an ice cover in producing ice jamming, including ice thickness and mechanical strength. Assemble the necessary meteorological data from Peace River stations and employ predictive models where required to quantify the major atmospheric heat fluxes that have affected "ice resistance" before and after the commencement of flow regulation.

3. Analyze the sources of flow contributing to downstream forcing during the period of ice break-up. In particular, separate those contributions derived upstream of the flow regulation point from downstream sources.

4. Interpret the above hydrometeorological conditions relative to the prevailing synoptic climatologic conditions.

5. Present data results in year one and an interpretive report focussing on the pre- and post-regulation periods in year two.

III. PROJECT ORGANIZATION

This project will be managed by Dr. Terry D. Prowse of the National Hydrology Research Institute and NRBS Hydrology/Hydraulics/Sediment Project Leader. Scientific collaborators include Mr. Rick Lawford, Chief of the Hydrometeorological Research Division, NHRI.

IV. REPORTING REQUIREMENTS

as per NRBS

APPENDIX B: FIGURES

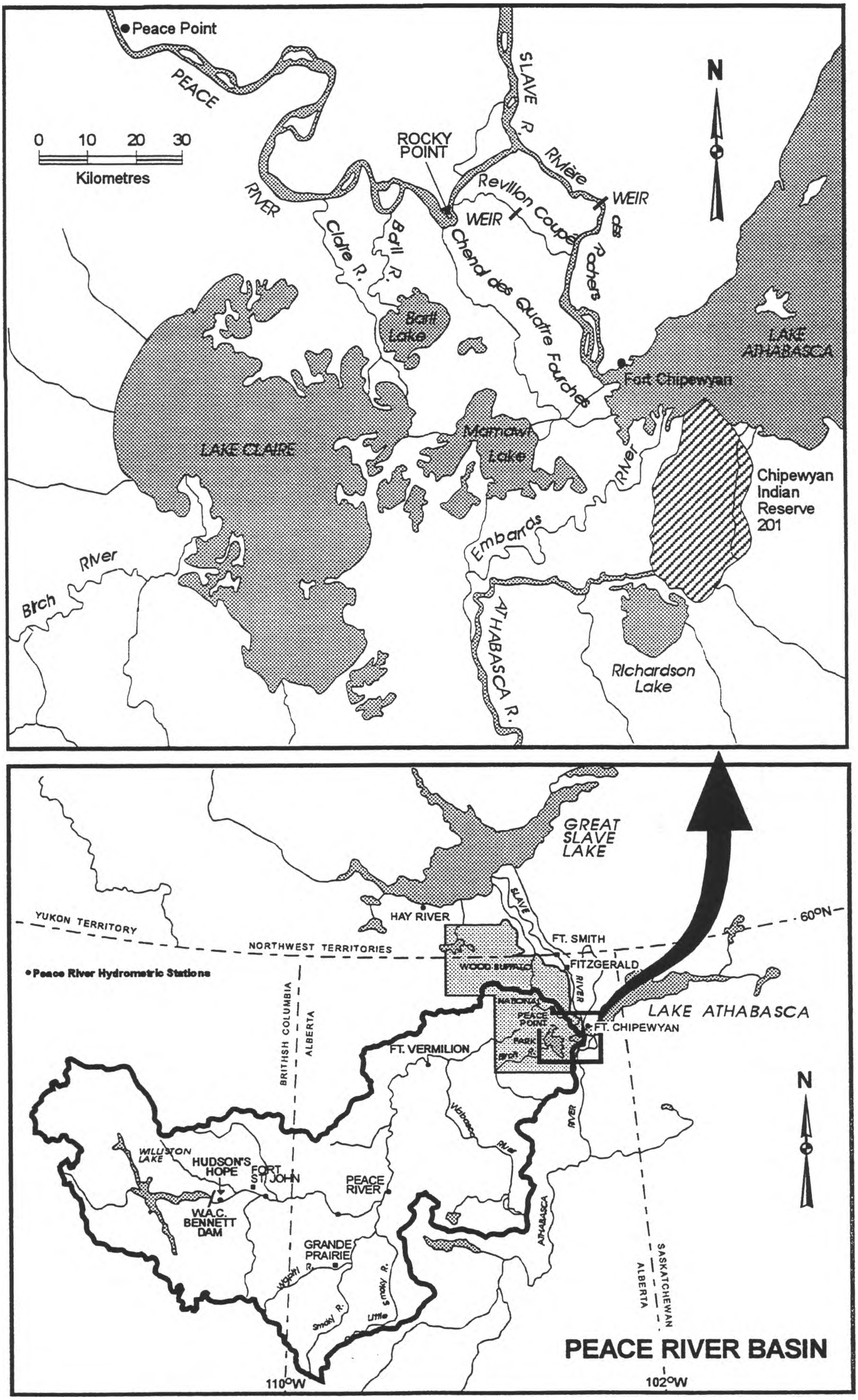

Figure 2.1 Location of Peace River Basin and the Peace-Athabasca Delta.

Figure 2.2 Water flow in the Peace-Athabasca Delta (after Prowse and Demuth, 1993)

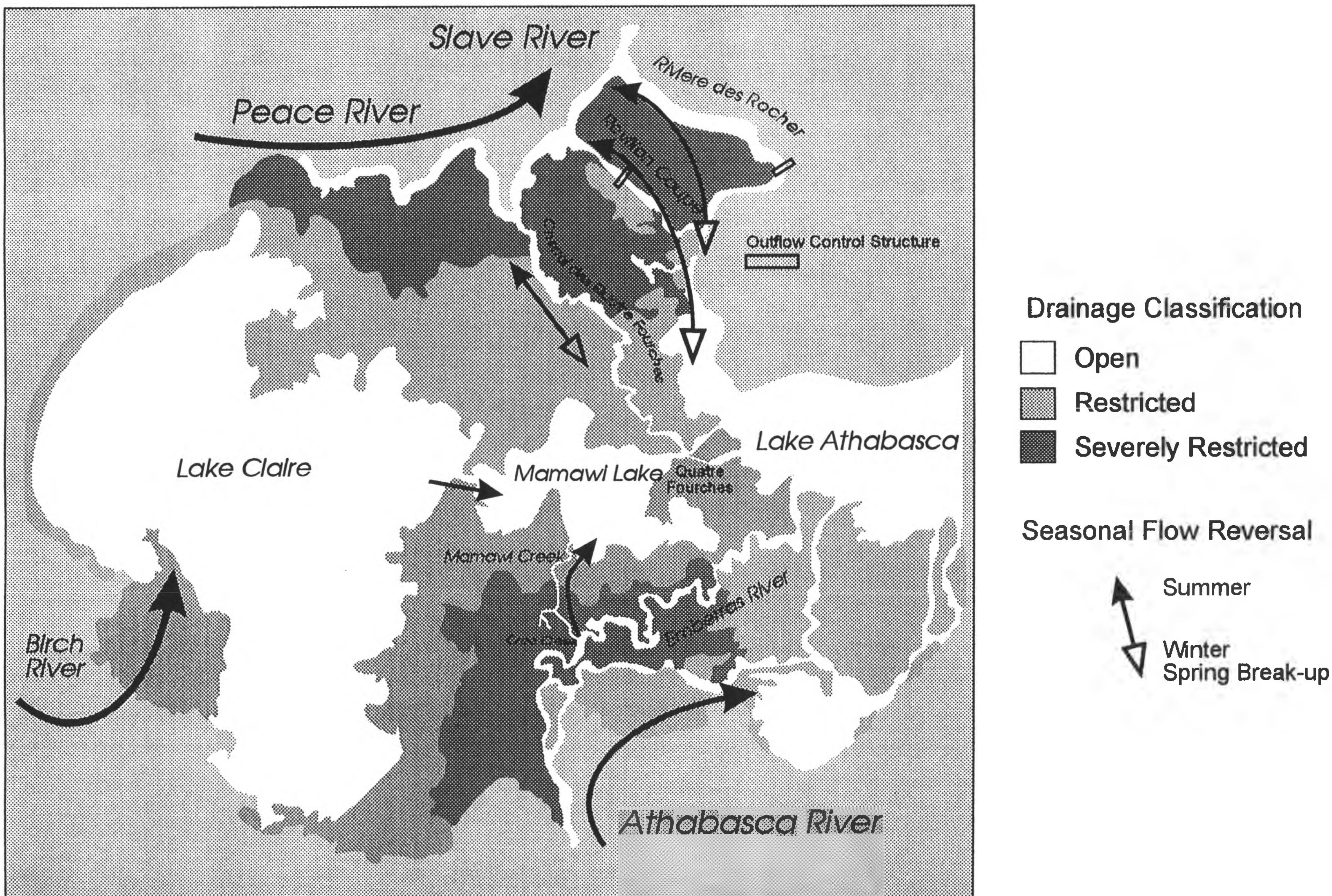

Figure 4.1. Mean monthly hydrograph for Peace River at Hudson's Hope: a) pre-dam 1960-67, b) post-dam 1972-92.

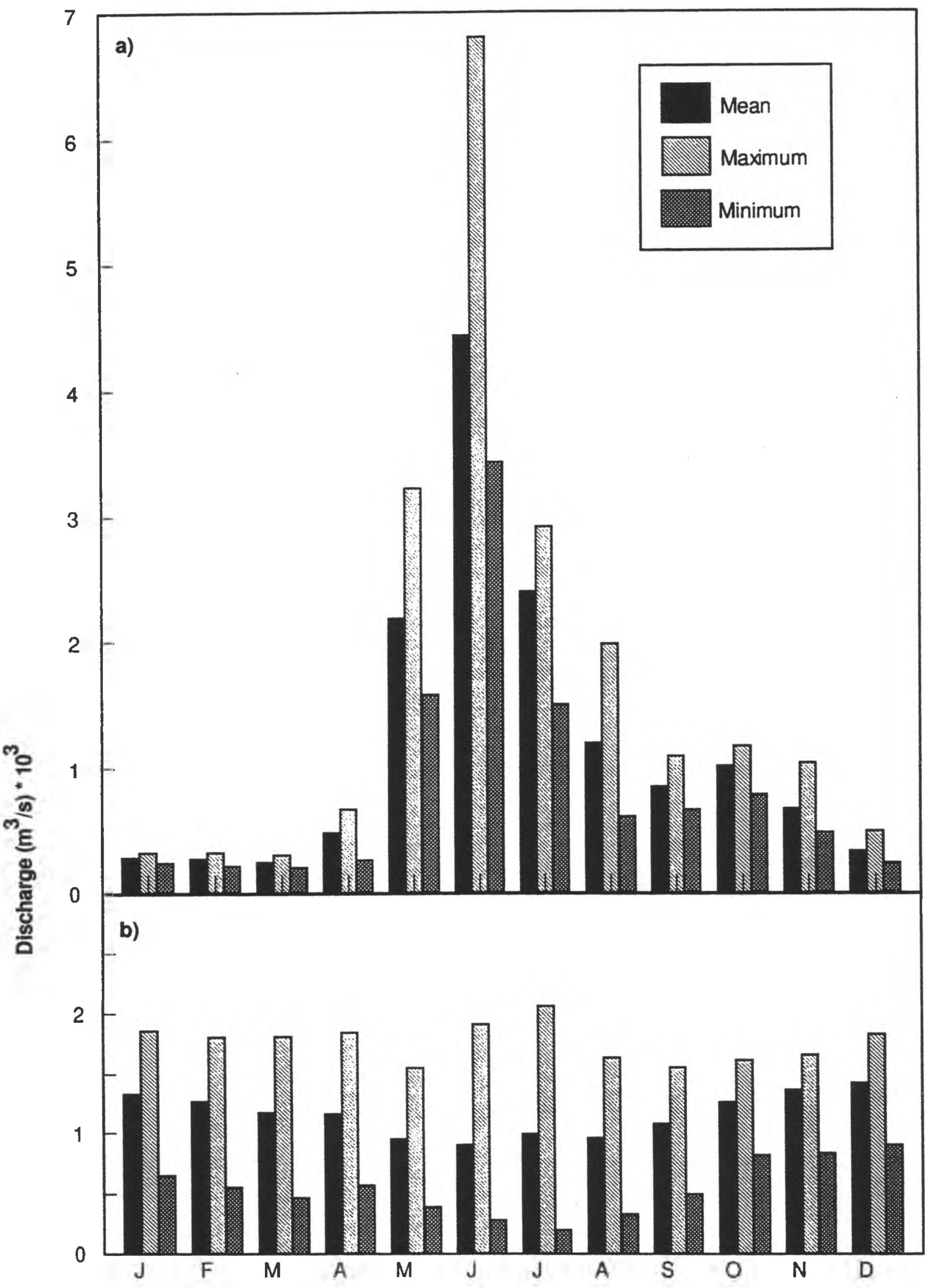

Figure 4.2. Mean monthly hydrograph for Peace River at Peace Point:
a) pre-dam 1960-67, b) post-dam 1972-92.

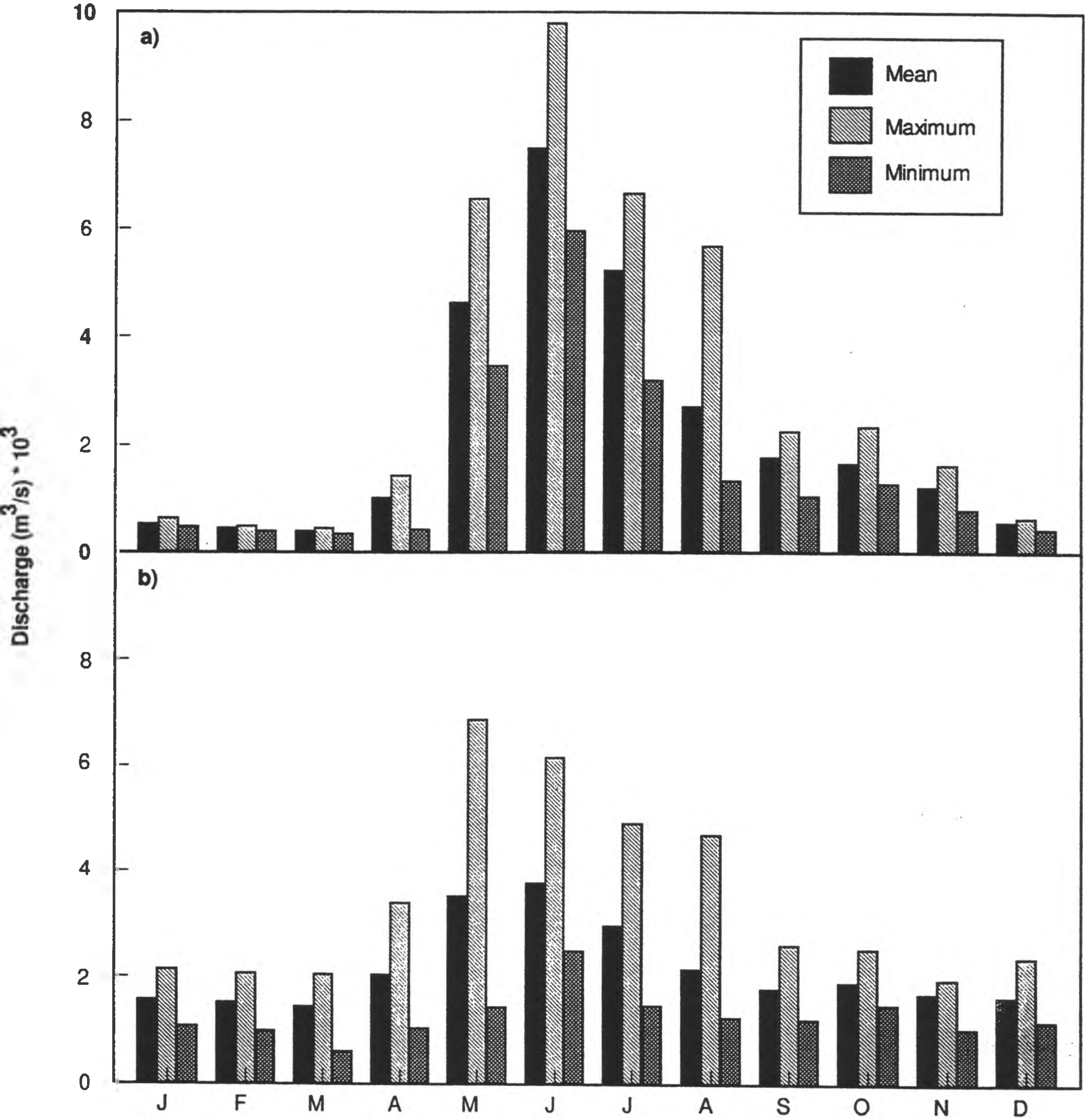

Figure 4.3. Open water peaks for the Peace River at Peace Point. Lines show mean values for the periods 1959-1967 and 1972-1992.

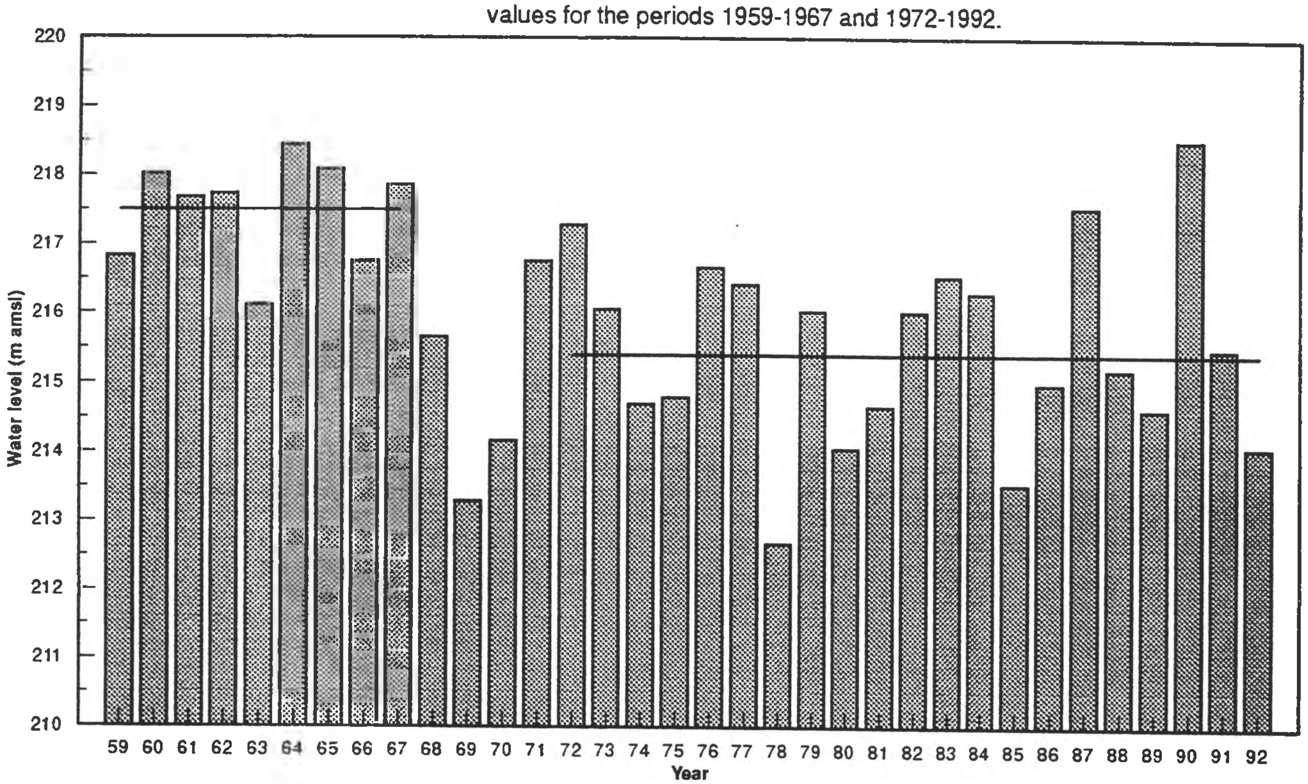

Figure 4.4. Annual peak water level versus discharge under break-up conditions.

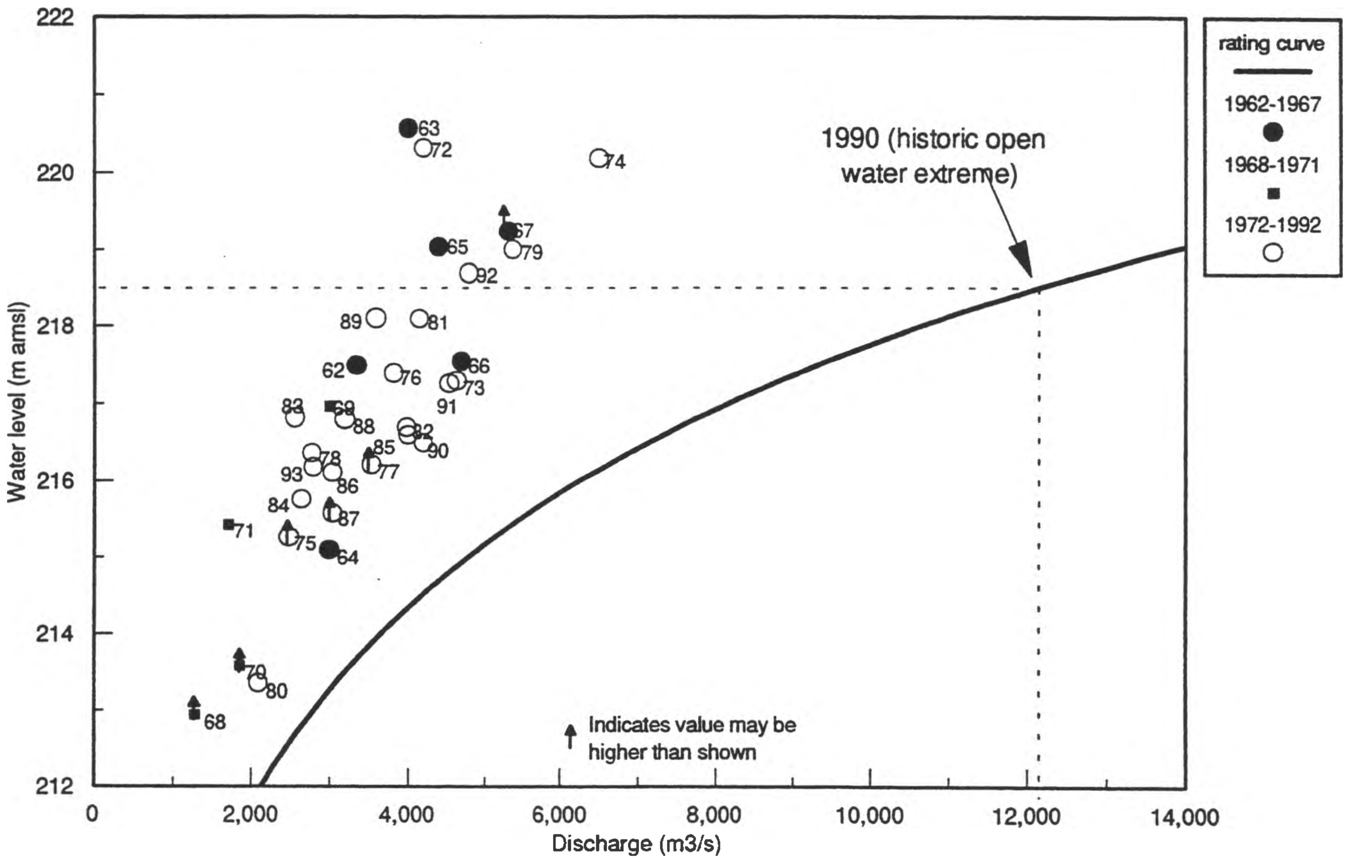

Figure 5.1. Ice conditions for mainstem Peace River stations: Hudson Hope 1917-93.

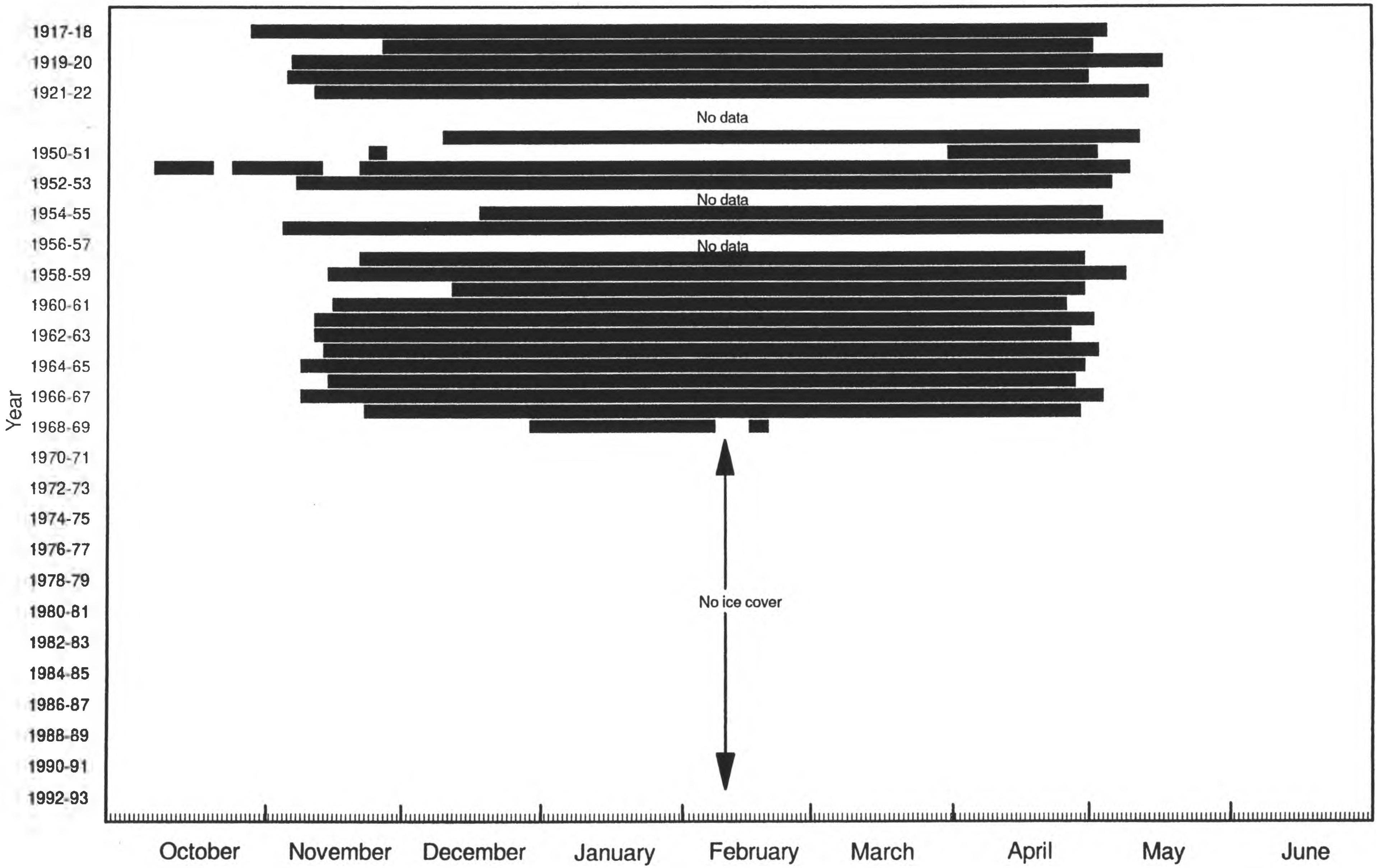

Figure 5.2 Ice conditions for mainstem Peace River stations: Taylor 1917-93.

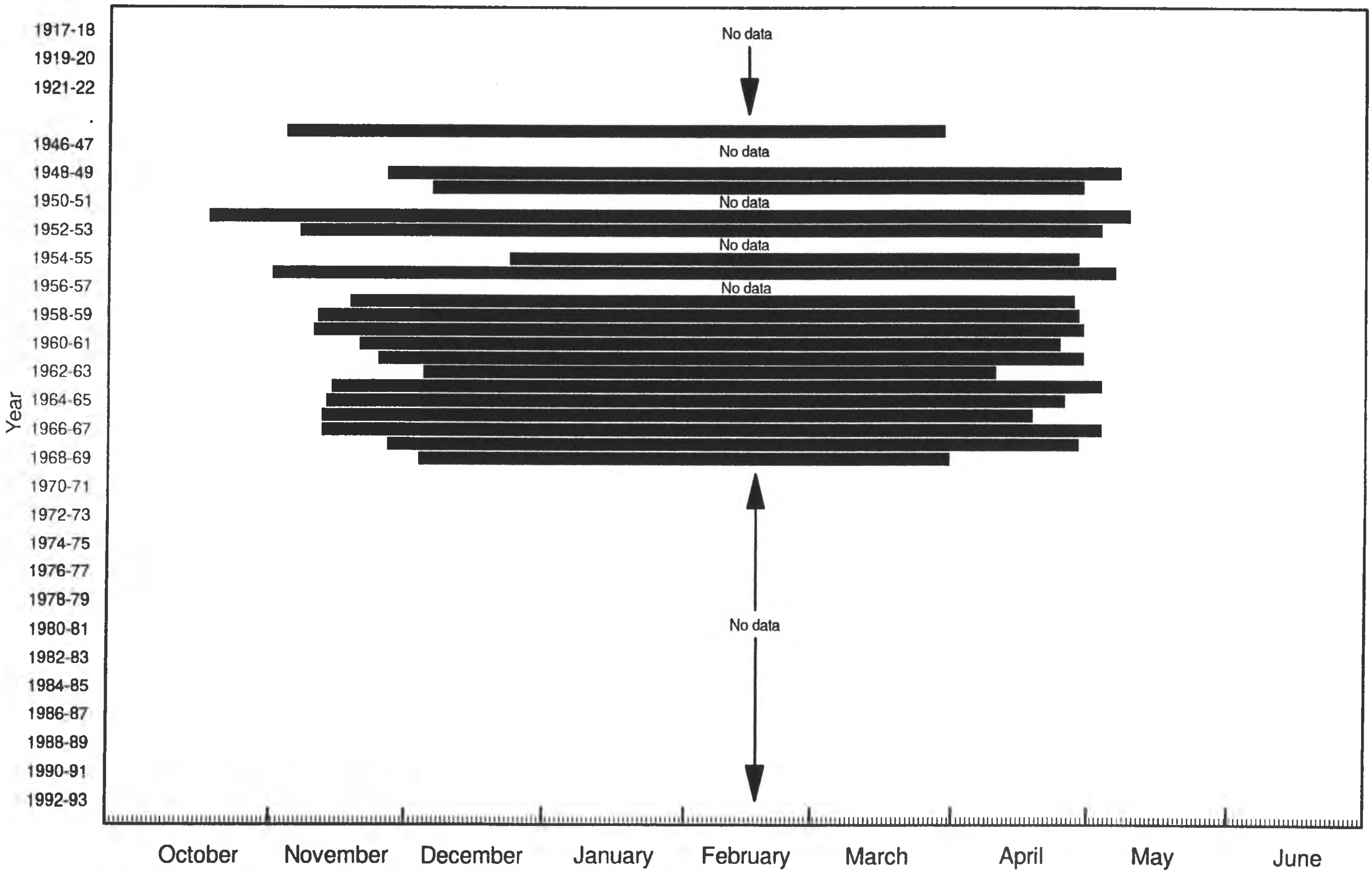

Figure 5.3. Ice conditions for mainstem Peace River stations: Peace River 1917-93.

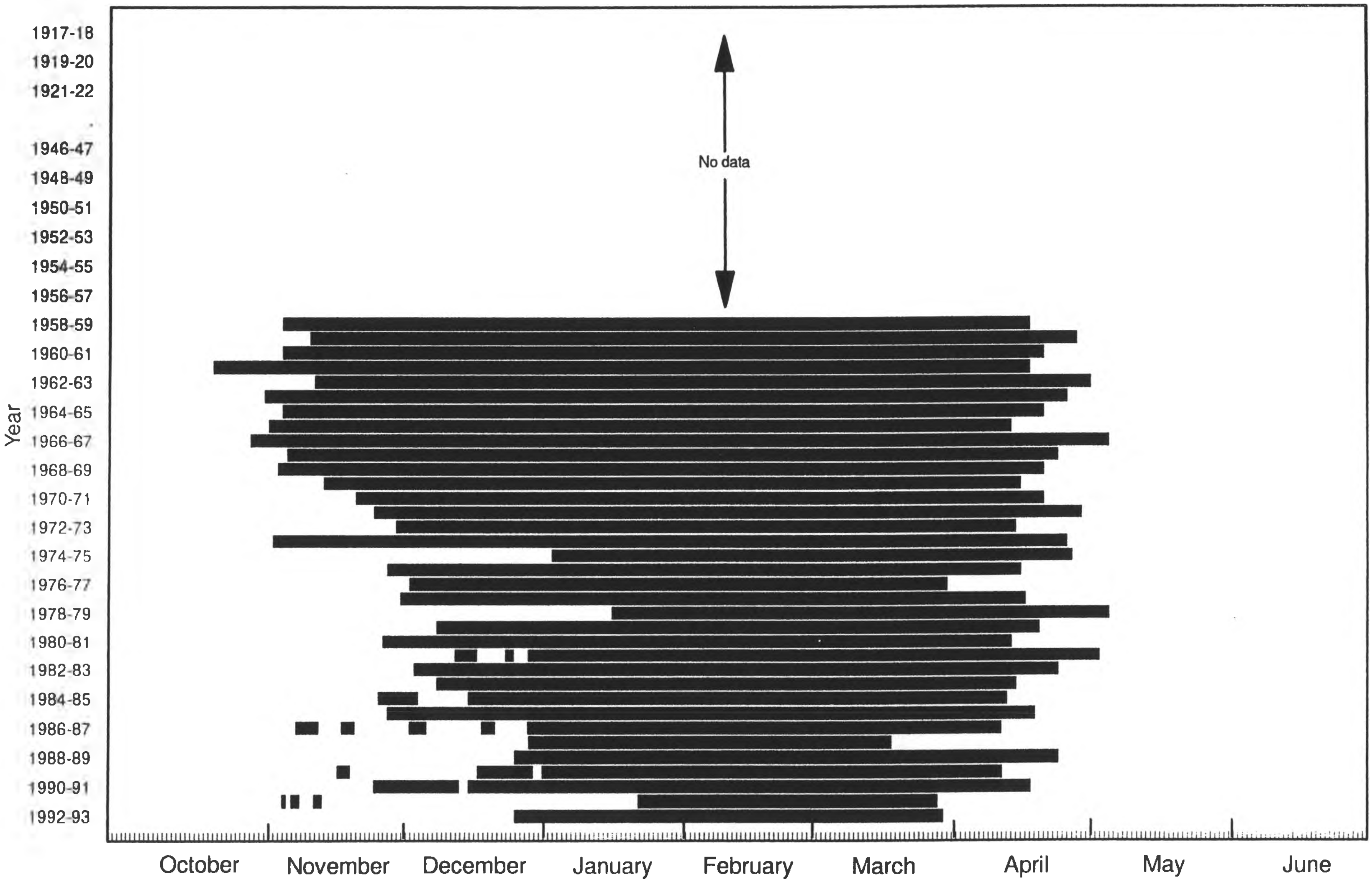

Figure 5.4. Ice conditions for mainstem Peace River stations: Fort Vermilion 1917-93.

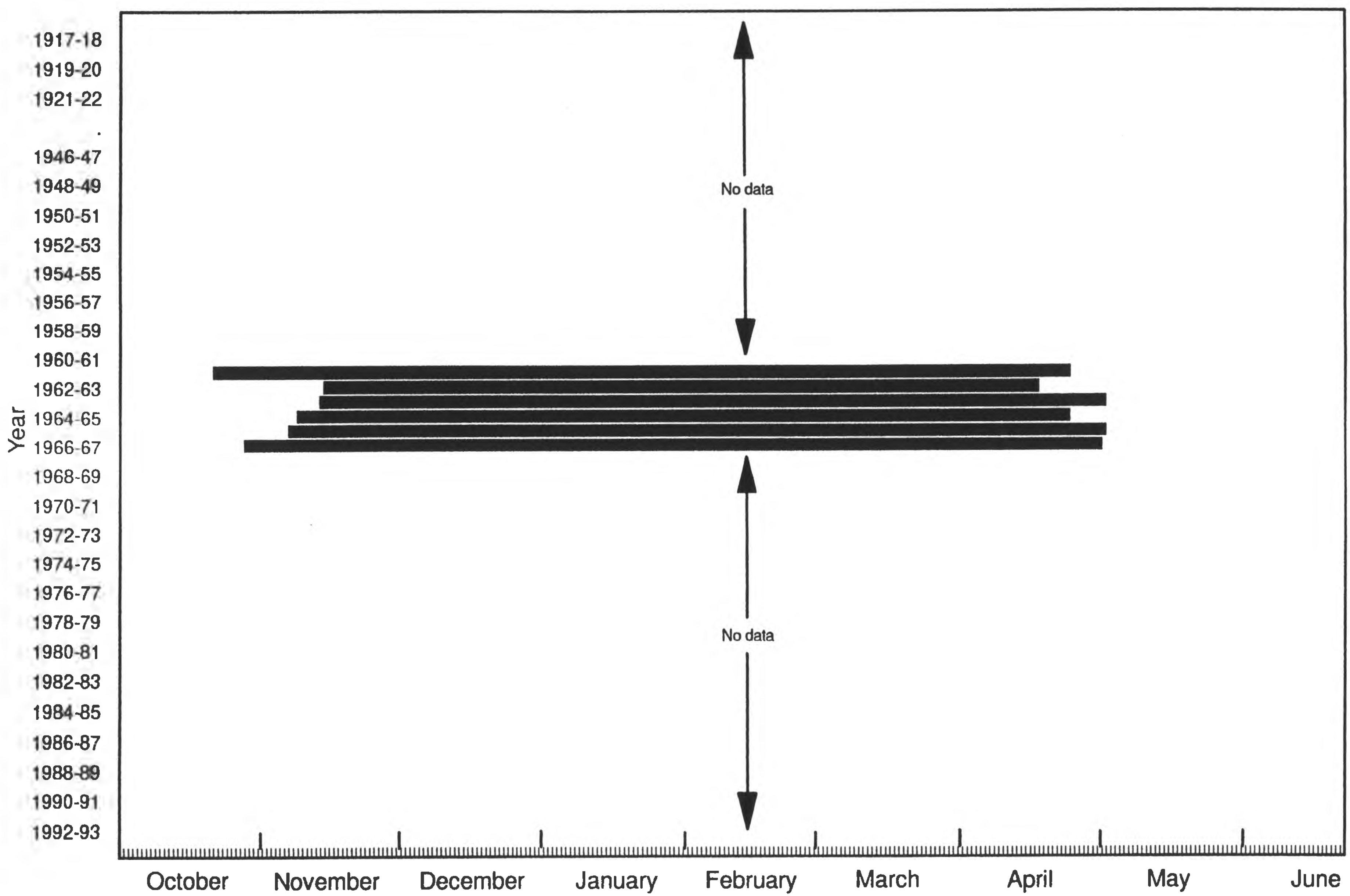

Figure 5.5. Ice conditions for mainstem Peace River stations: Peace Point 1917-93.

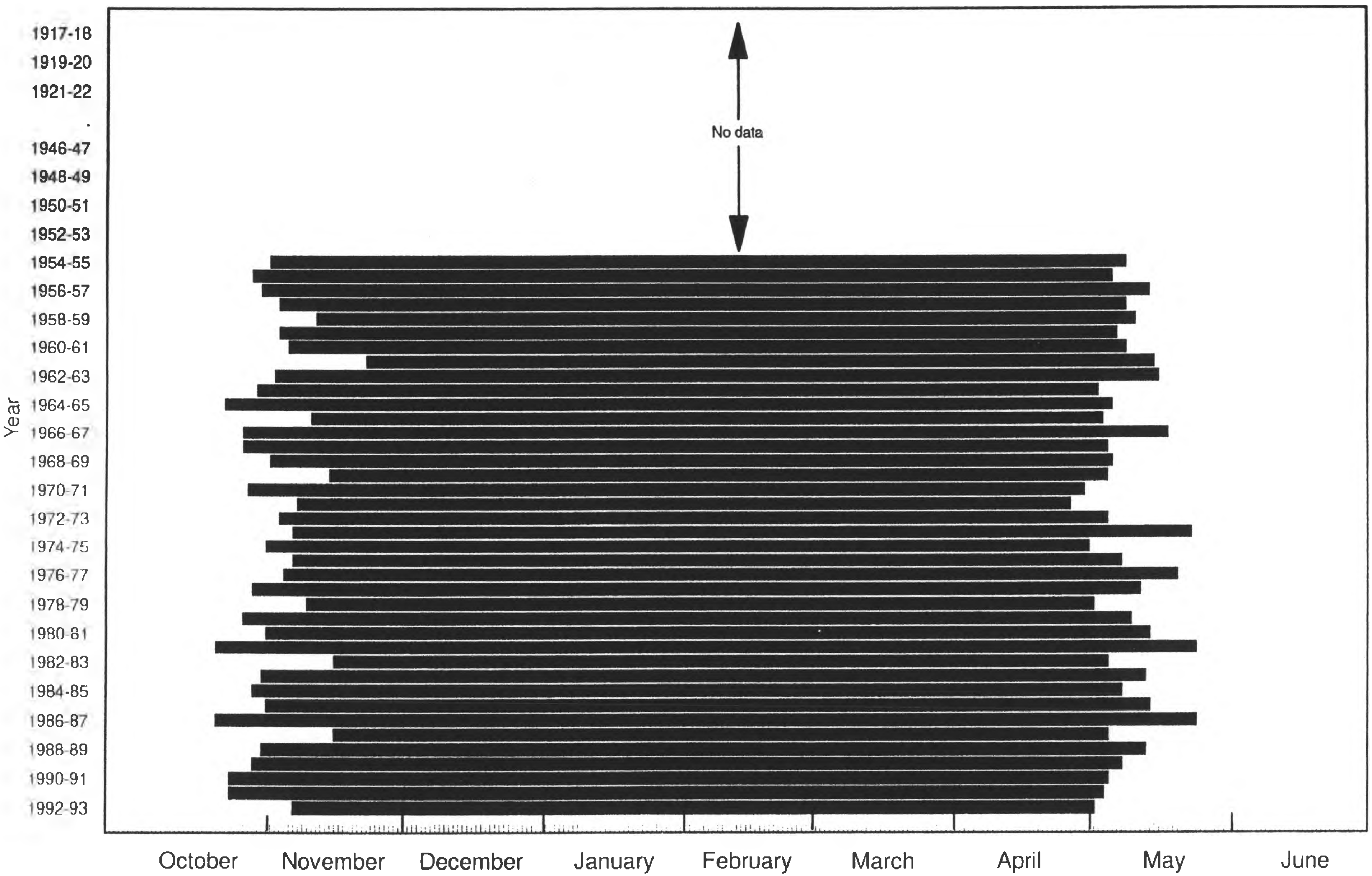

Figure 5.6. Average period of solid ice cover for the Peace River at Peace River.

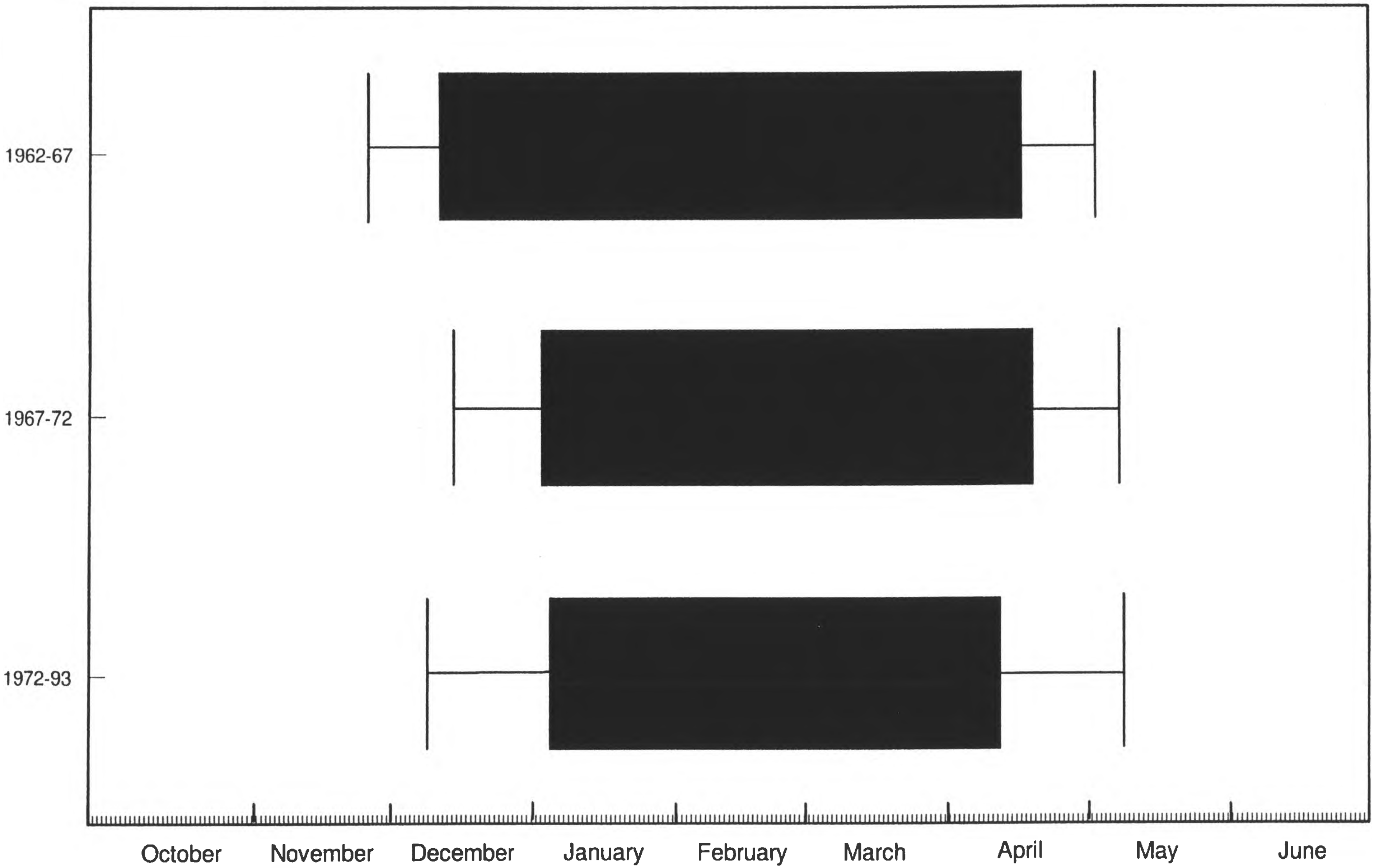

* Whiskers indicate one standard deviation

Figure 5.7. Average period of solid ice cover for the Peace River at Peace Point.

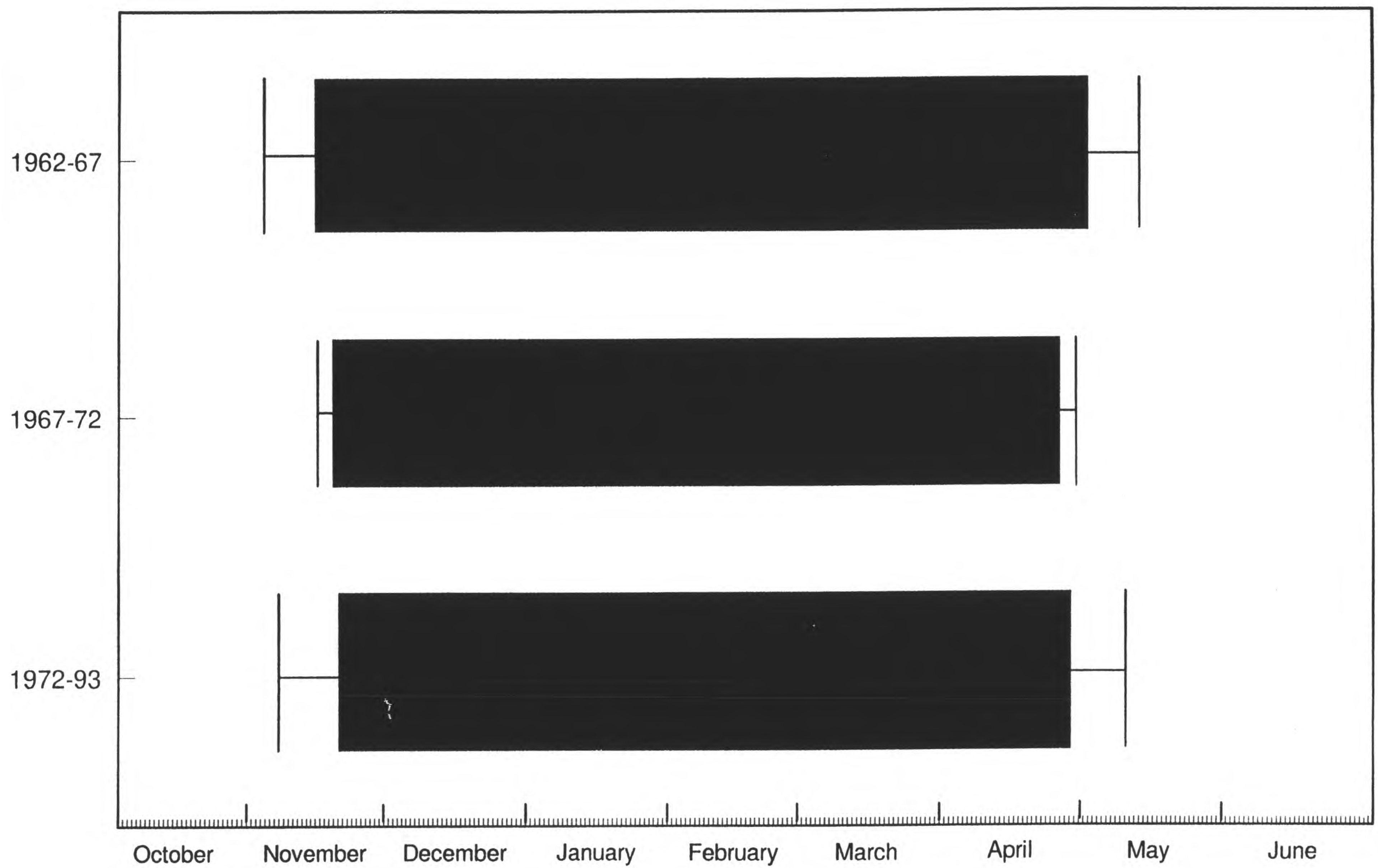

* Whiskers indicate one standard deviation.

Figure 6.1. Ice thickness determination.

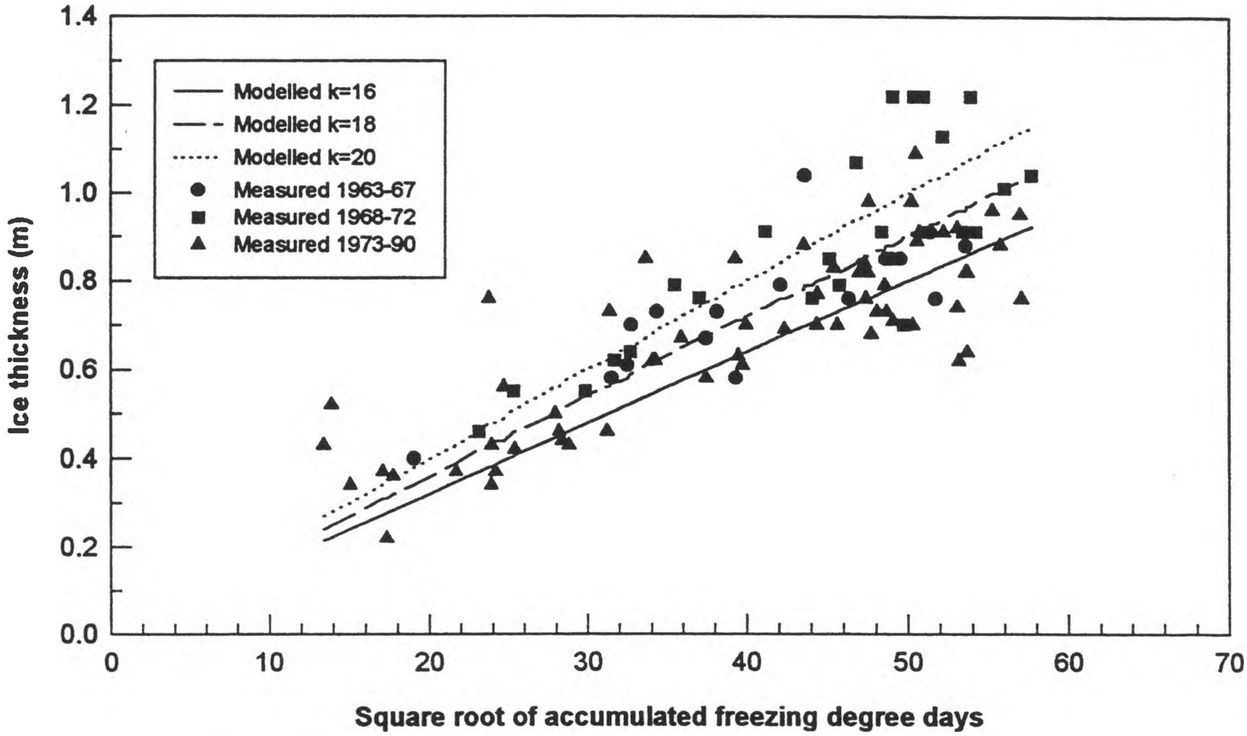

Figure 6.2. Modelled ice thickness based on degree day index.

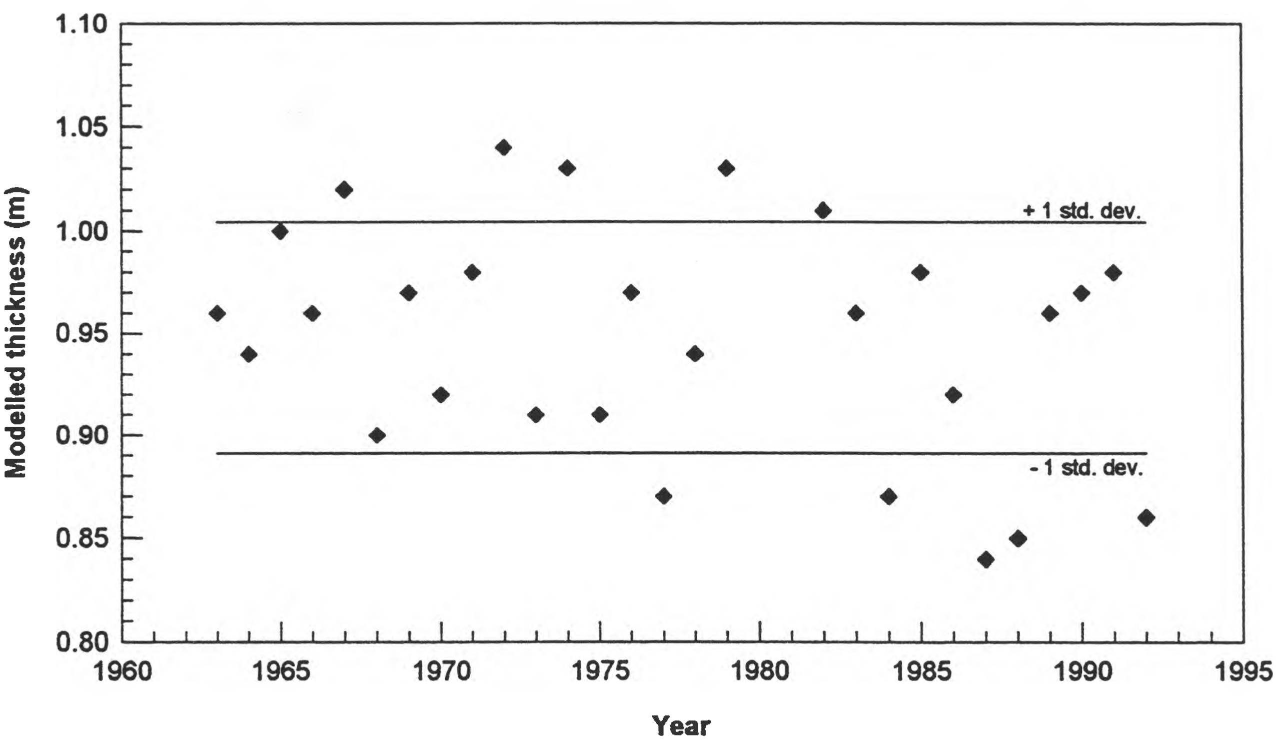

Figure 6.3 Model calibrations for albedo at Fort Smith

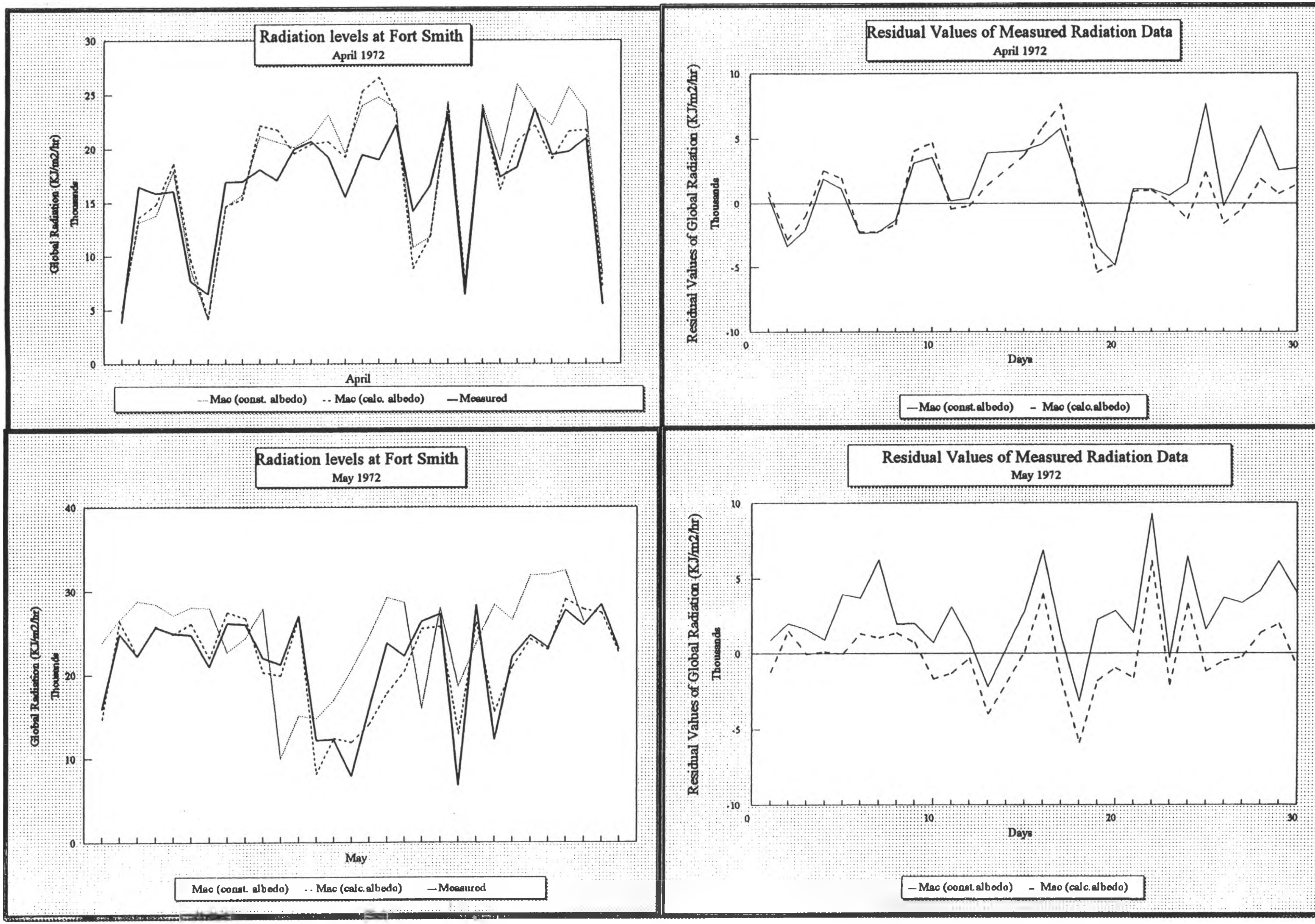

Figure 6.4 Model calibrations for albedo at Fort Smith

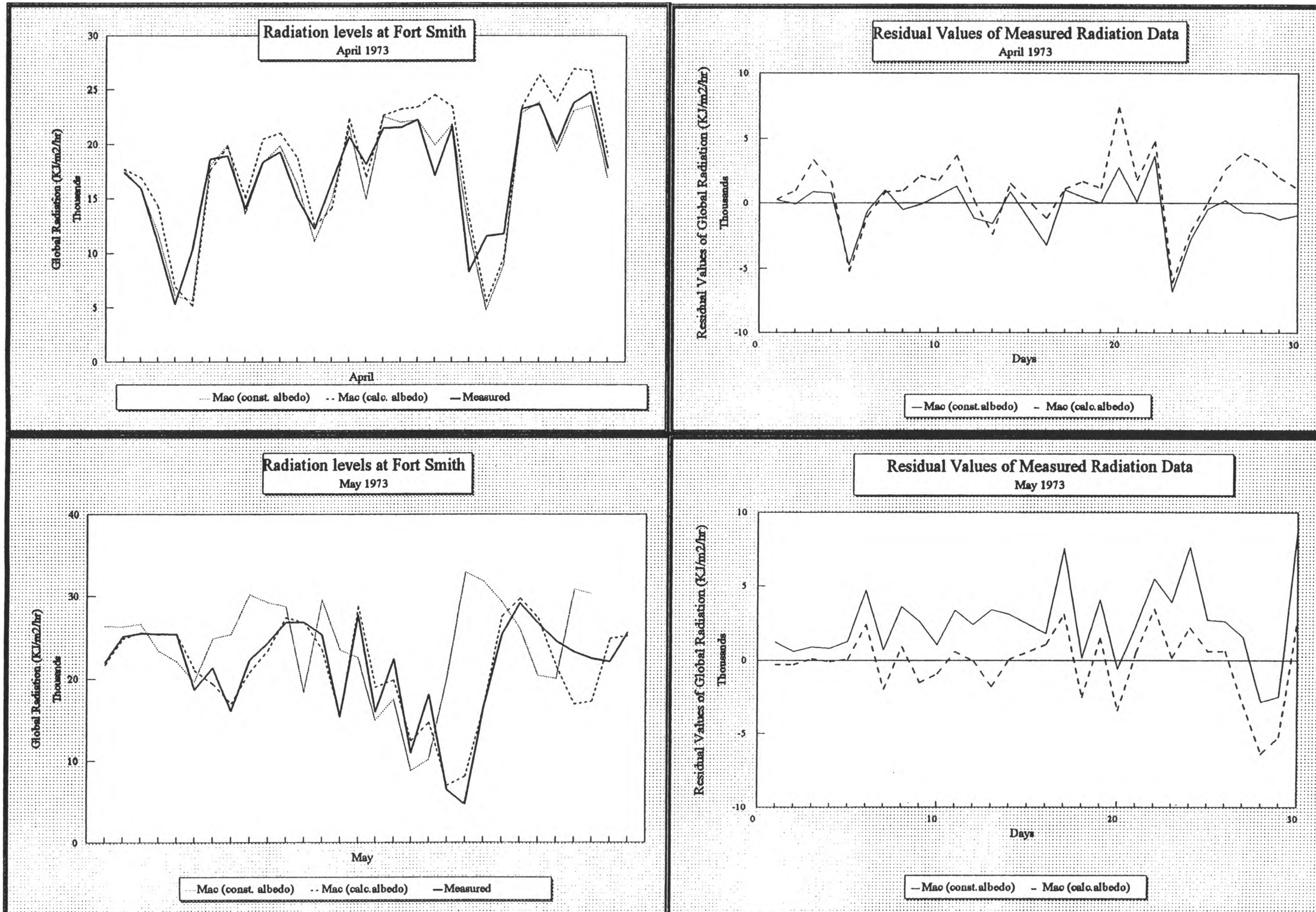

Figure 6.5 Model calibrations for albedo at Fort Smith

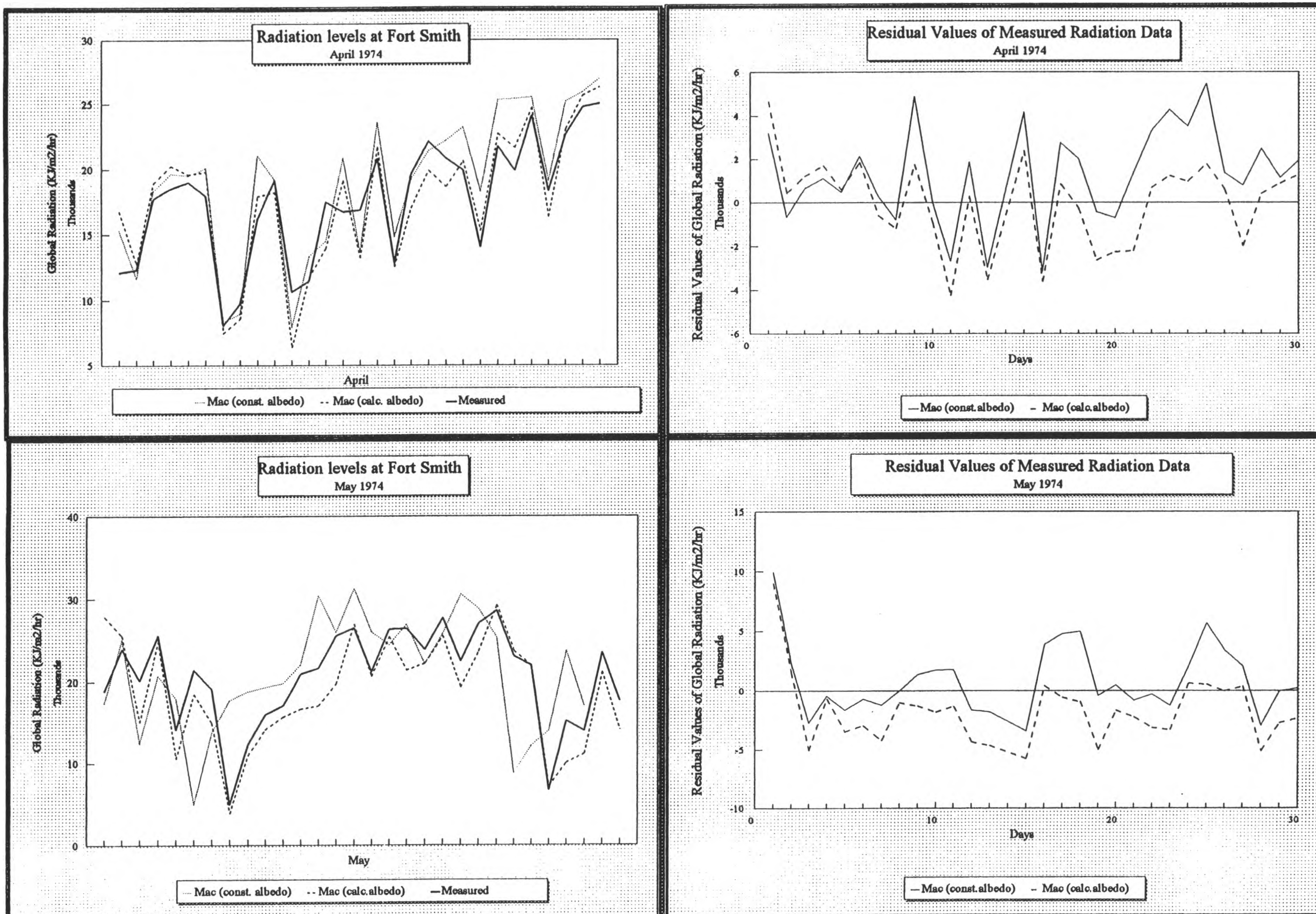

Figure 6.6 Model calibrations for albedo at Fort Smith

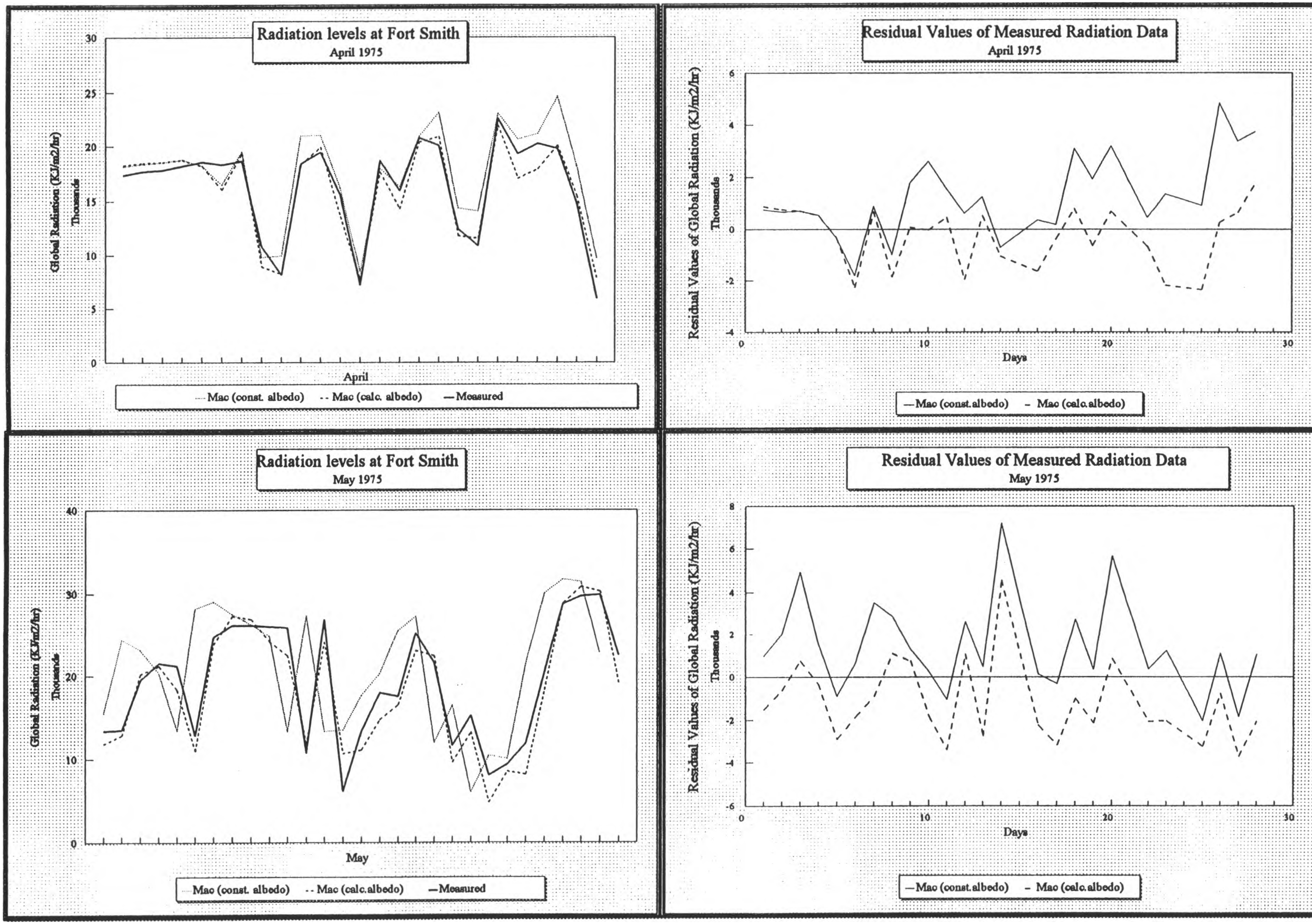

Figure 6.7 Model calibrations for albedo at Fort Smith

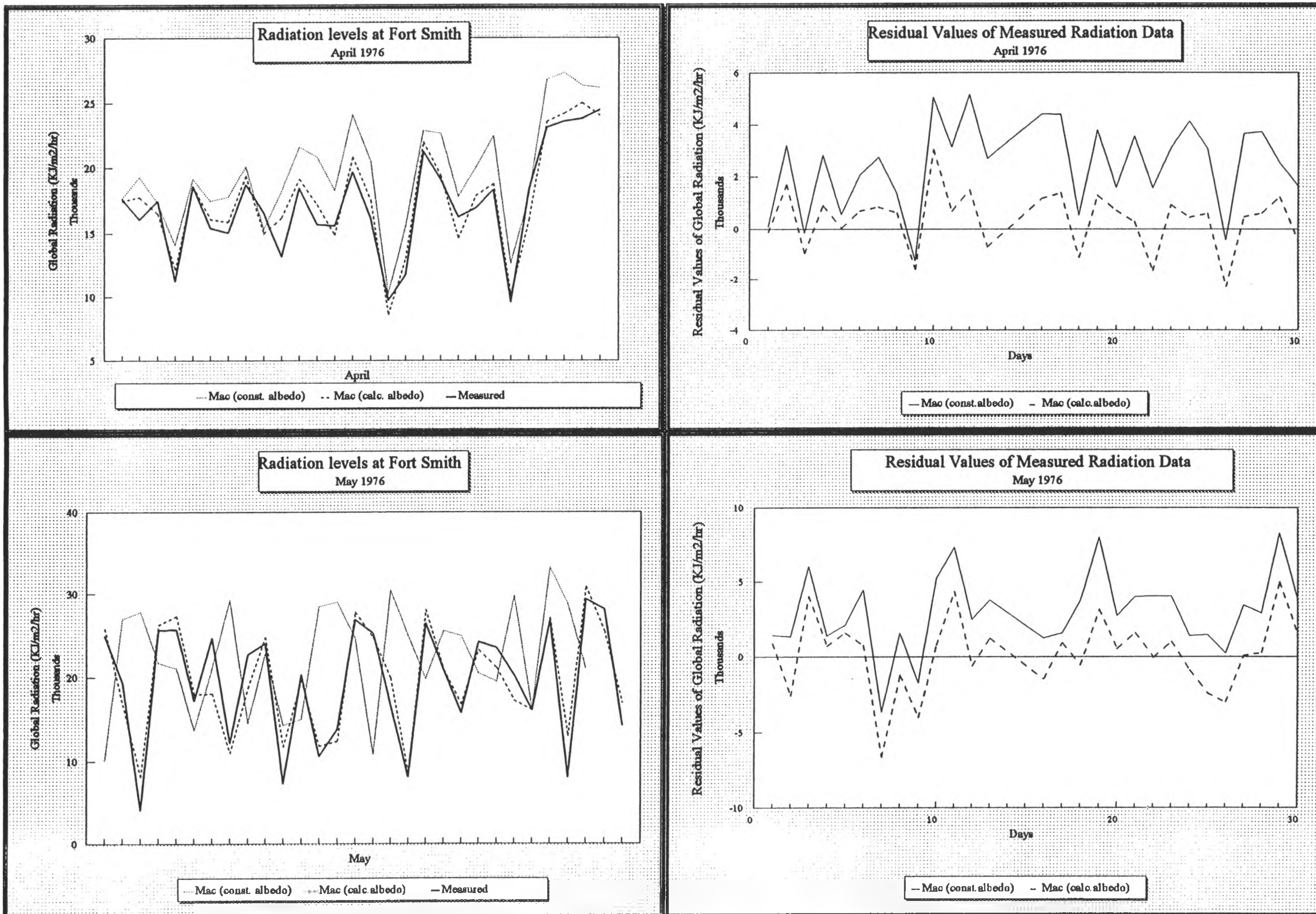

Figure 6.8 Model calibrations for albedo at Fort Smith

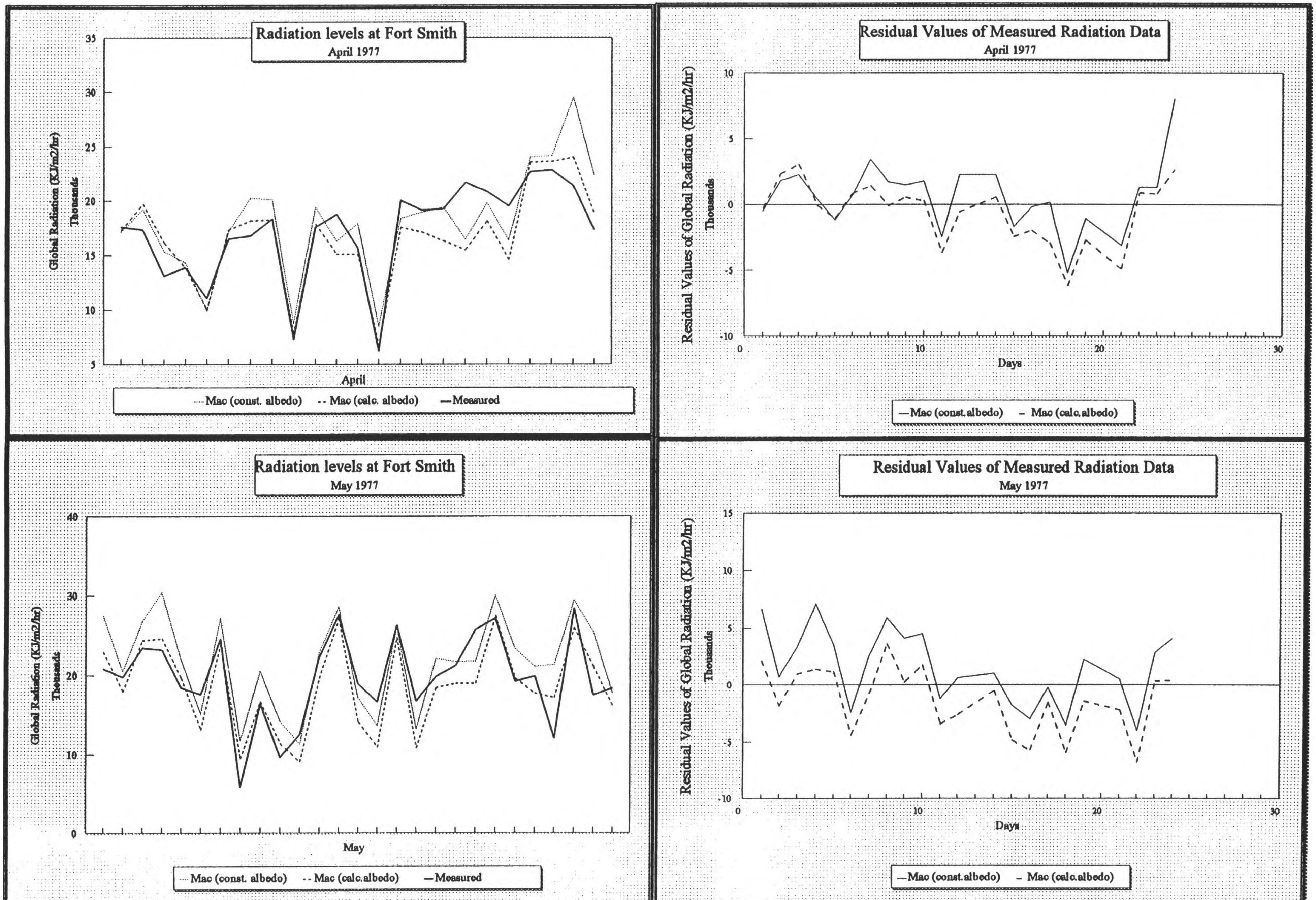

Figure 6.9 Model calibrations for albedo at Fort Smith

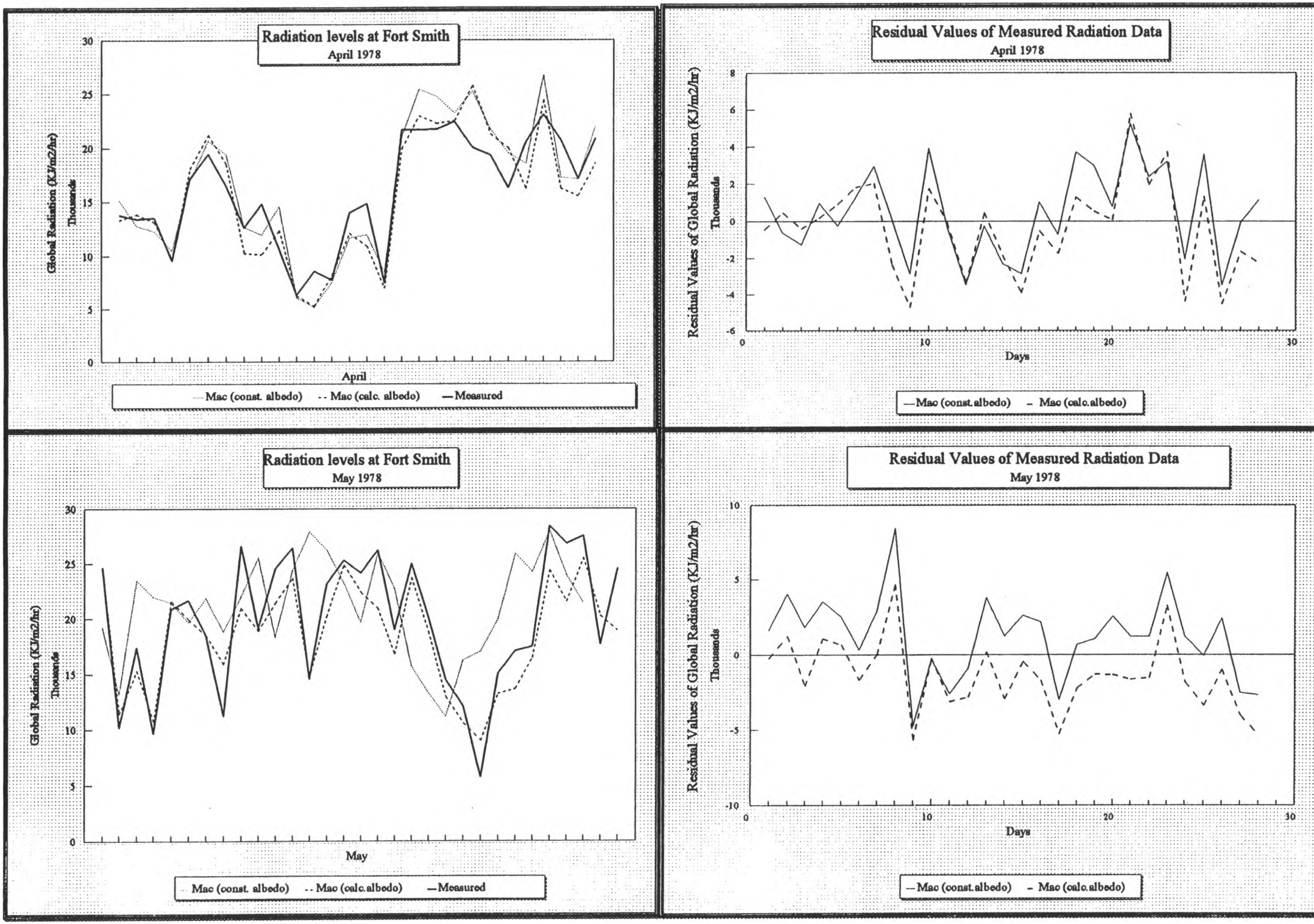

Figure 6.10. Melt initiation indices for the pre-break-up period, 1978.

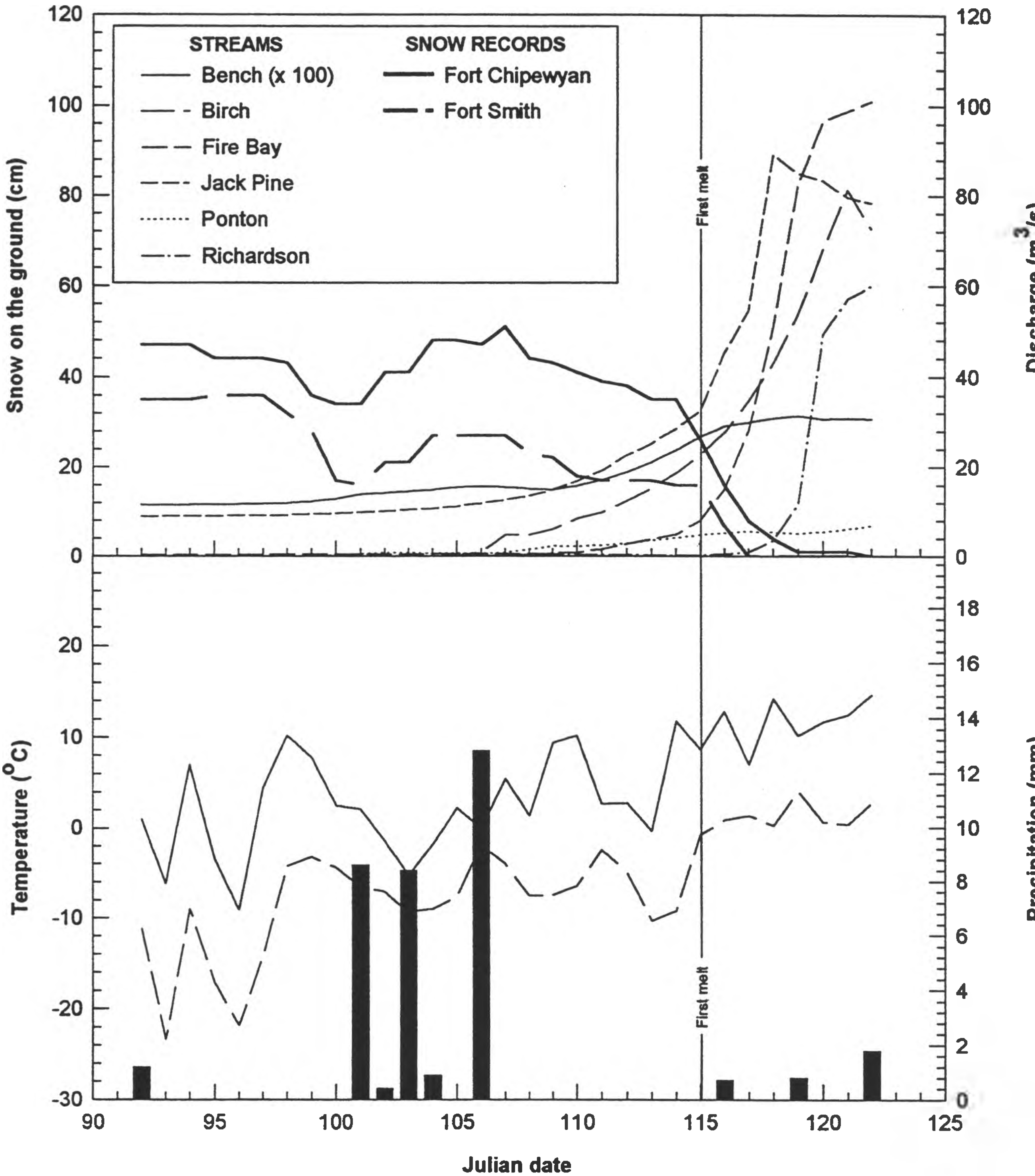

Figure 6.11 a) Daily heat flux calculations for Fort Chipewyan

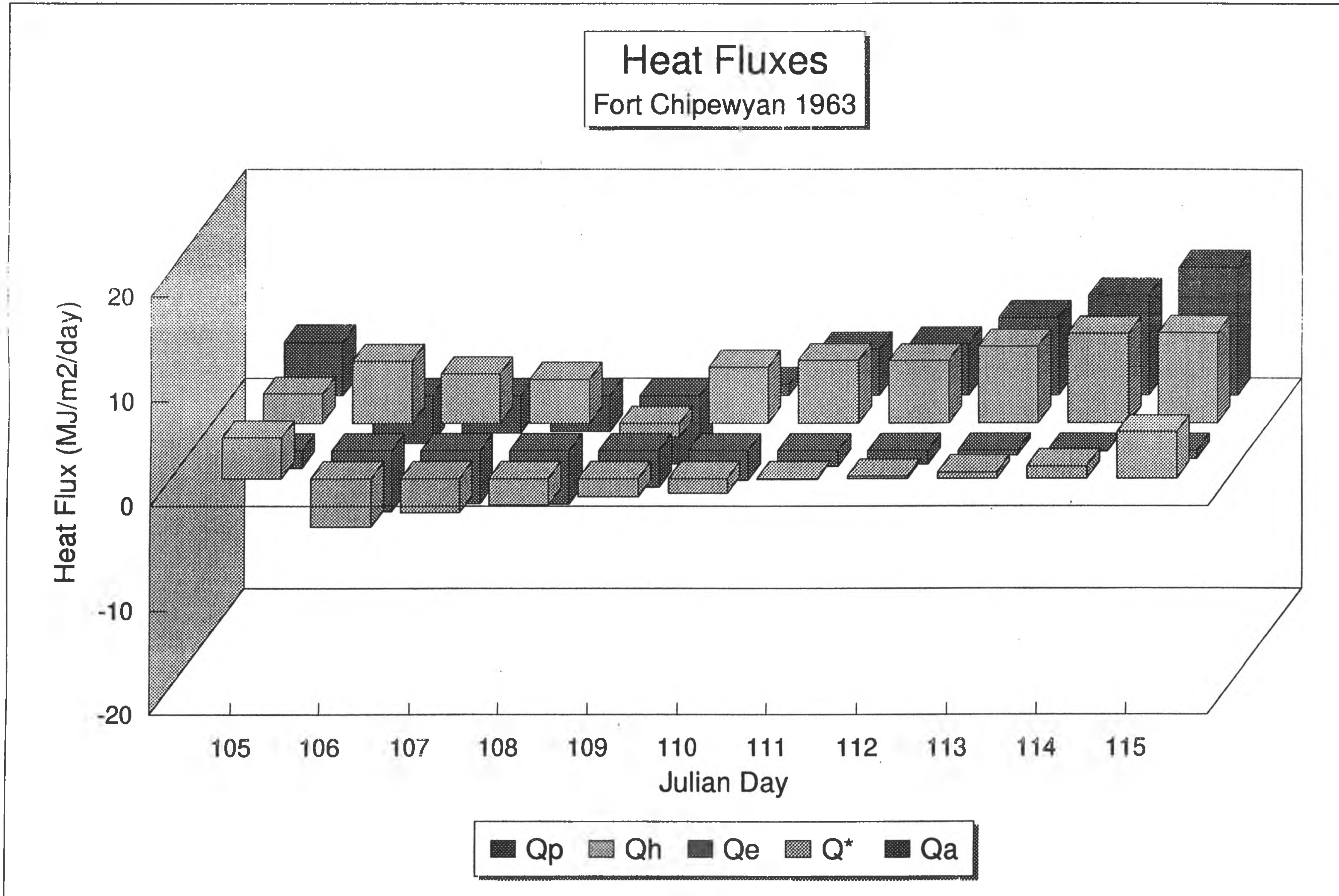

Figure 6.11 b) Daily heat flux calculations for Fort Chipewyan

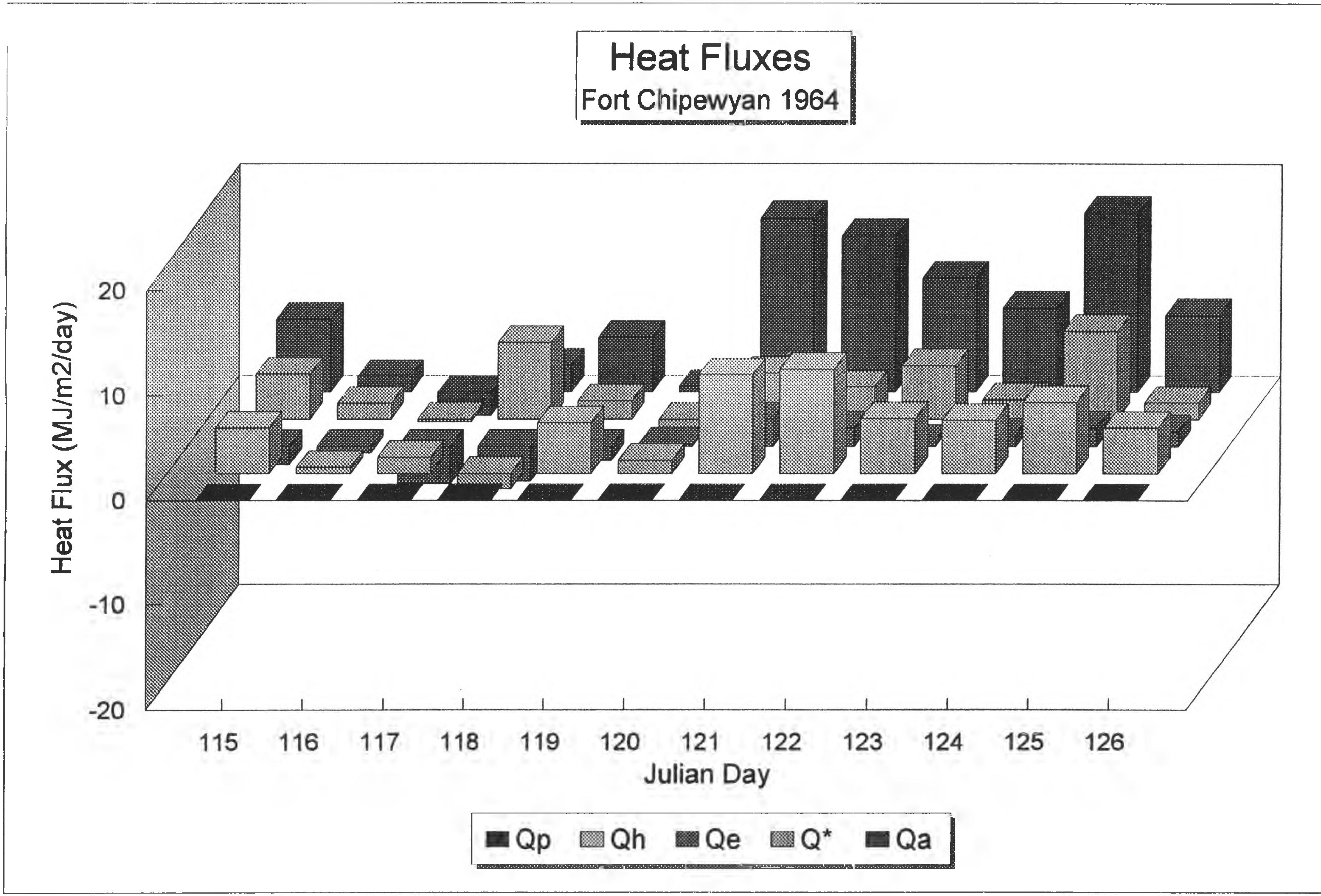

Figure 6.11 c) Daily heat flux calculations for Fort Chipewyan

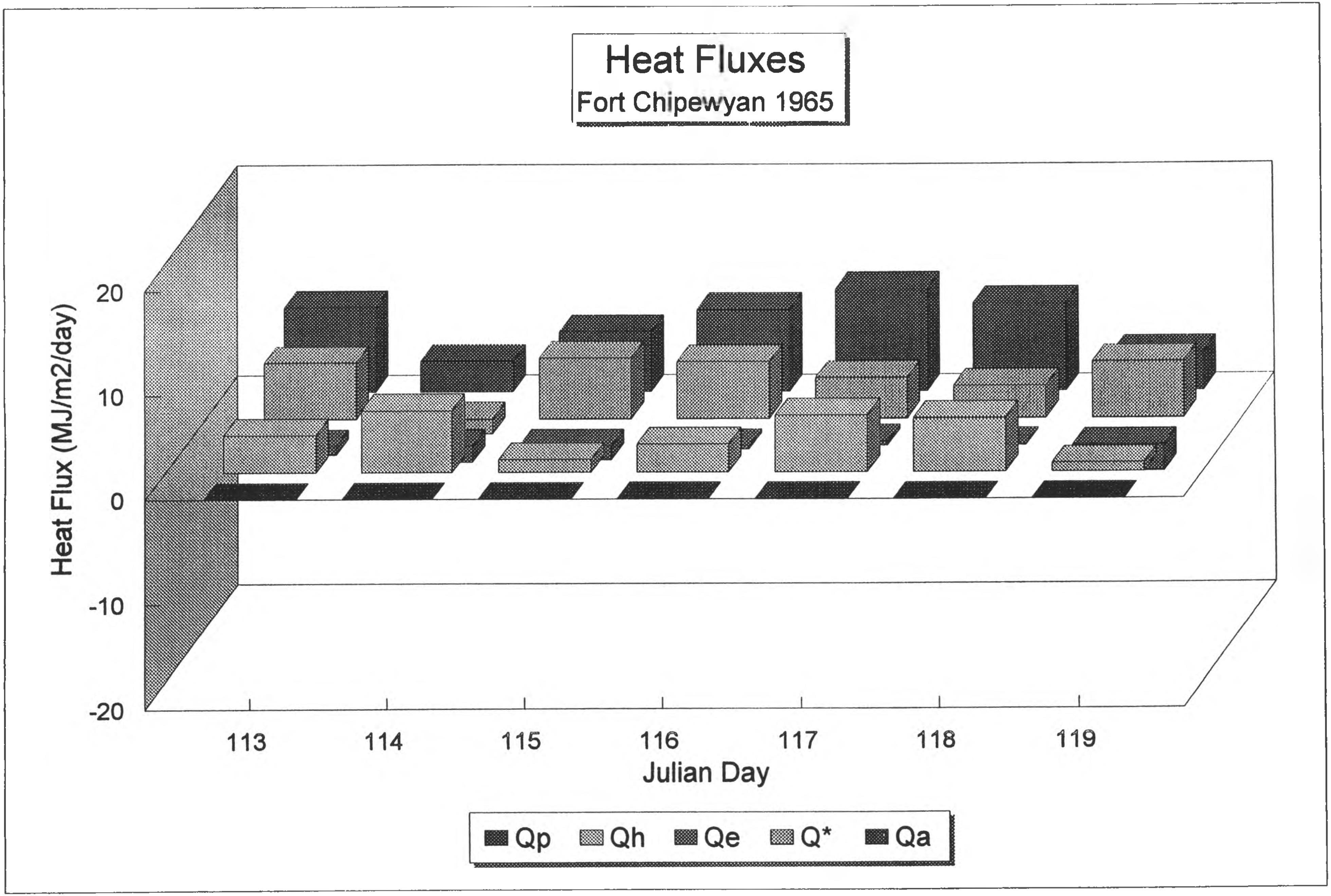

Figure 6.11 d) Daily heat flux calculations for Fort Chipewyan

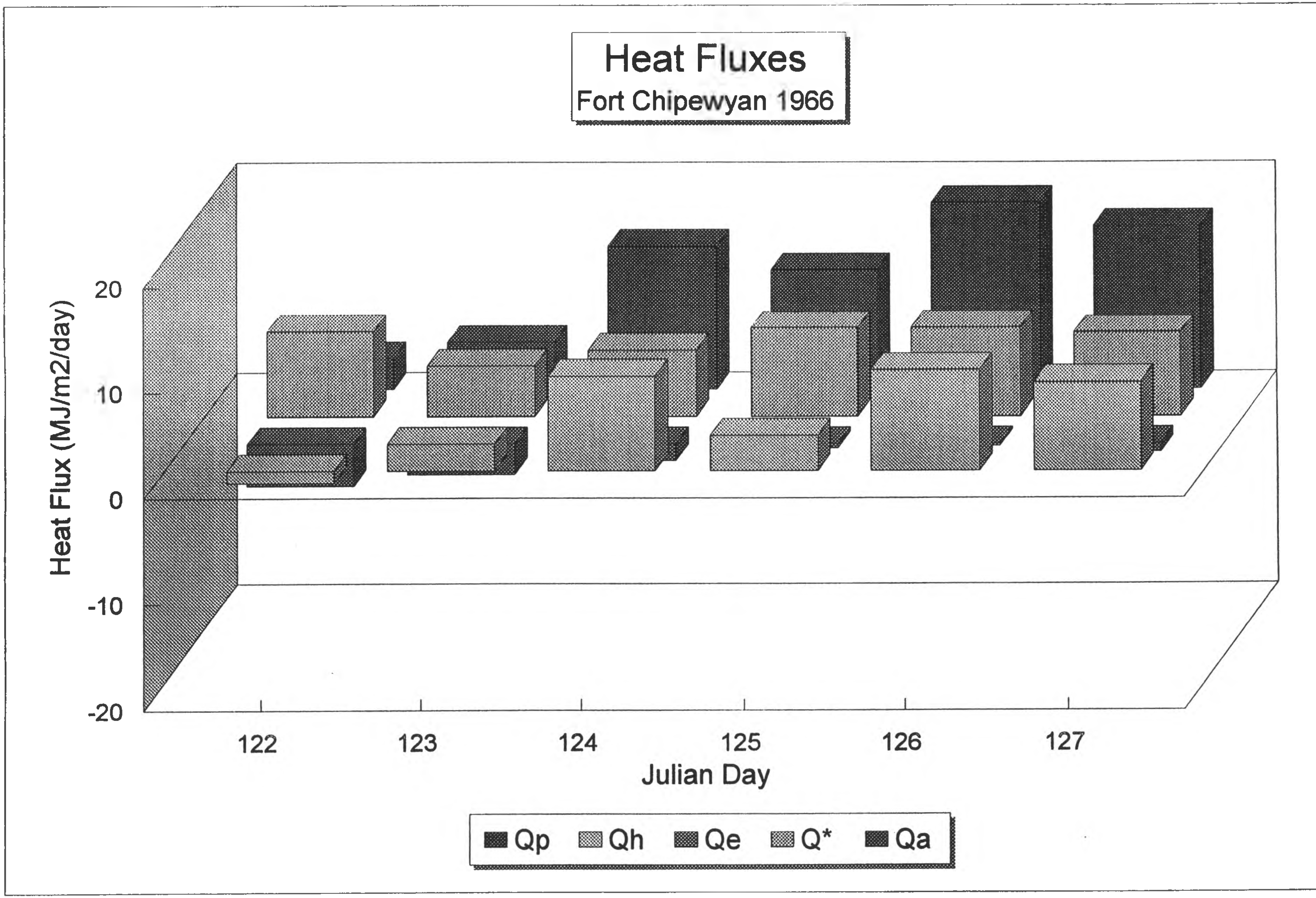

Figure 6.11 e) Daily heat flux calculations for Fort Chipewyan

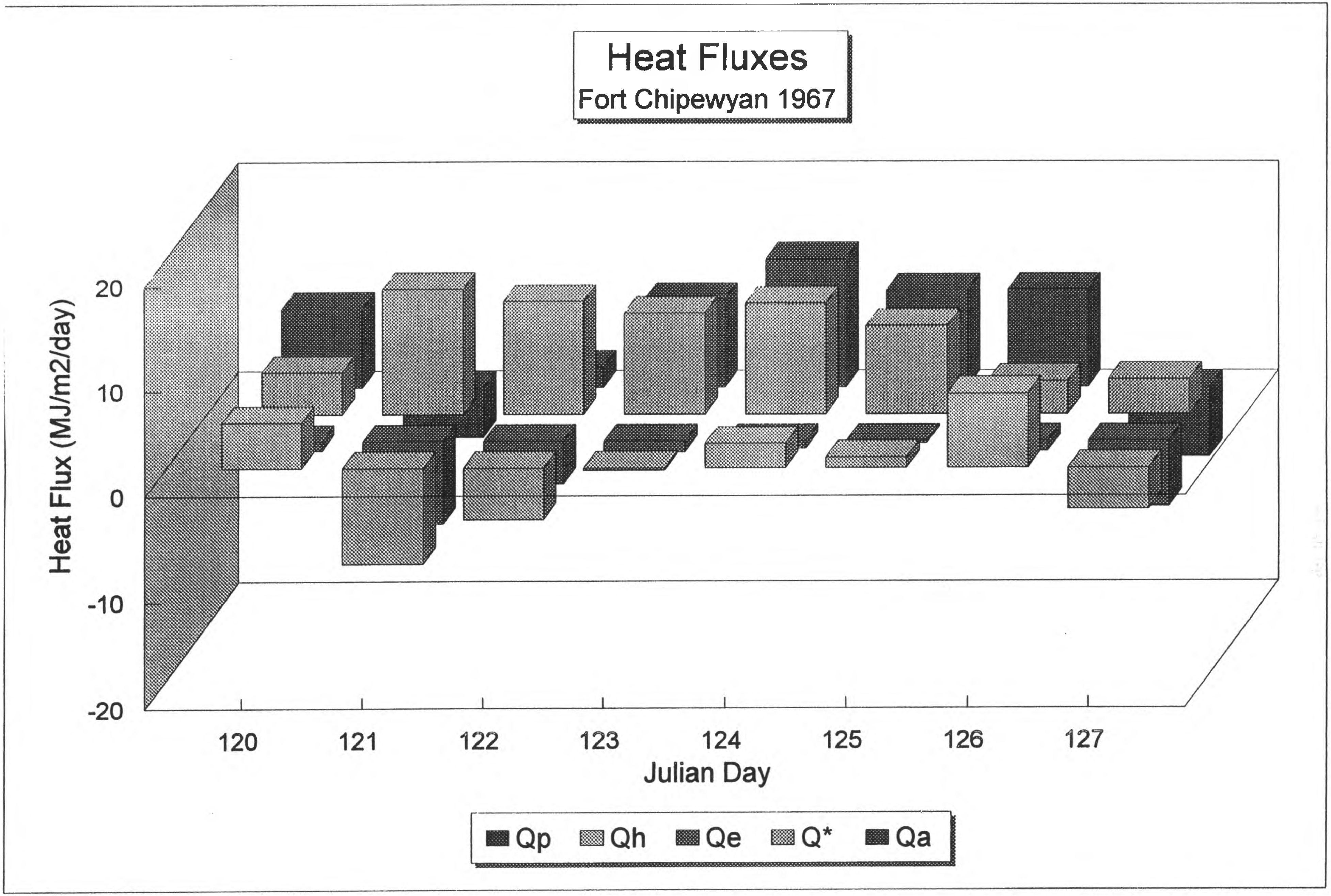

Figure 6.11 f) Daily heat flux calculations for Fort Chipewyan

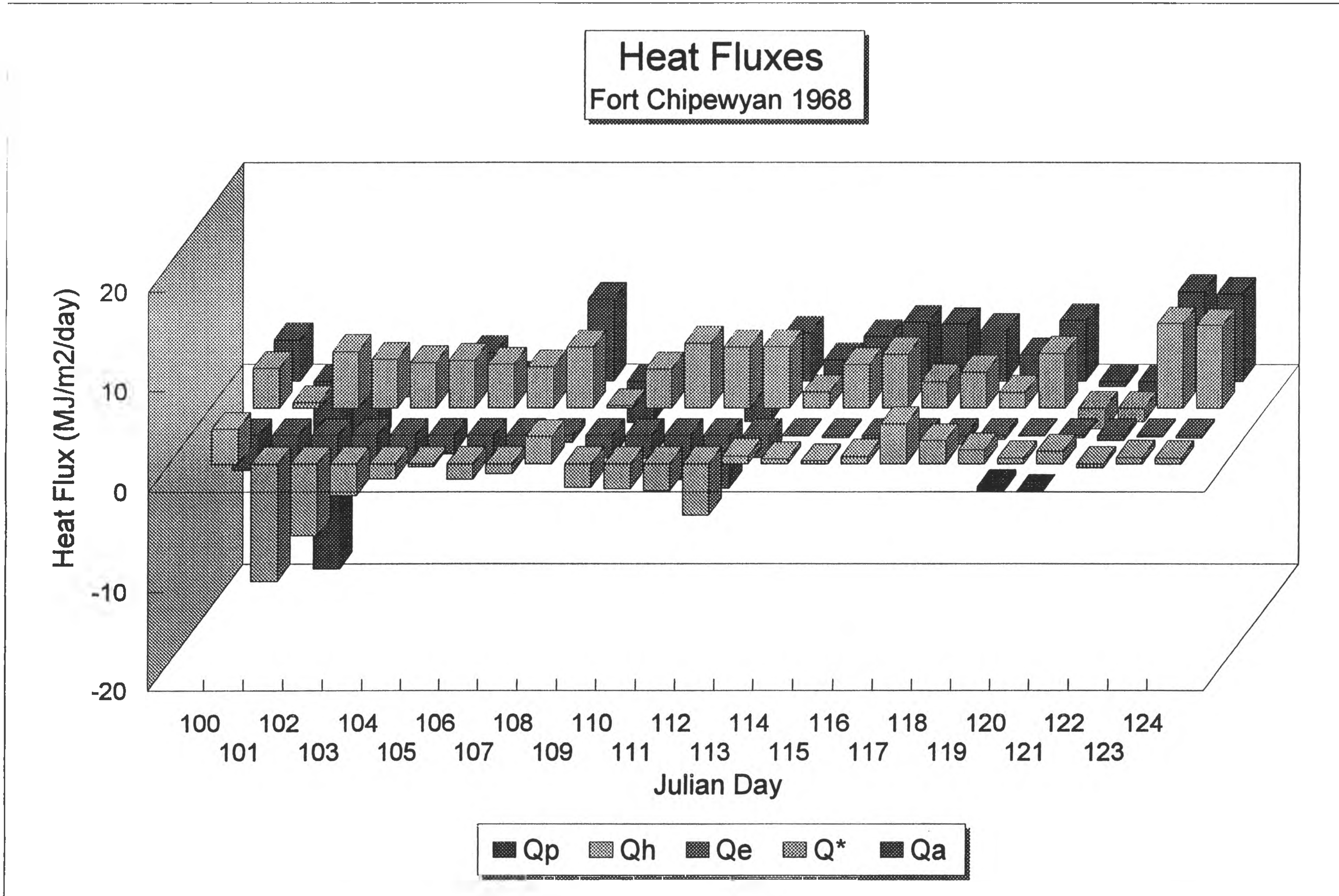

Figure 6.11 g) Daily heat flux calculations for Fort Chipewyan

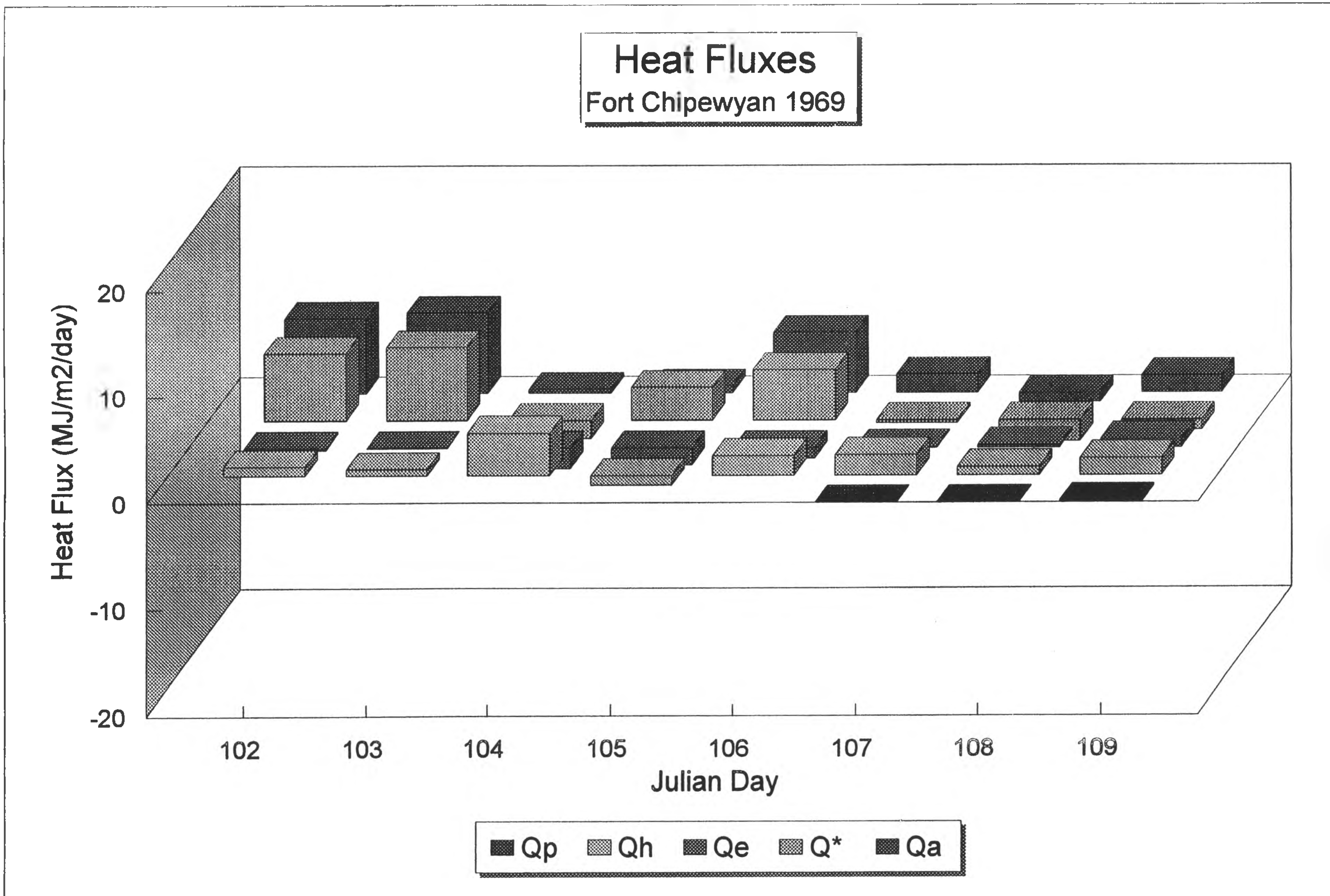

Figure 6.11 h) Daily heat flux calculations for Fort Chipewyan

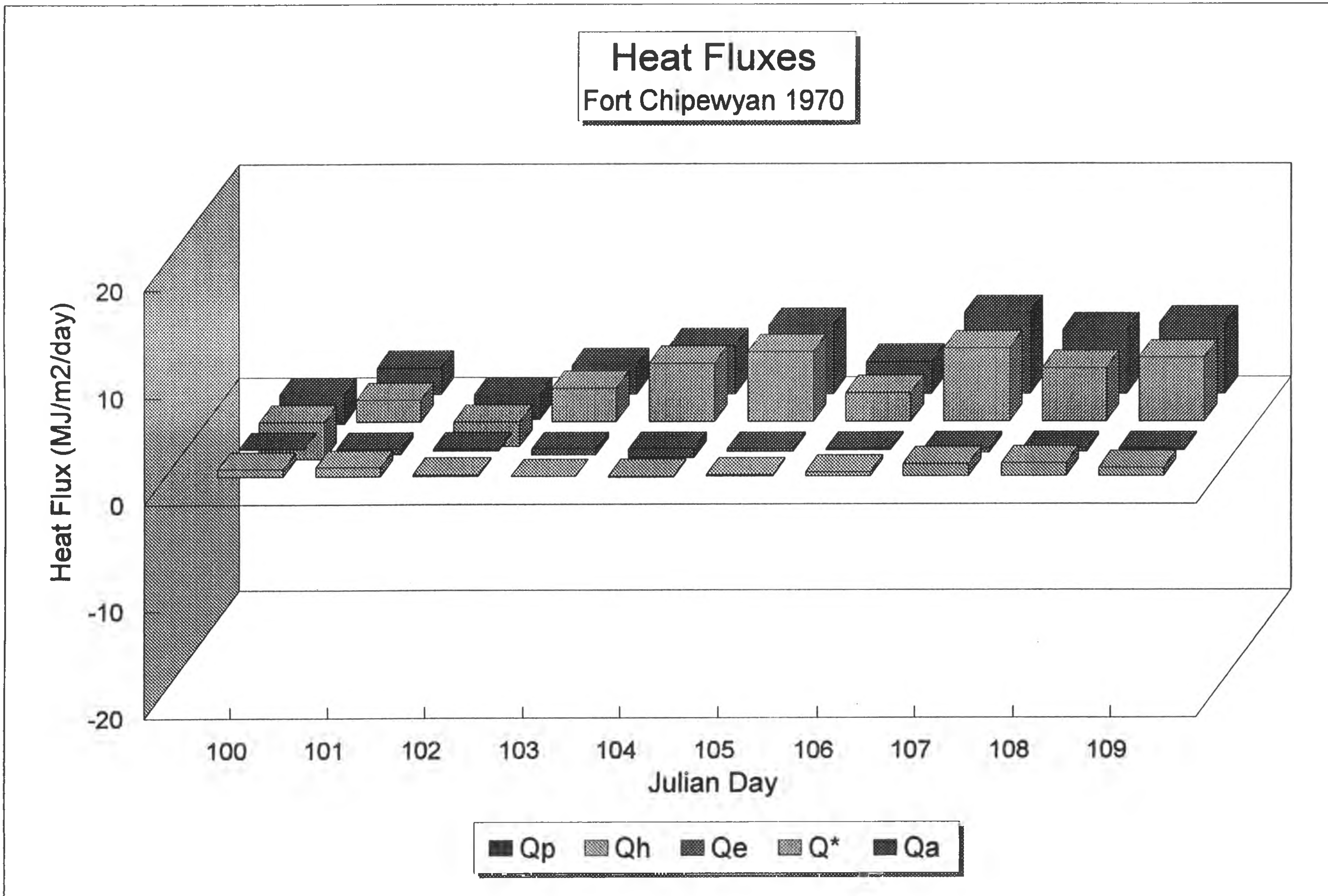

Figure 6.11 i) Daily heat flux calculations for Fort Chipewyan

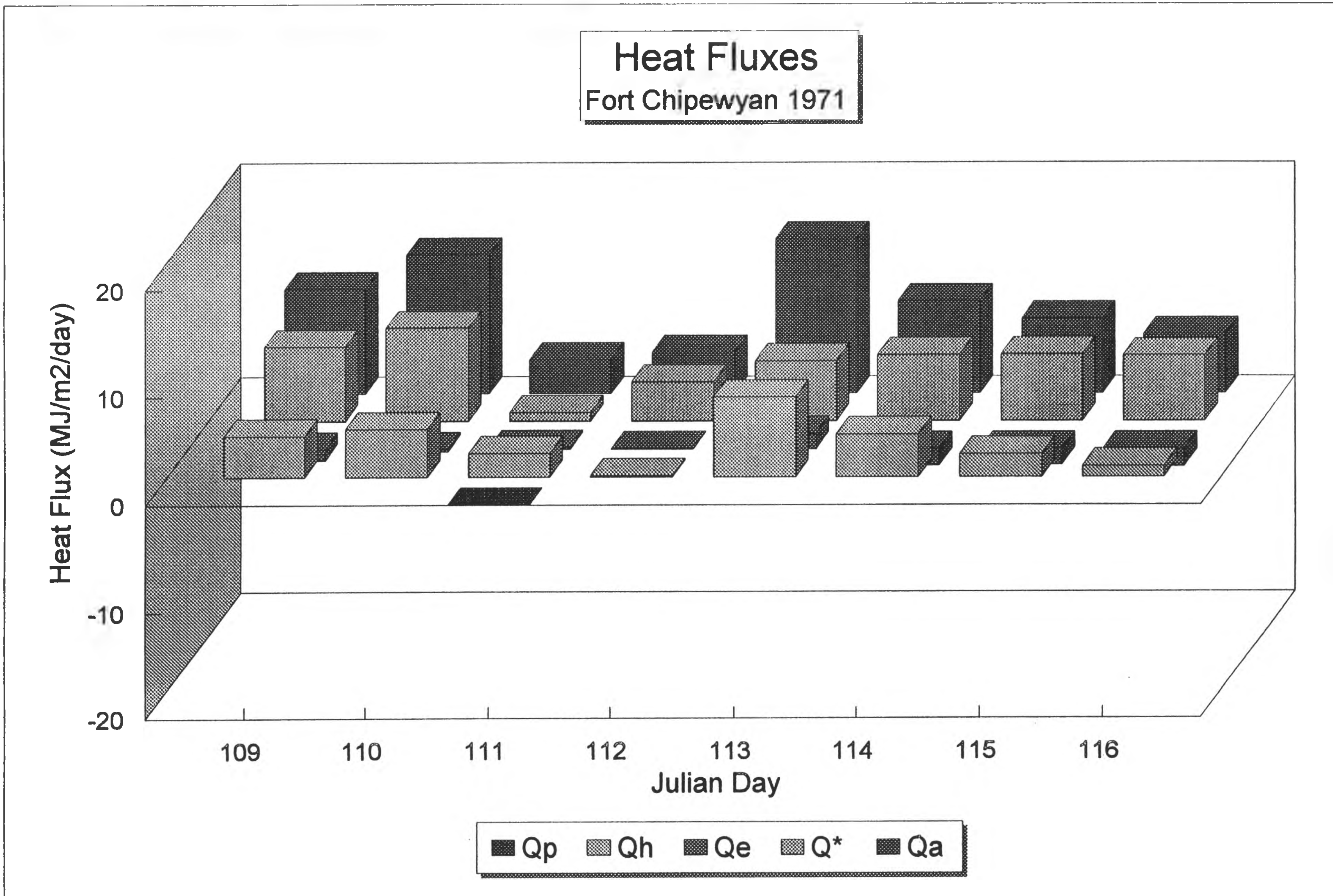

Figure 6.11 j) Daily heat flux calculations for Fort Chipewyan

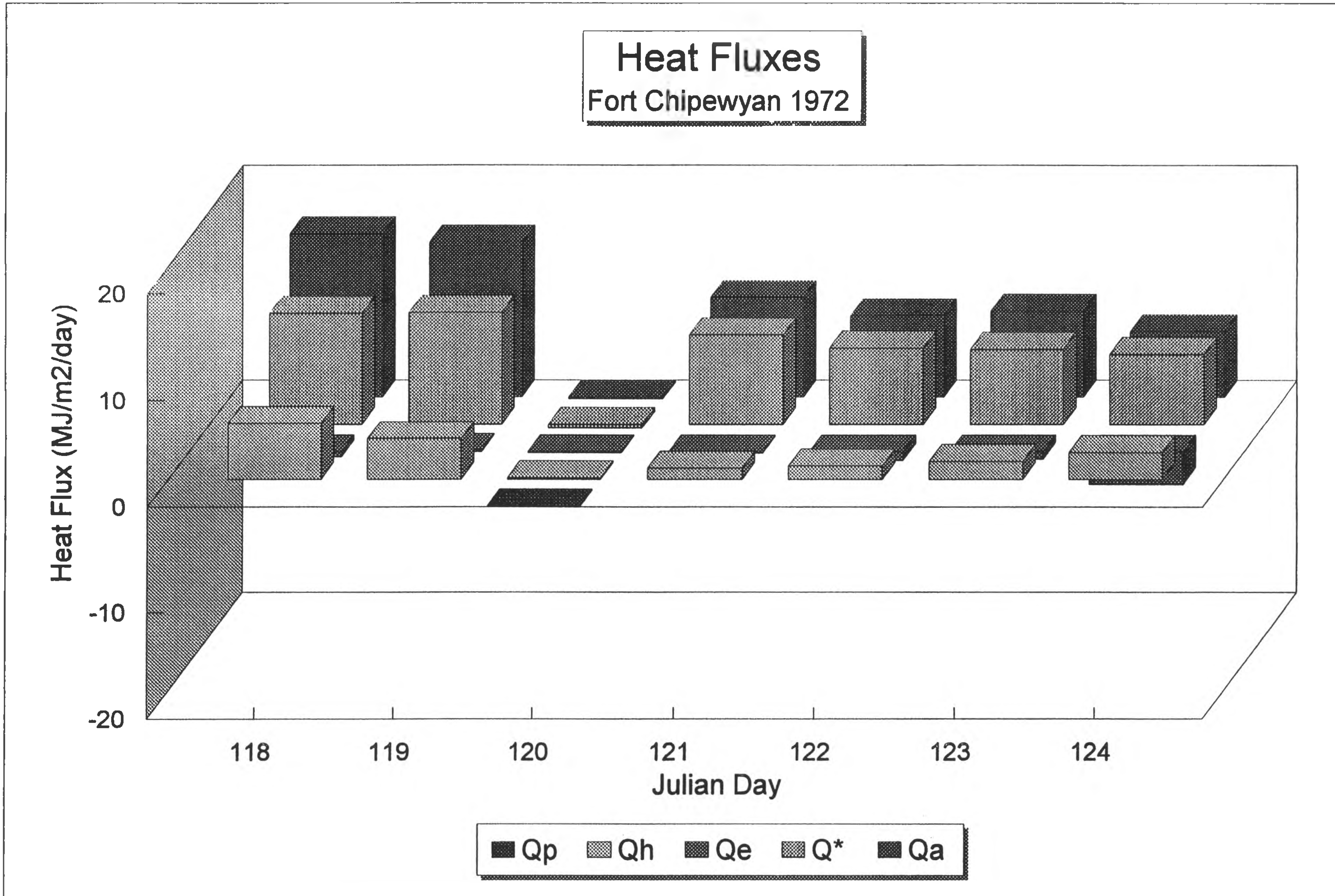

Figure 6.11 k) Daily heat flux calculations for Fort Chipewyan

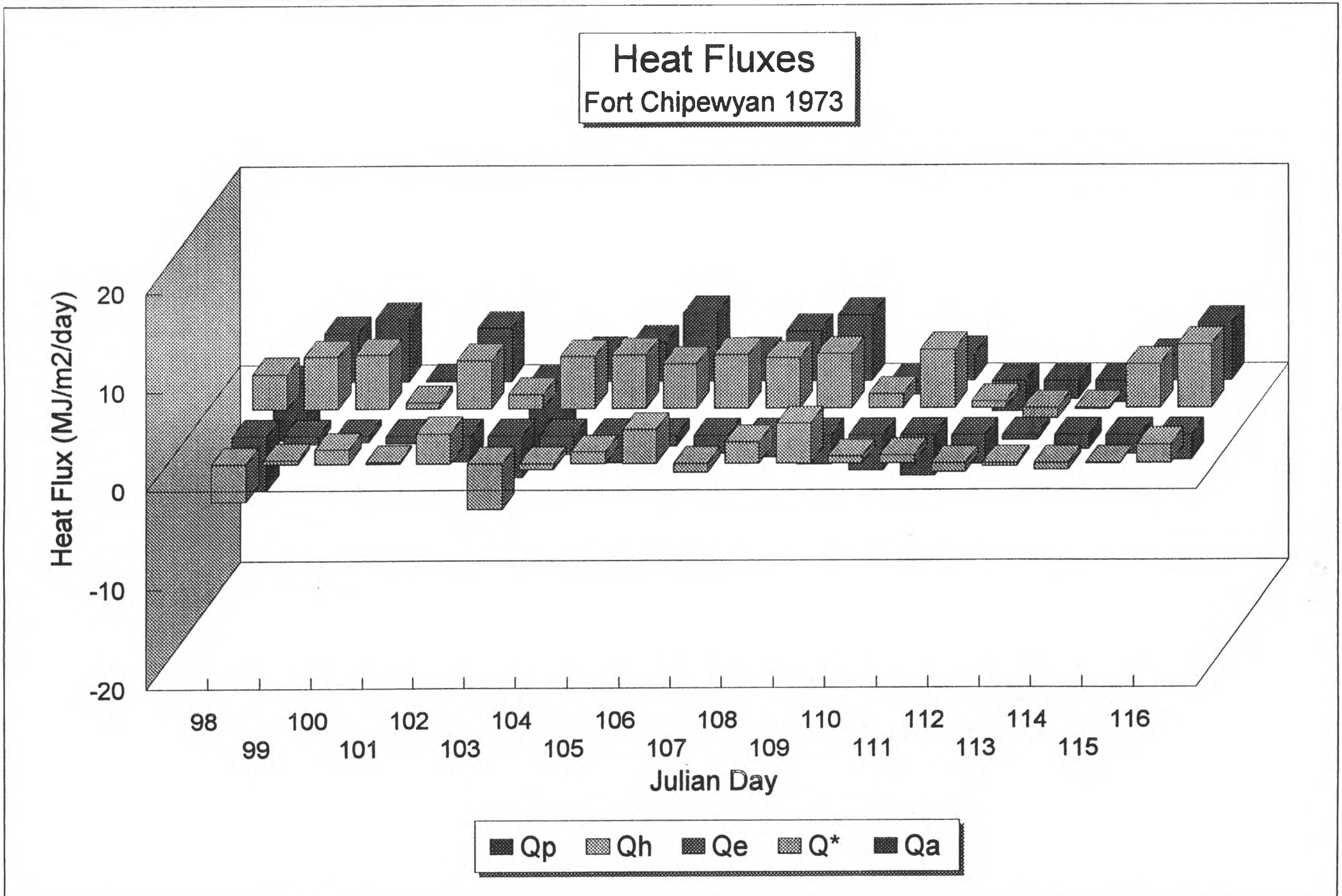

Figure 6.11 l) Daily heat flux calculations for Fort Chipewyan

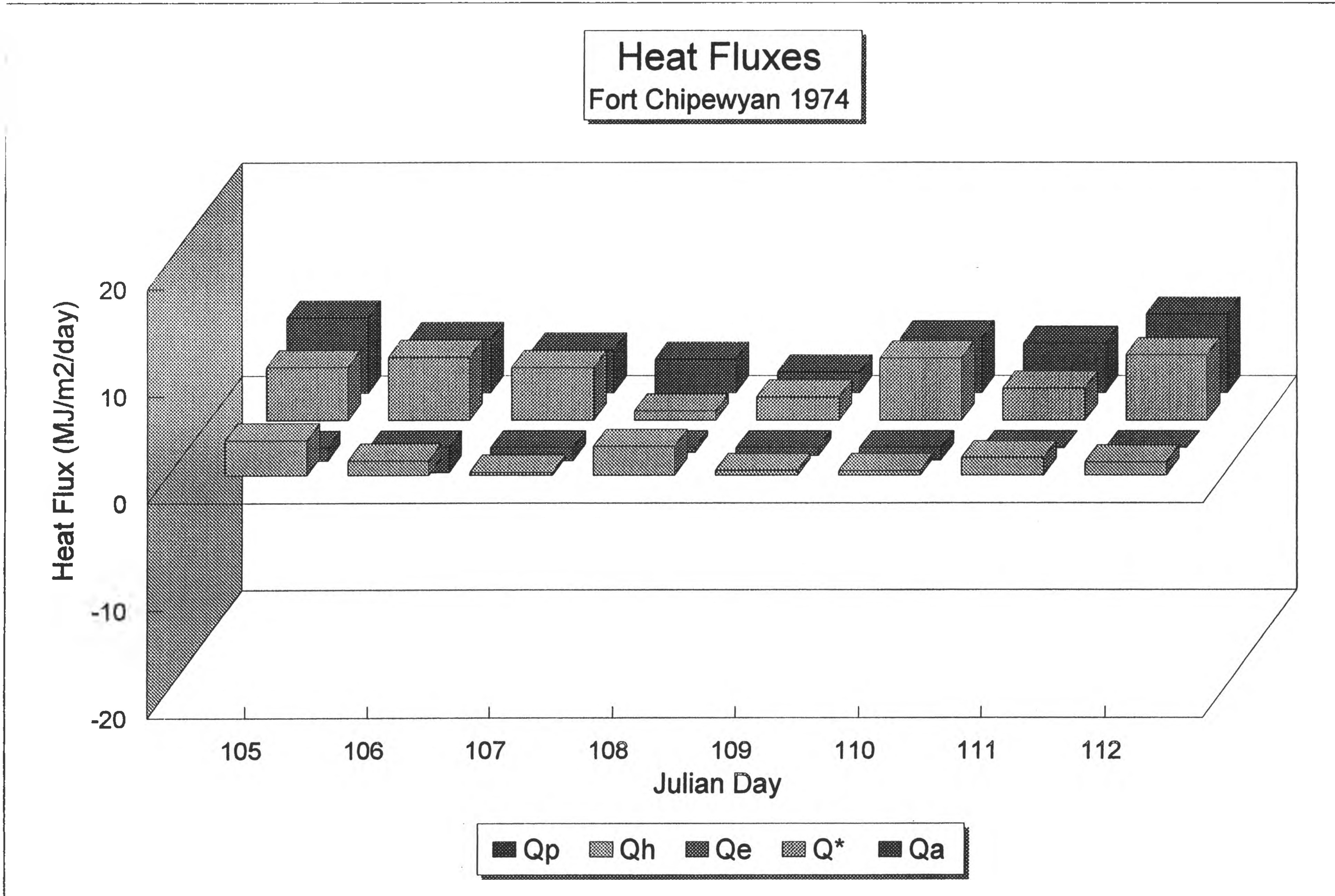

Figure 6.11 m) Daily heat flux calculations for Fort Chipewyan

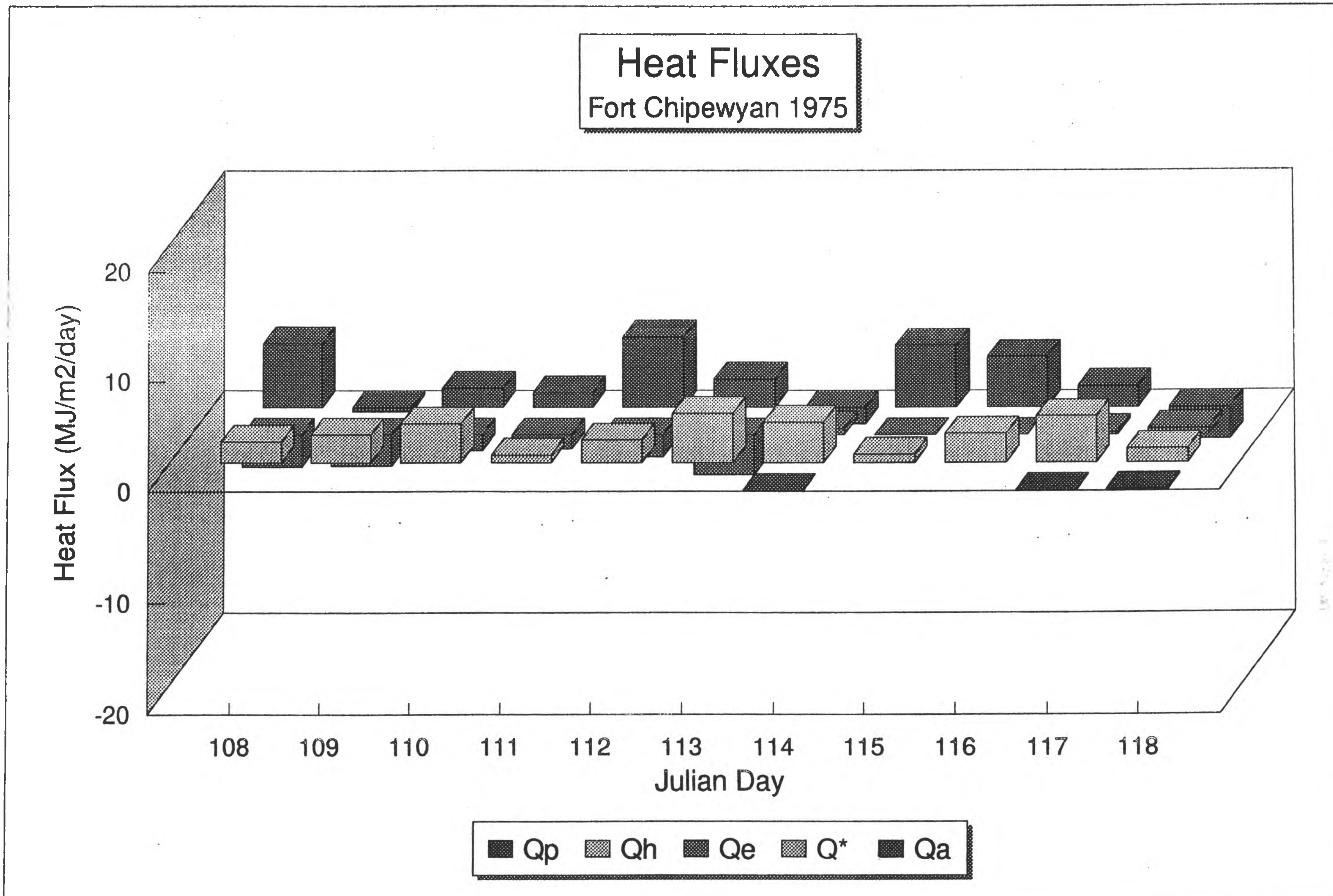

Figure 6.11 n) Daily heat flux calculations for Fort Chipewyan

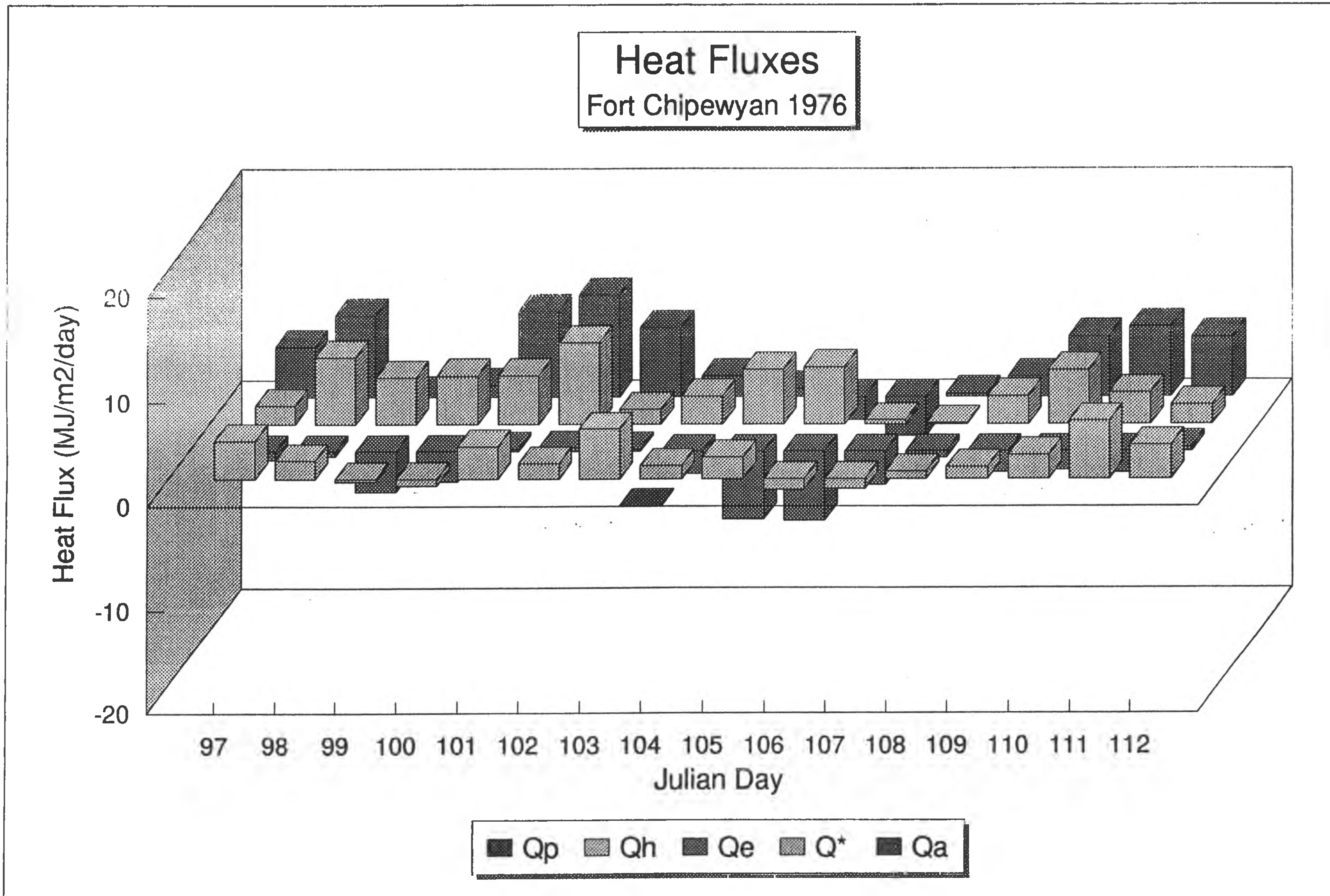

Figure 6.11 o) Daily heat flux calculations for Fort Chipewyan

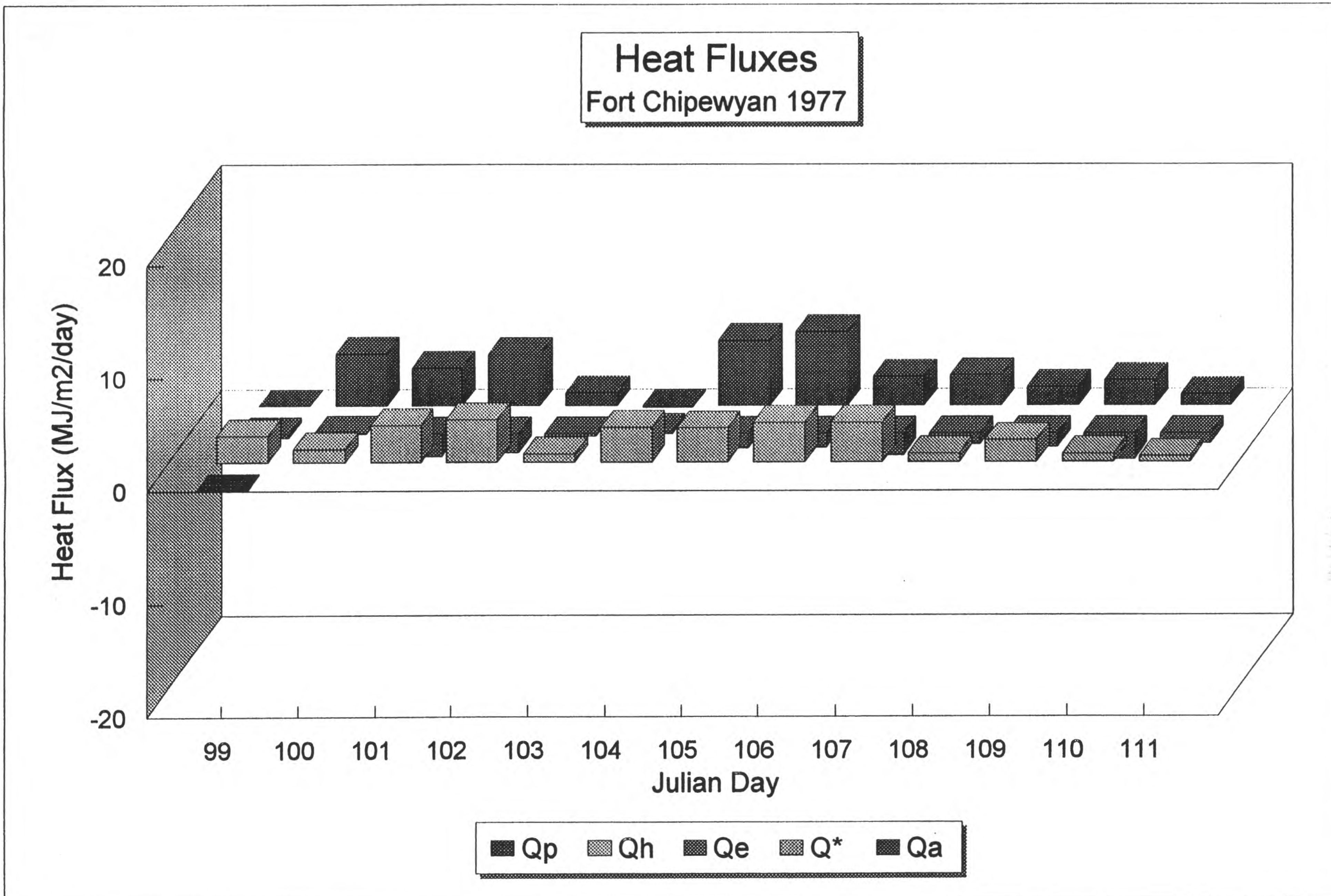

Figure 6.11 p) Daily heat flux calculations for Fort Chipewyan

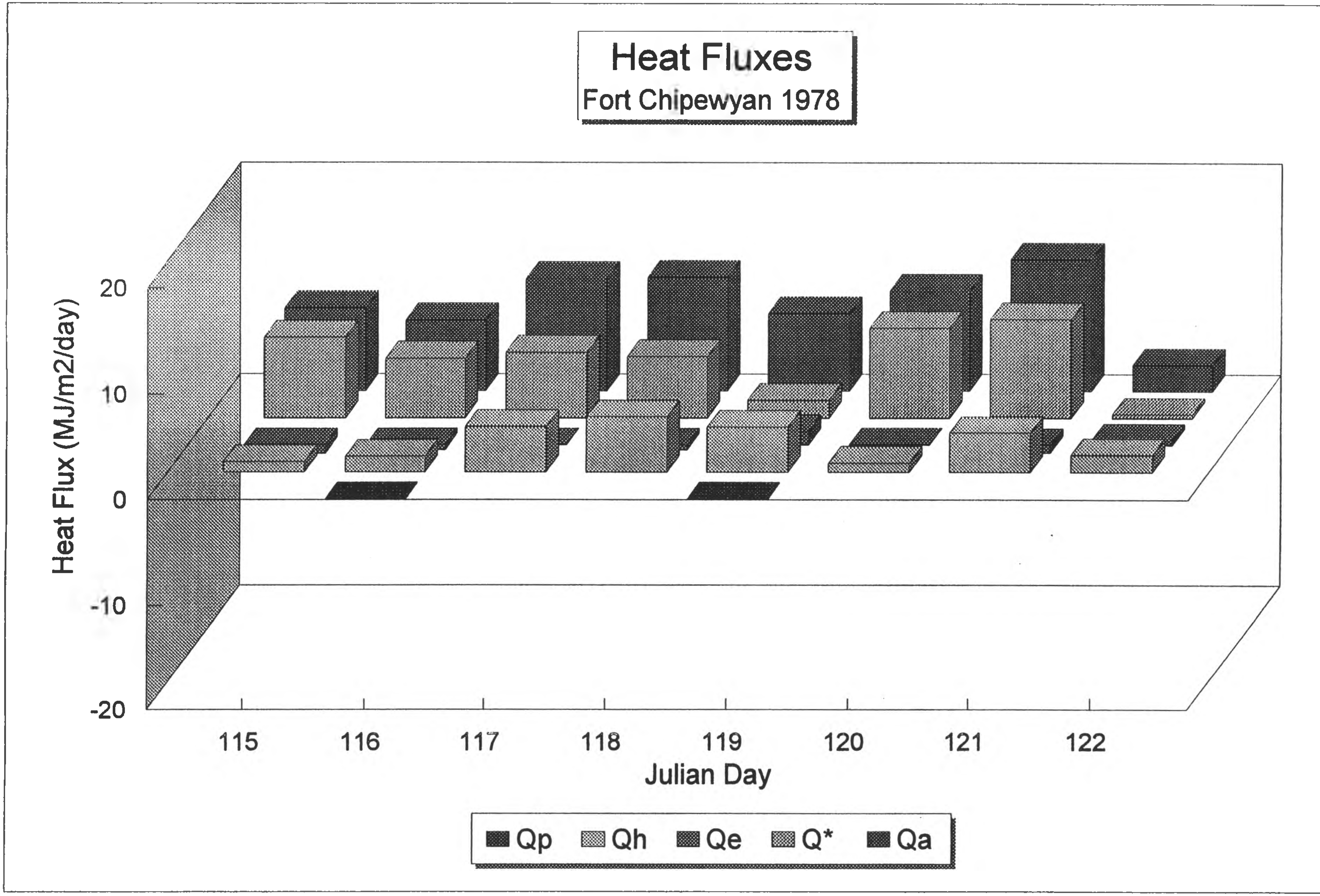

Figure 6.11 q) Daily heat flux calculations for Fort Chipewyan

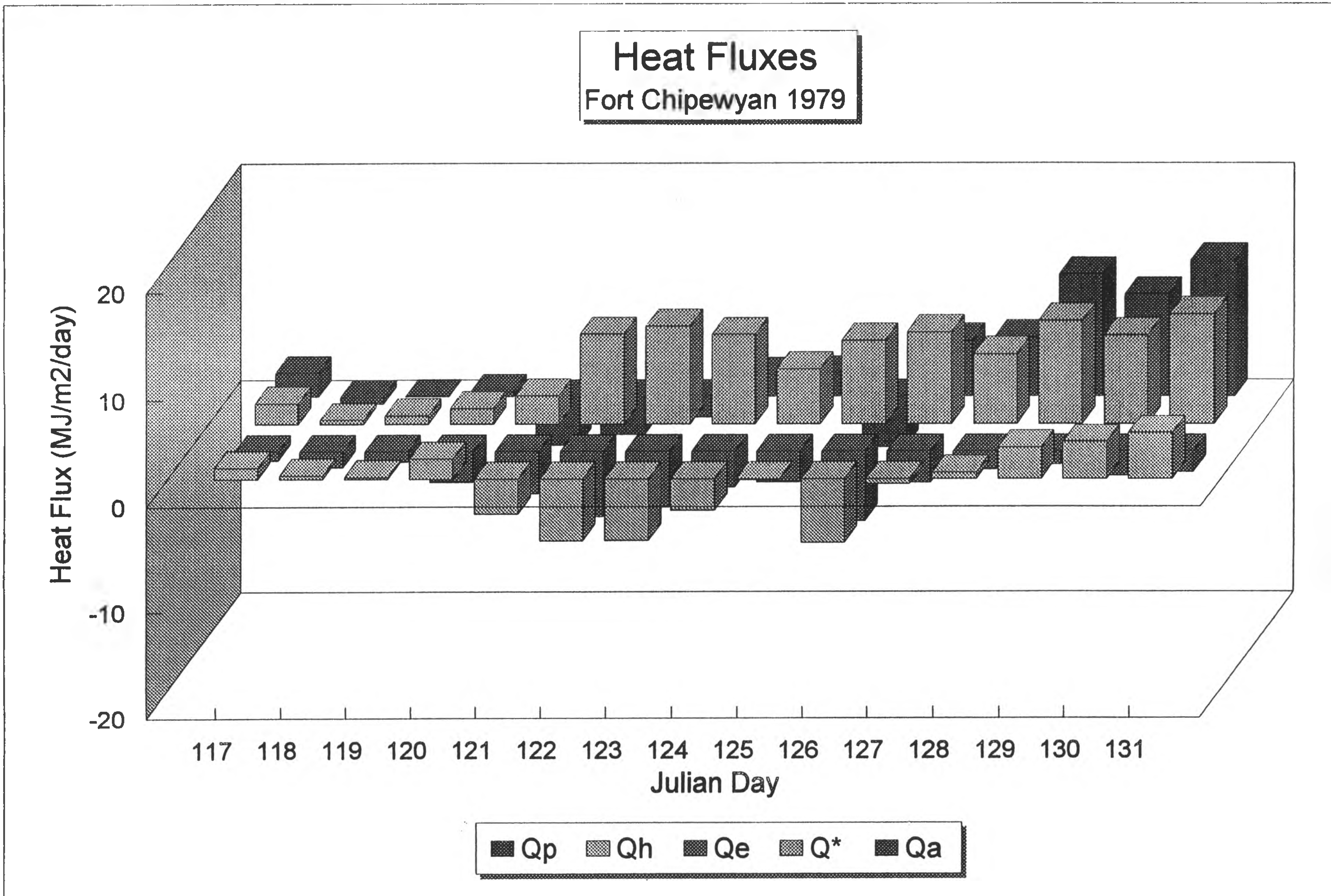

Figure 6.12. Net heat flux summary for Peace River 1963-79.

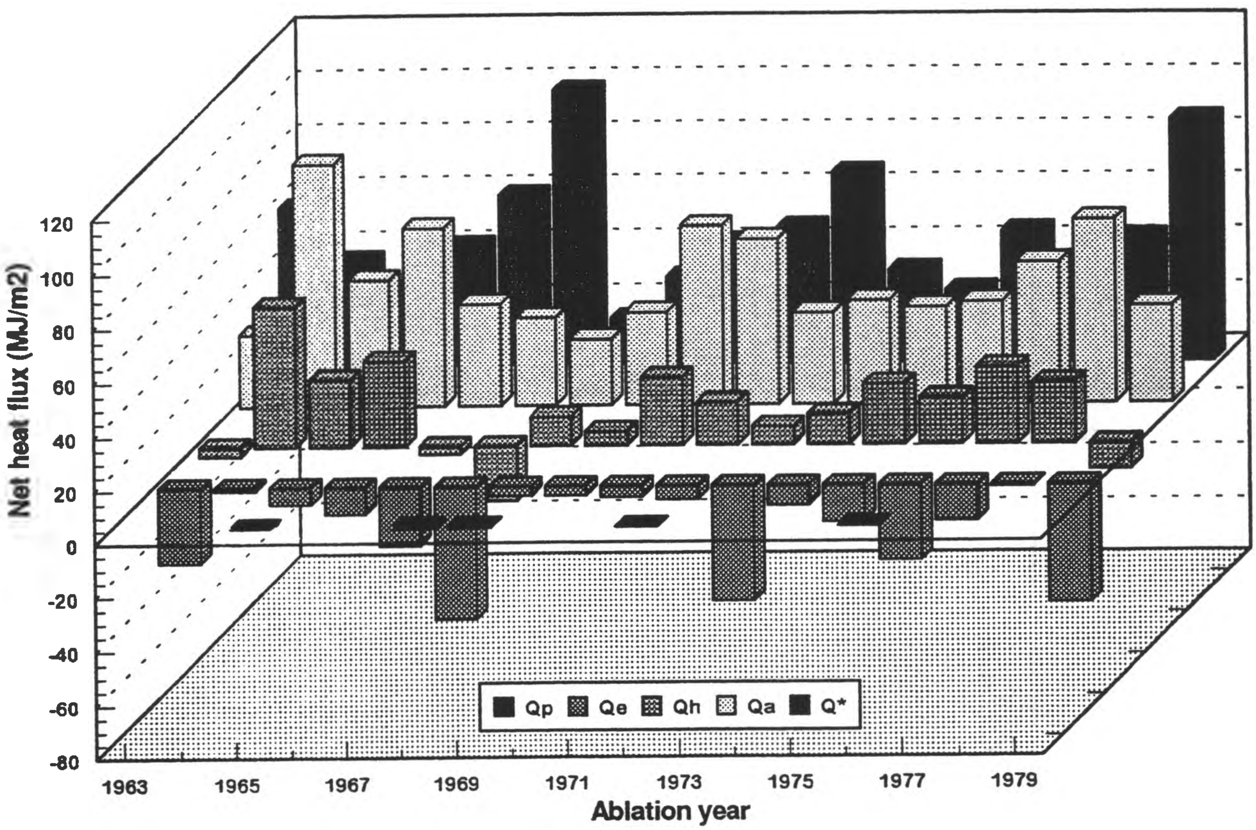

Figure 6.13 Positive heat flux summary for Peace River 1963-79

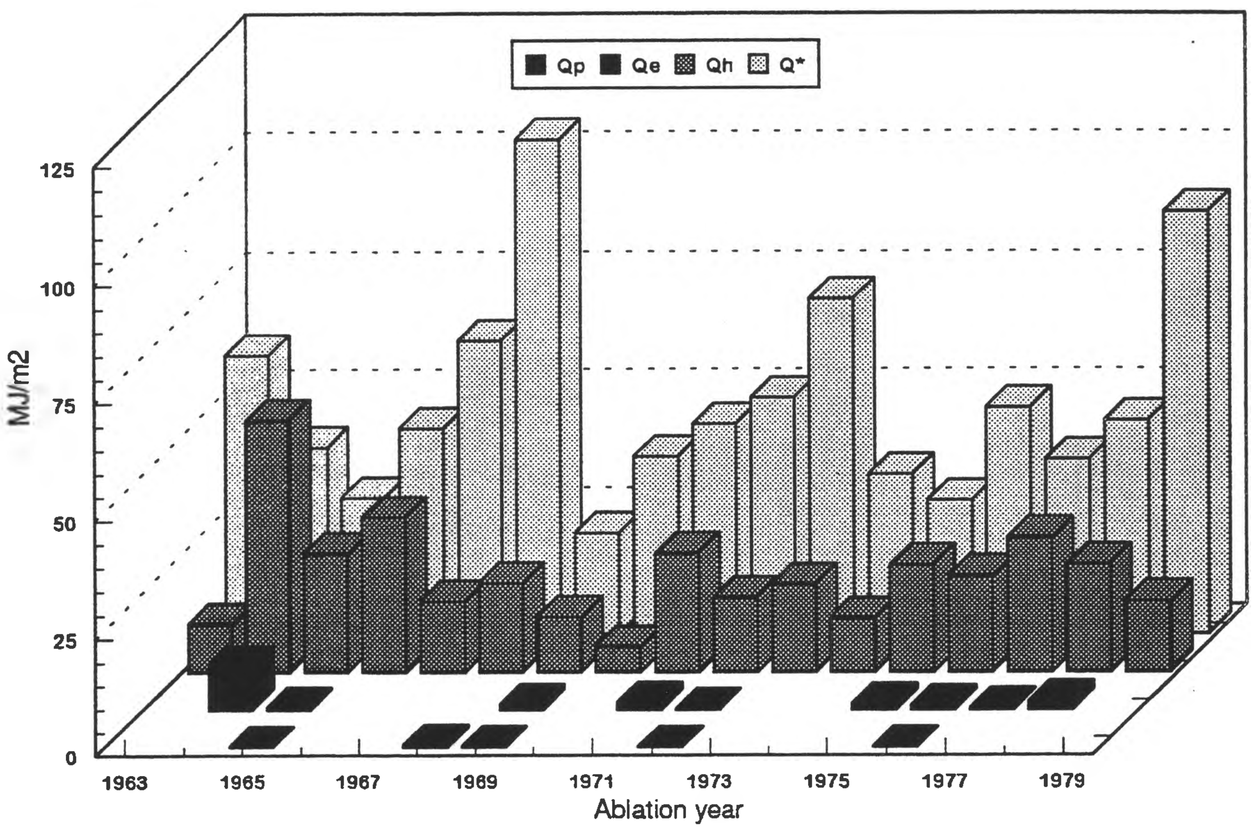

Figure 6.14. Relative net heat flux summary for the Peace River, 1963-79.

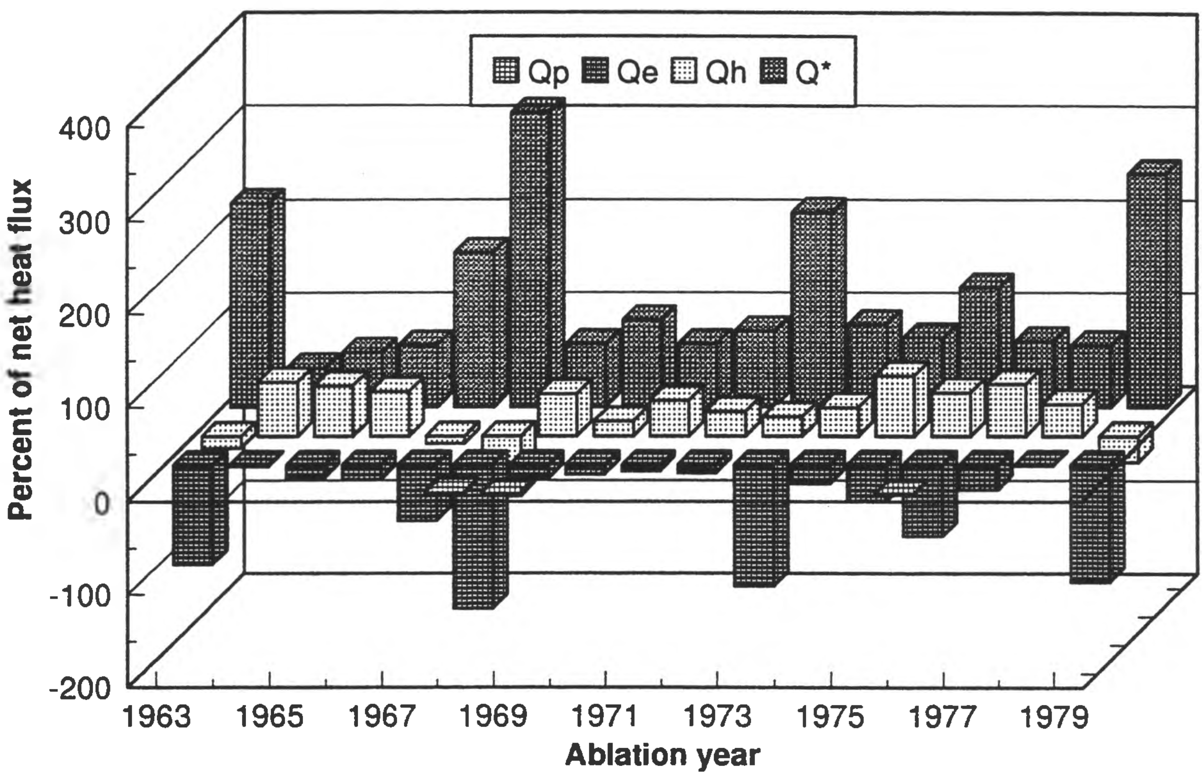

Figure 6.15. Relative positive heat flux summary for the Peace River, 1963-79.

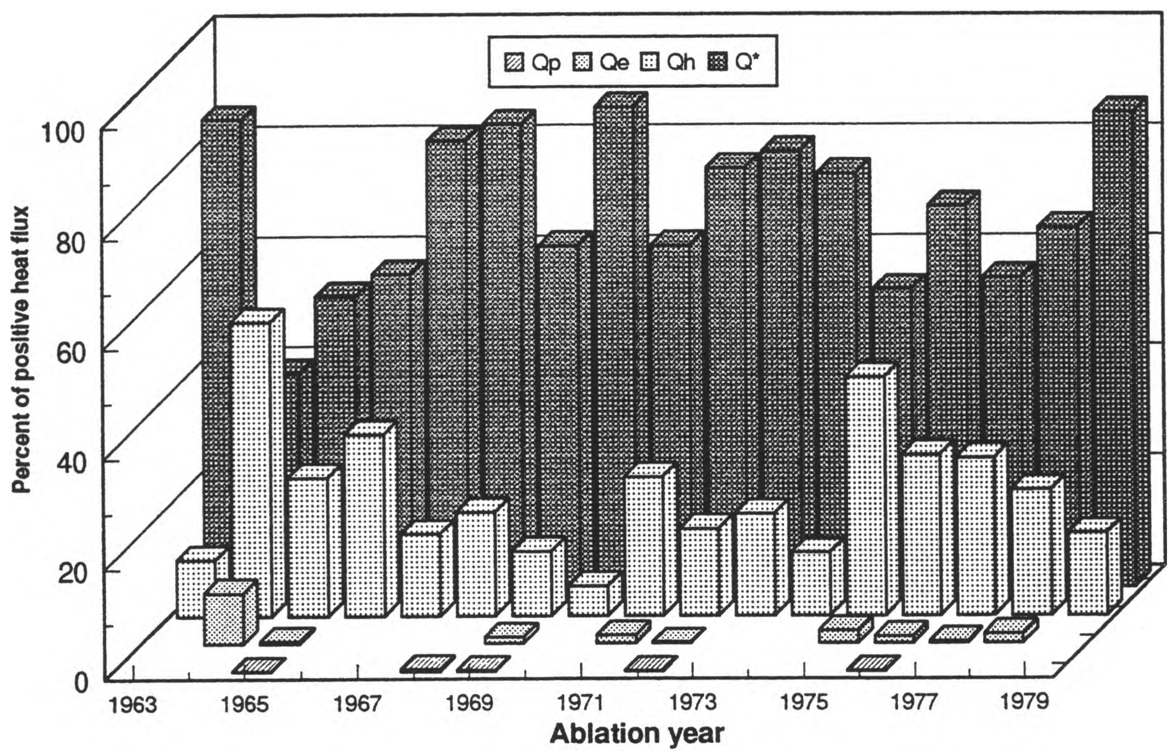

Figure 6.16. Radiation flux summary for Peace River 1963-79.

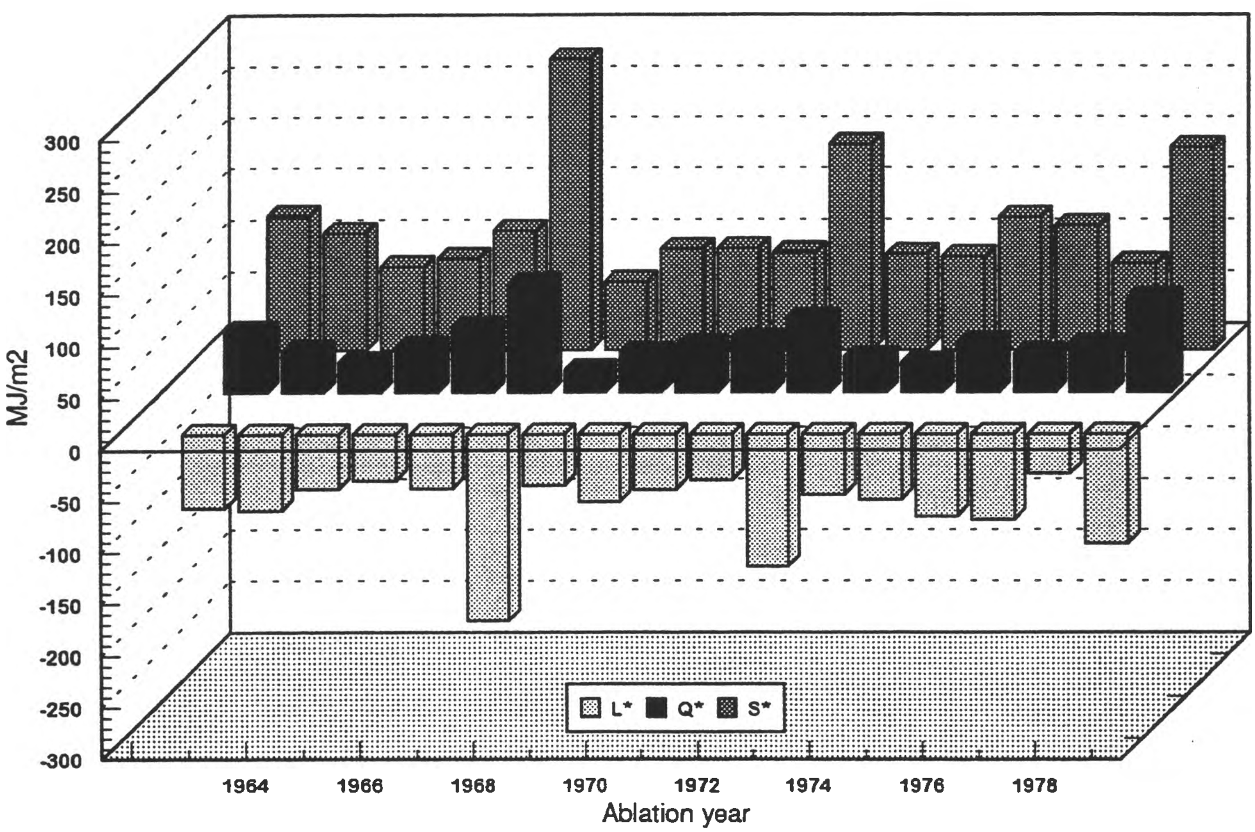

Figure 6.17. Net heat flux versus stage increase for Peace Point 1963-79. (Circles indicate years 1968-72).

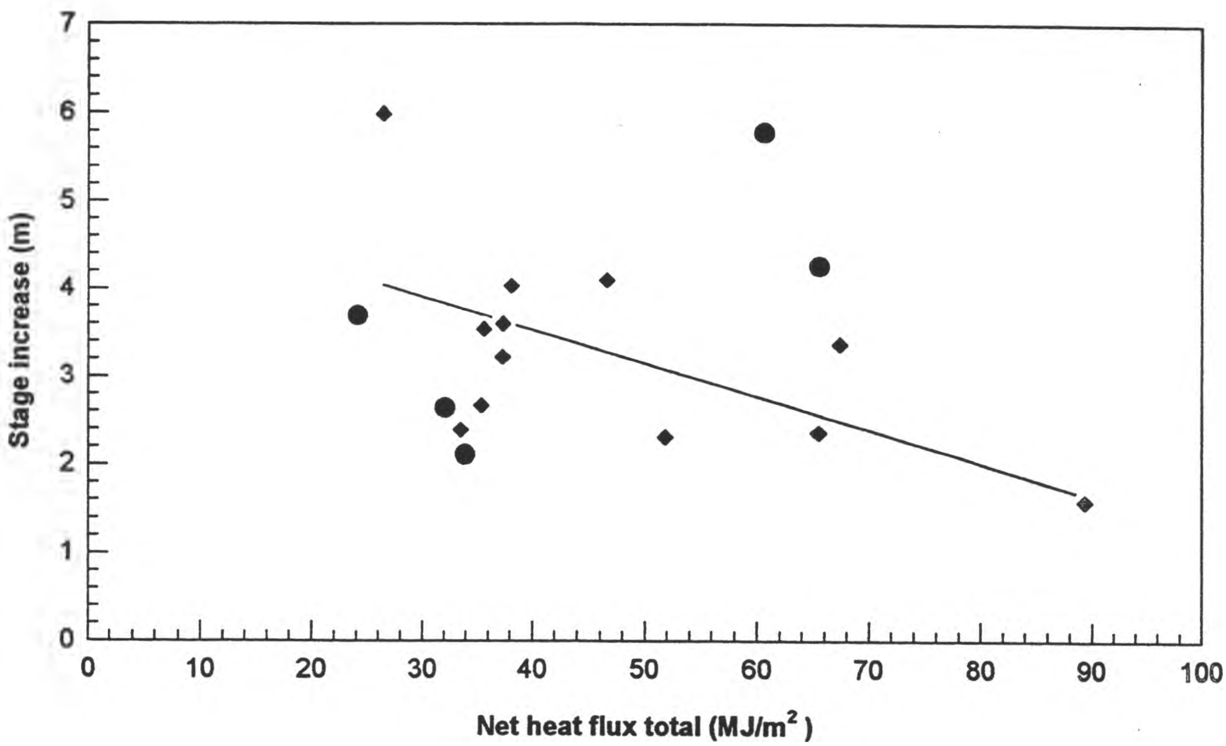

Figure 6.18. Positive heat flux versus stage increase for Peace Point 1963-79. (Circles indicate years 1968-72).

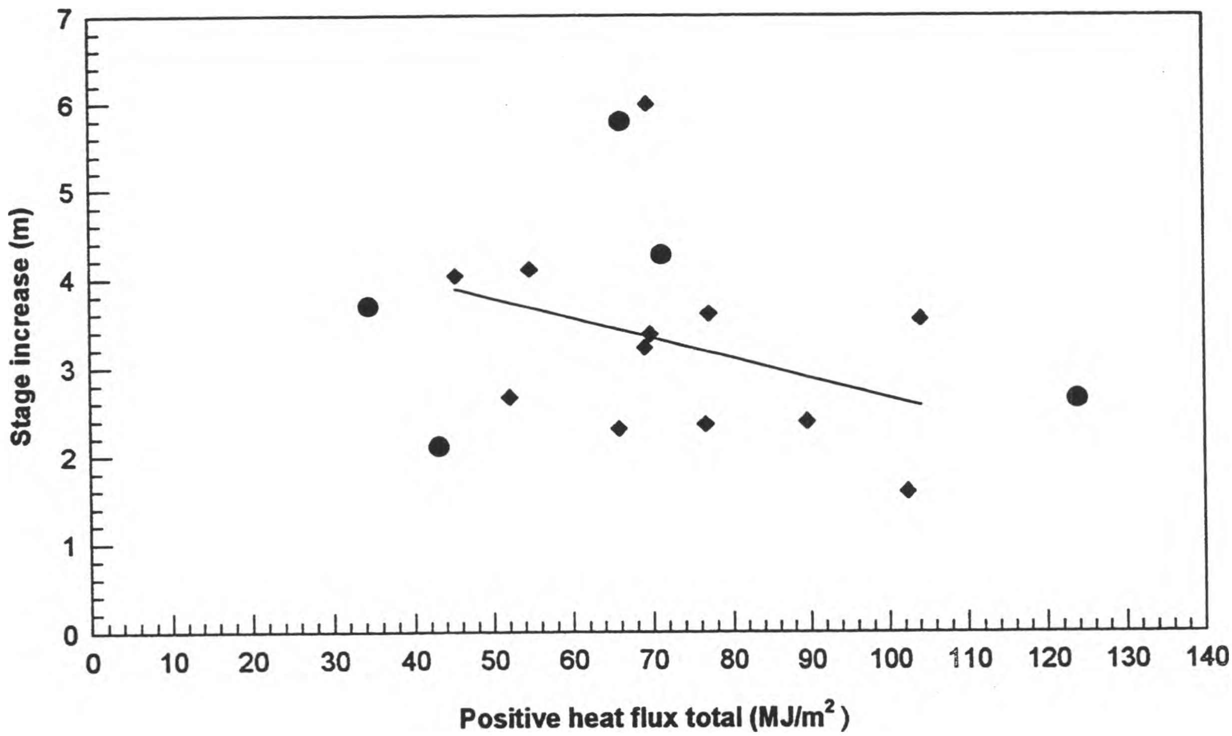

Figure 6.19. Melting degree days for Fort Chipewyan 1963-92, using a base of -5° C.

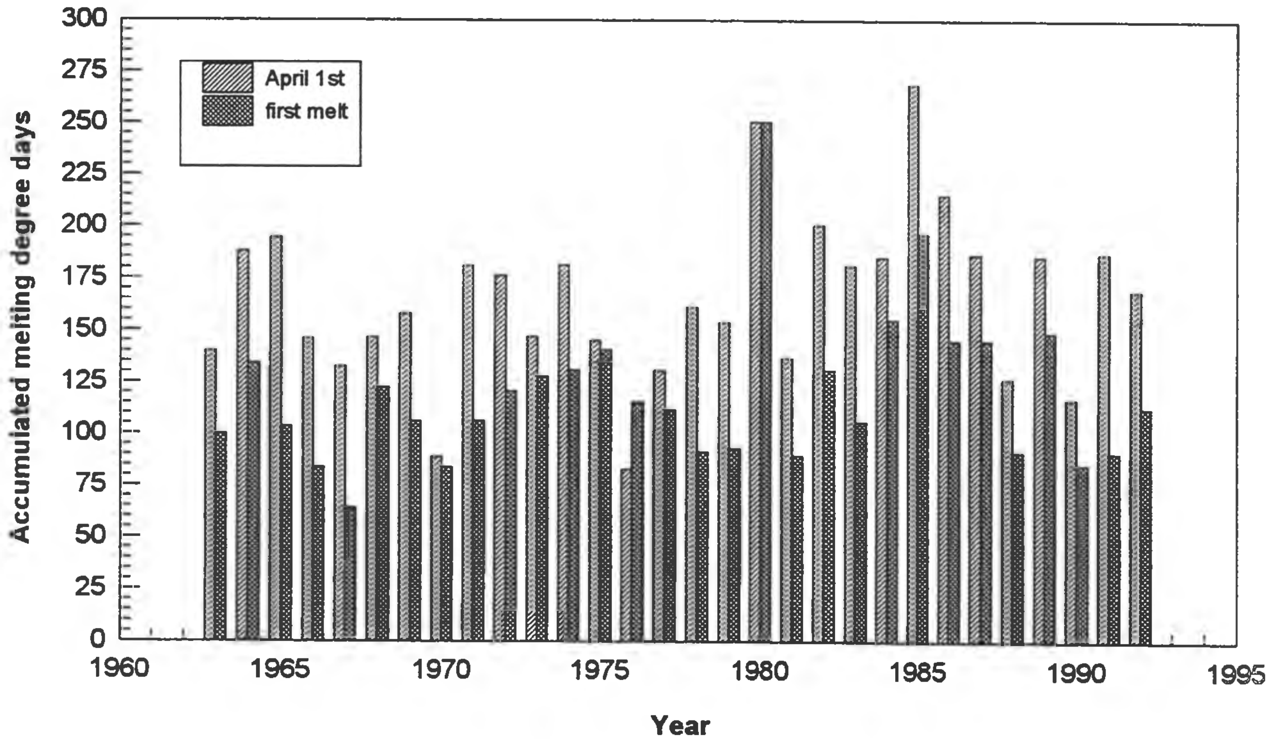

Figure 6.20. Melting degree days from April 1st to break-up versus stage increase for Peace Point 1963-92. (Circles indicate years 1968-72).

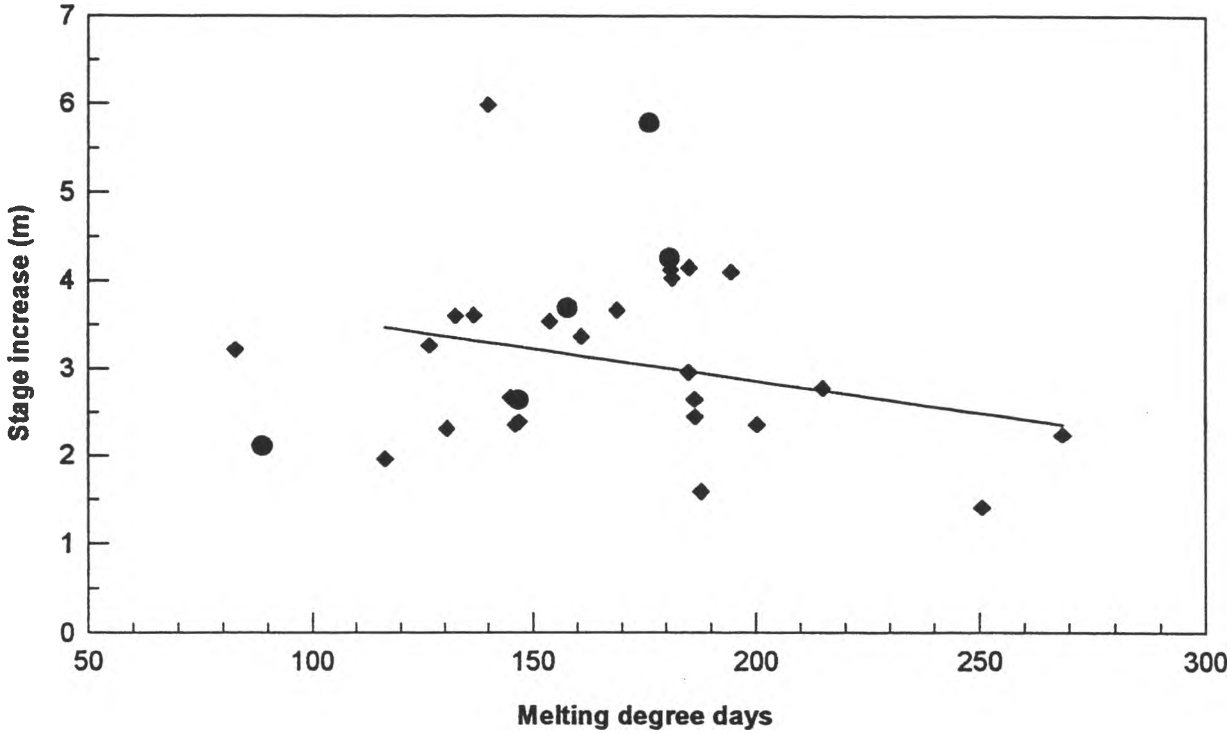

Figure 6.21. Melting degree days from first melt to break-up versus stage increase for Peace Point 1963-92. (Circles indicate years 1968-72).

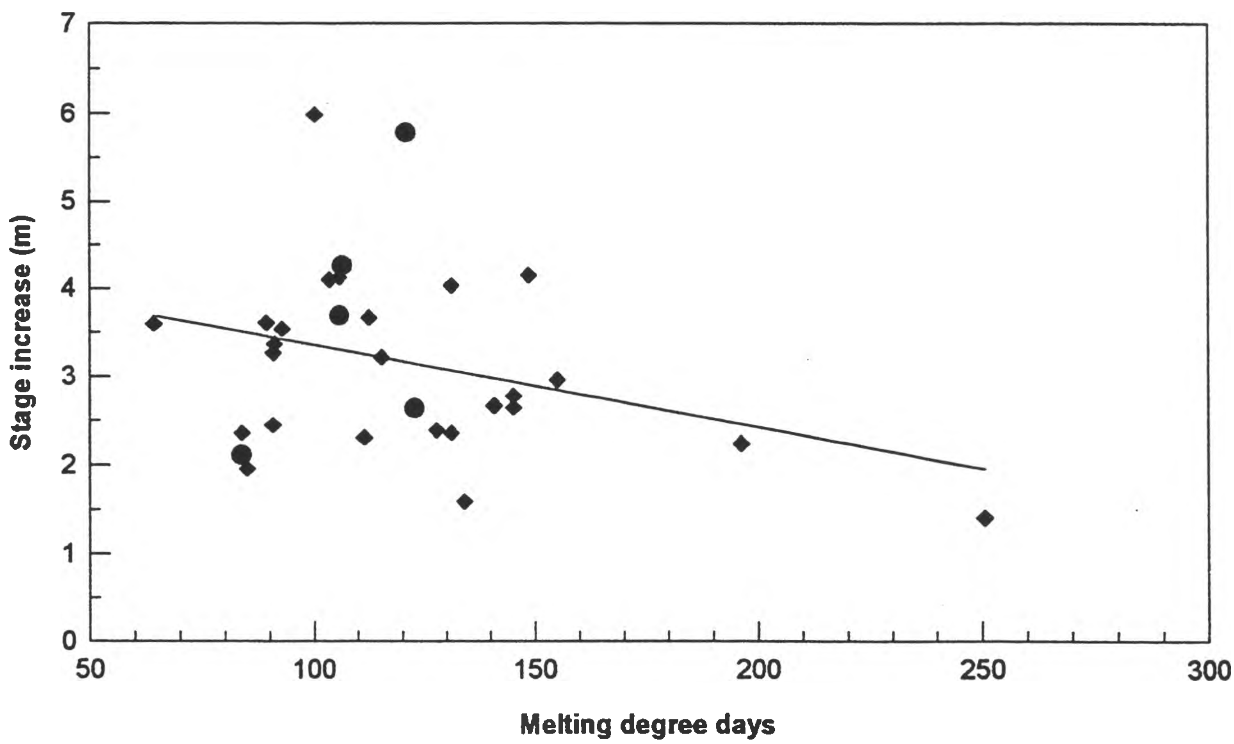

Figure 6.22. Standardized melting degree days from melt initiation to break-up for Fort Chipewyan 1963-92.

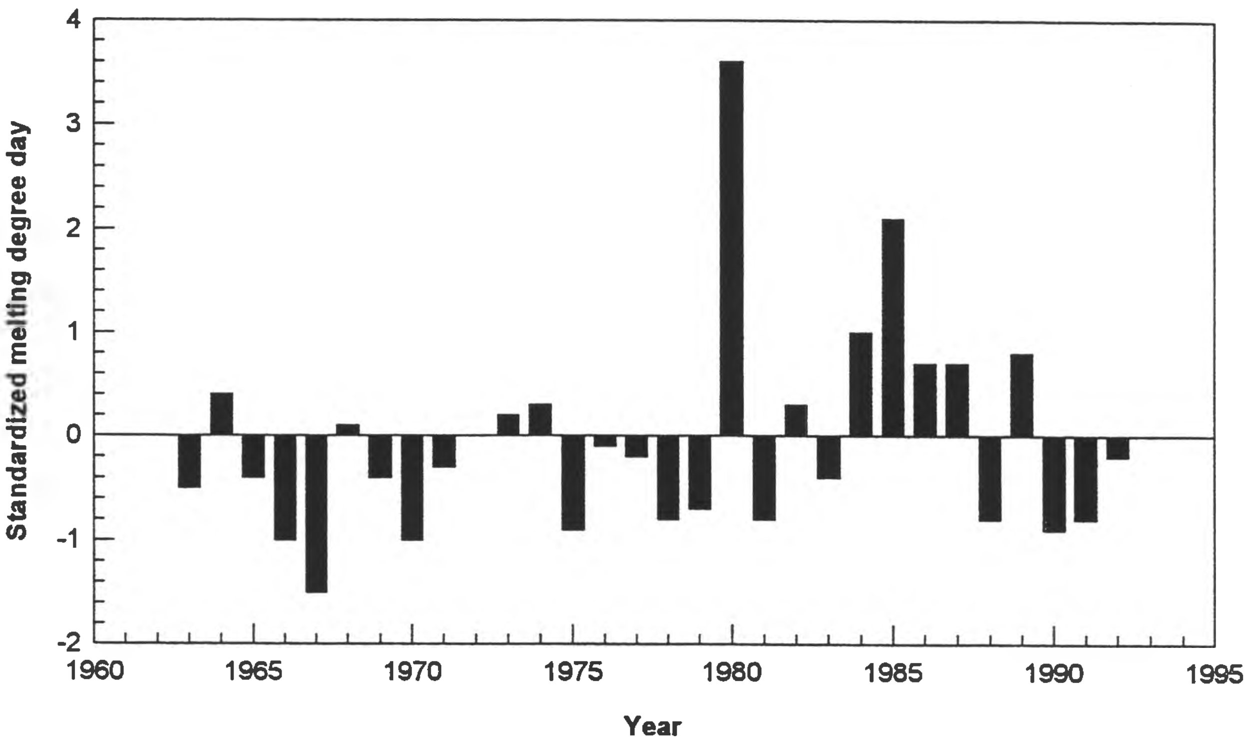

Figure 6.23. Trend in melting degree days from first day of melt to break-up for Fort Chipewyan 1963-92.

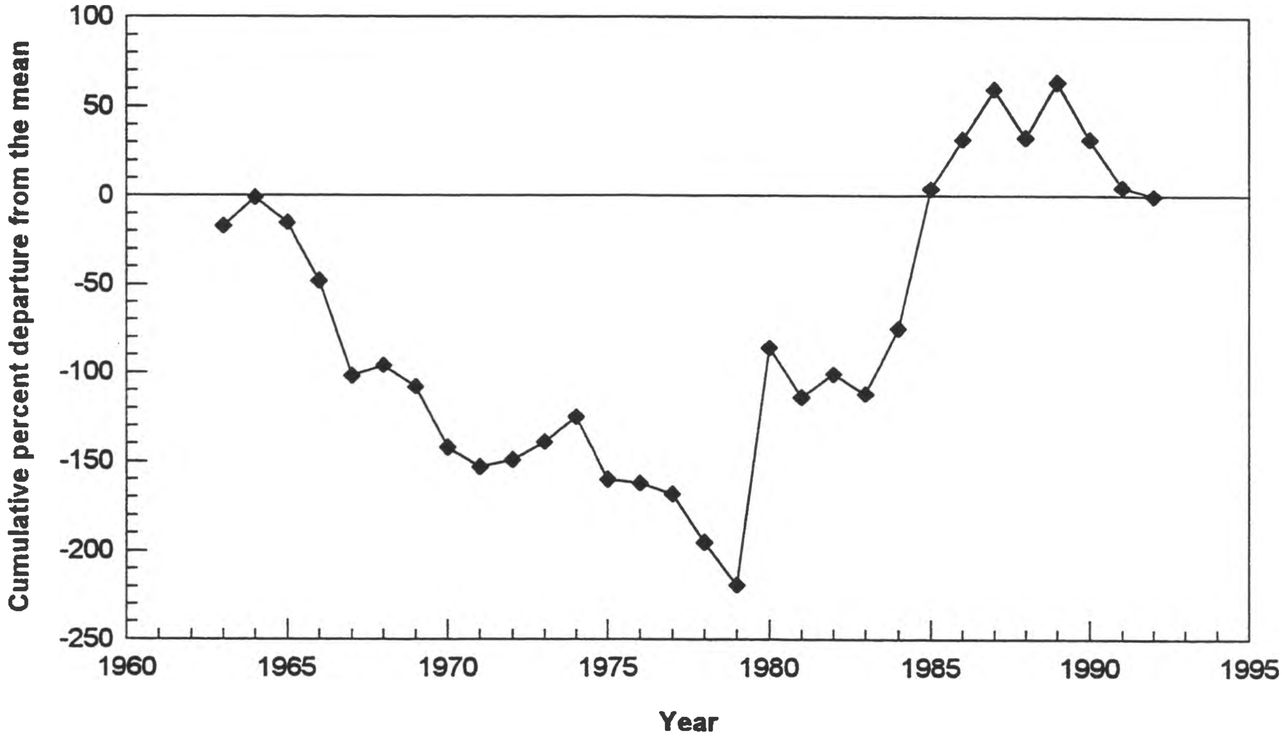

Figure 6.24. Annual ice strength ratio during break-up for Fort Chipewyan.

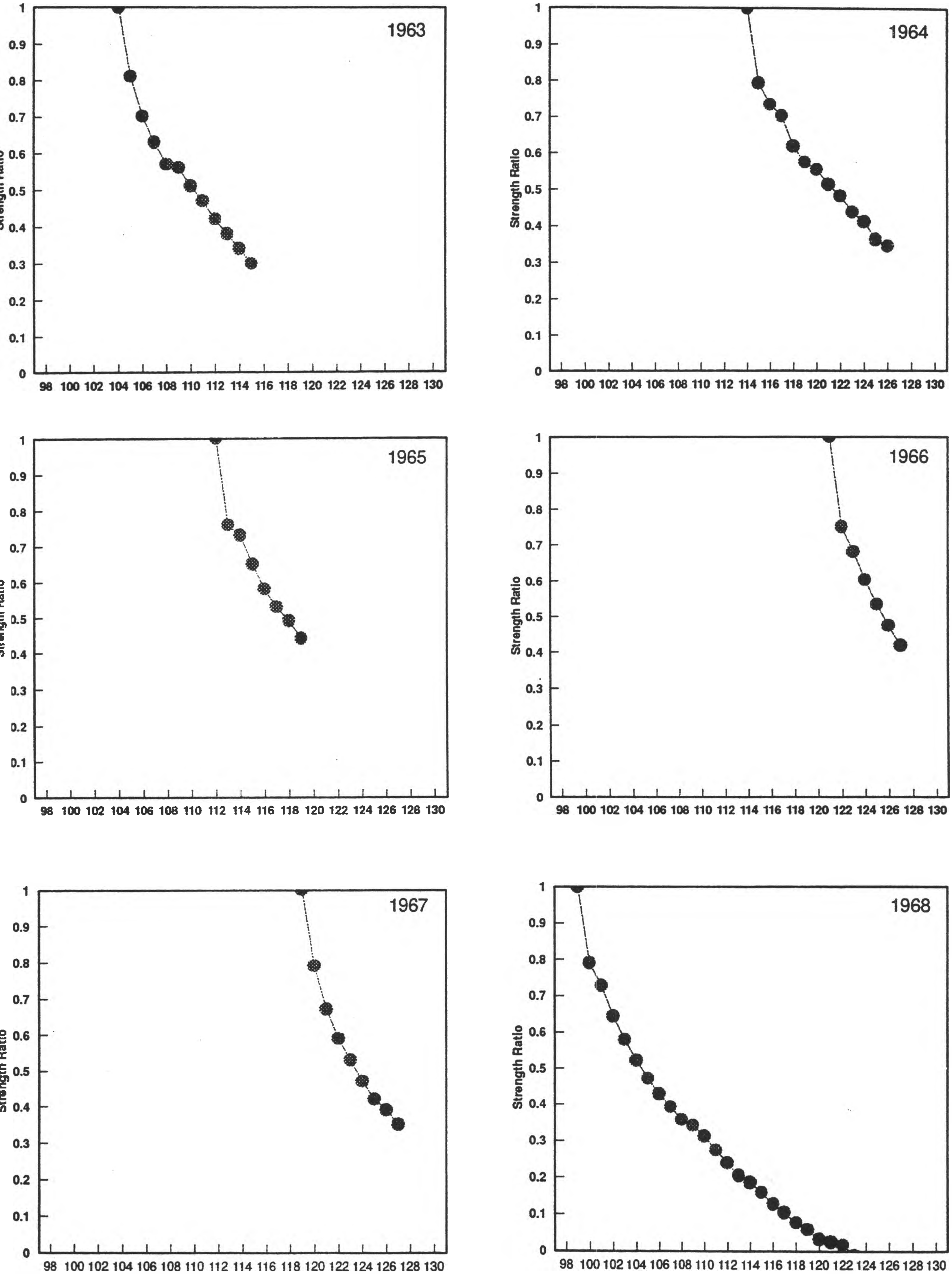

Figure 6.24 (continued).

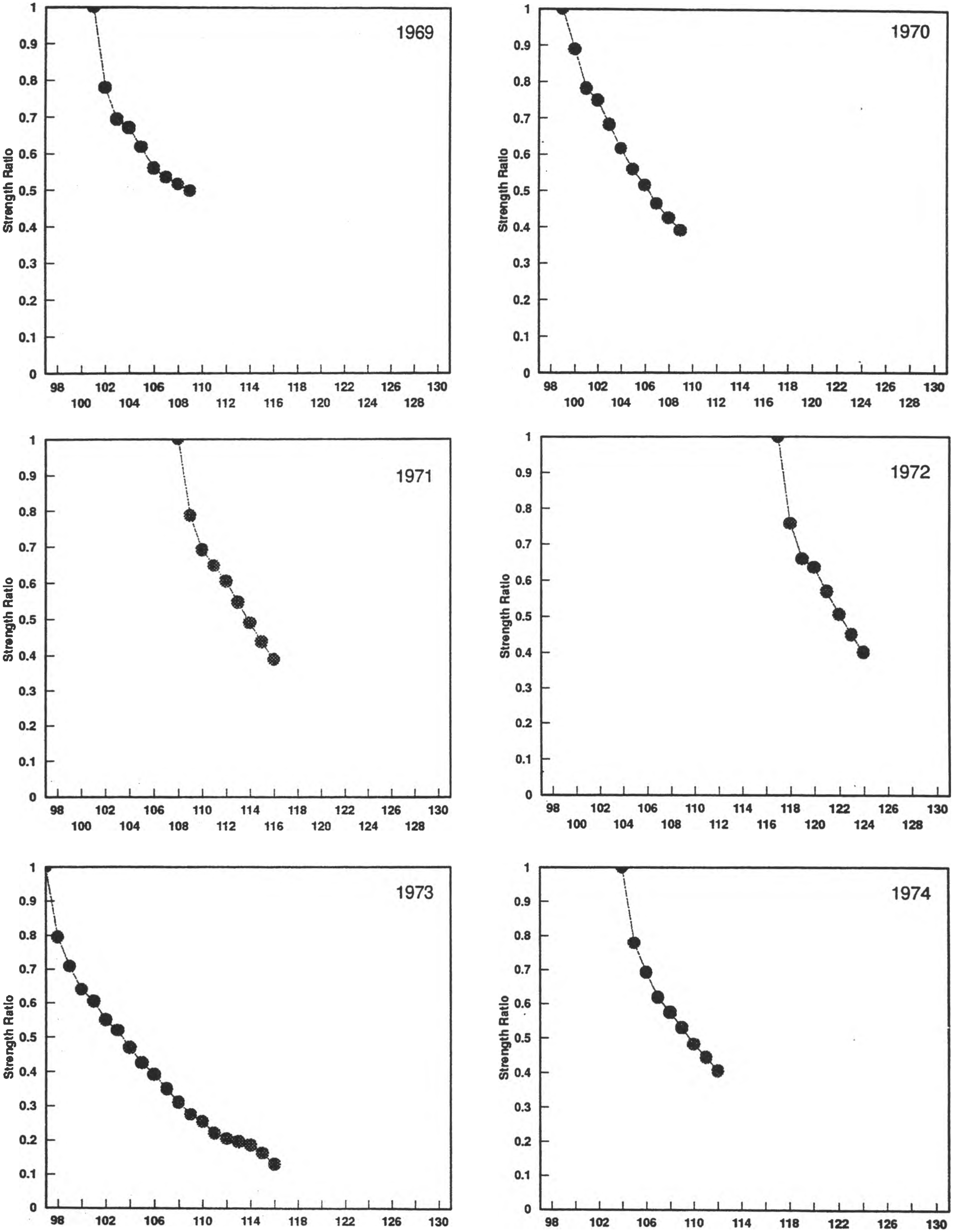

Figure 6.24 (continued).

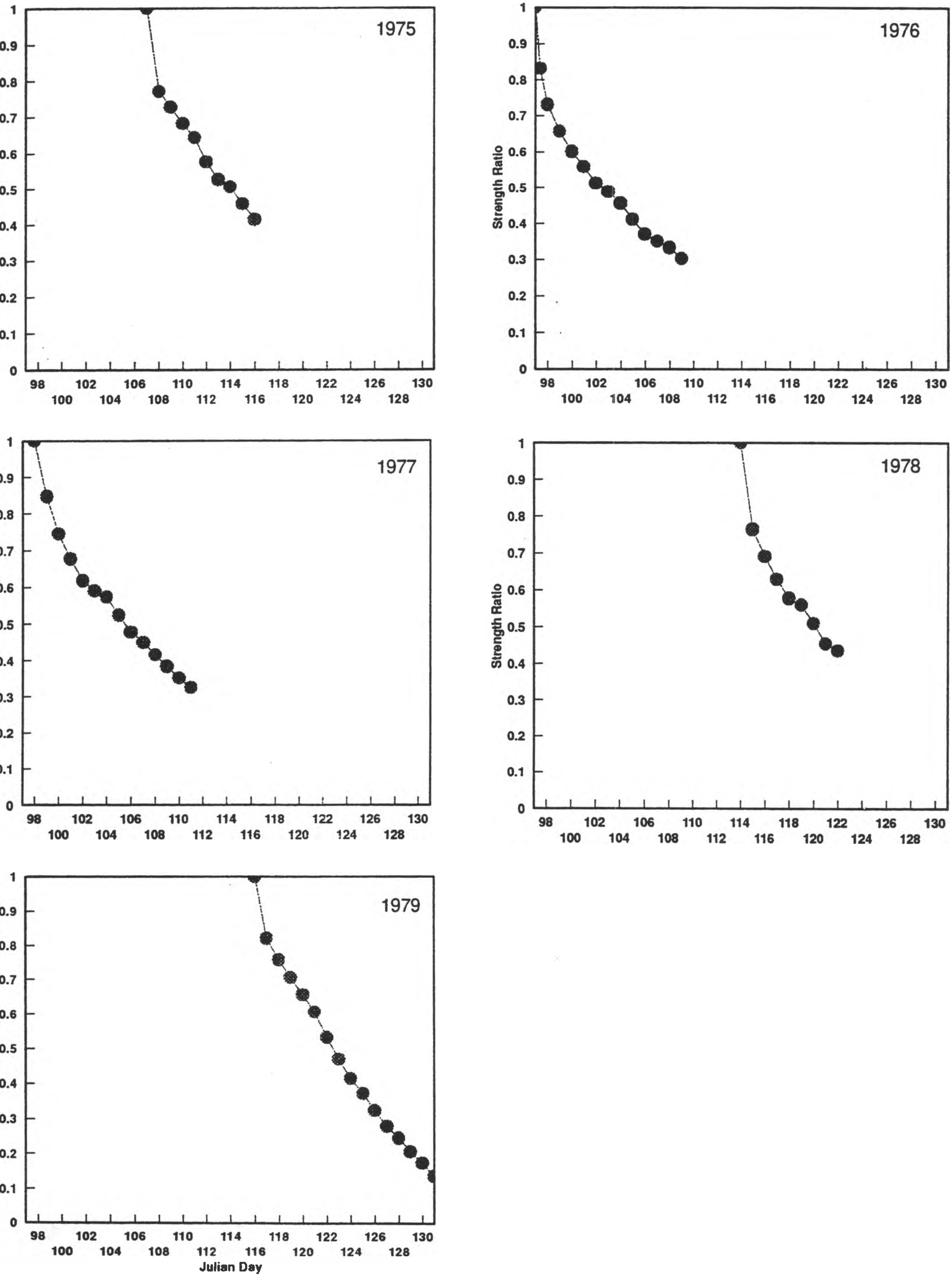

Figure 6.25. Residual ice strength at break-up for the lower Peace River 1963-79.

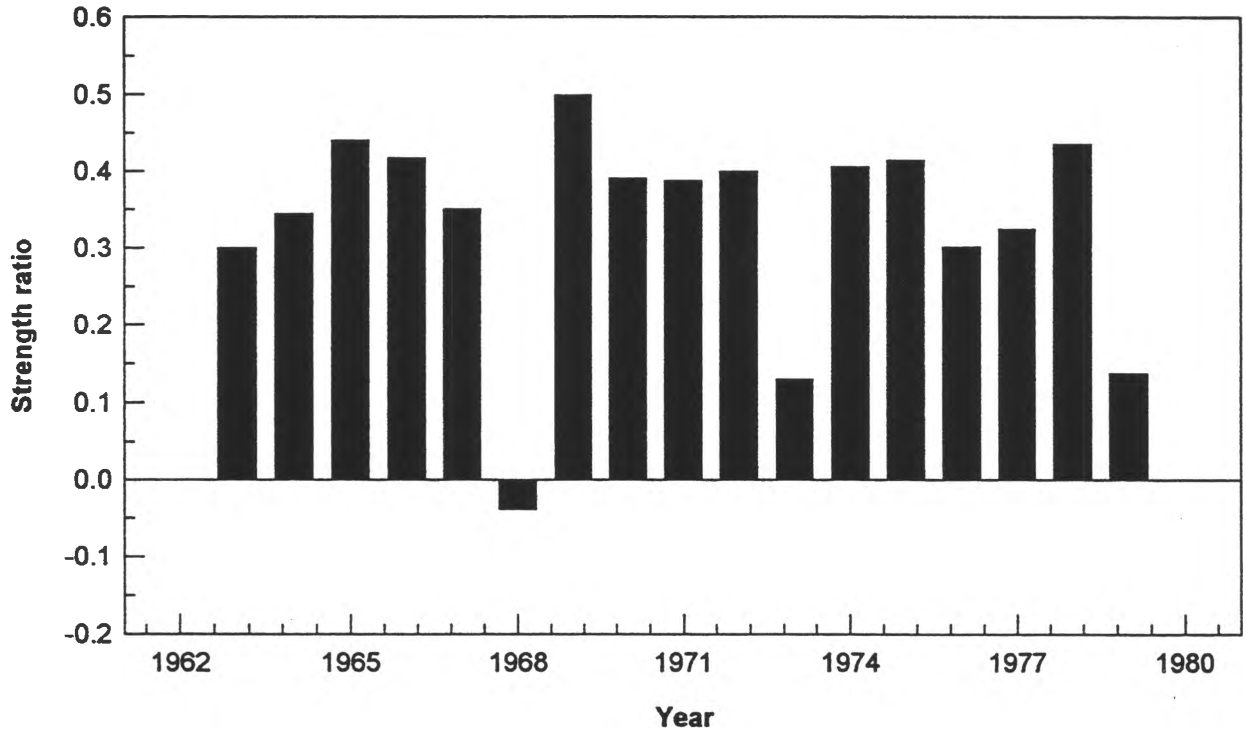

Figure 6.26. Residual strength ratio as cumulative percent departure from the mean for the lower Peace River 1963-80.

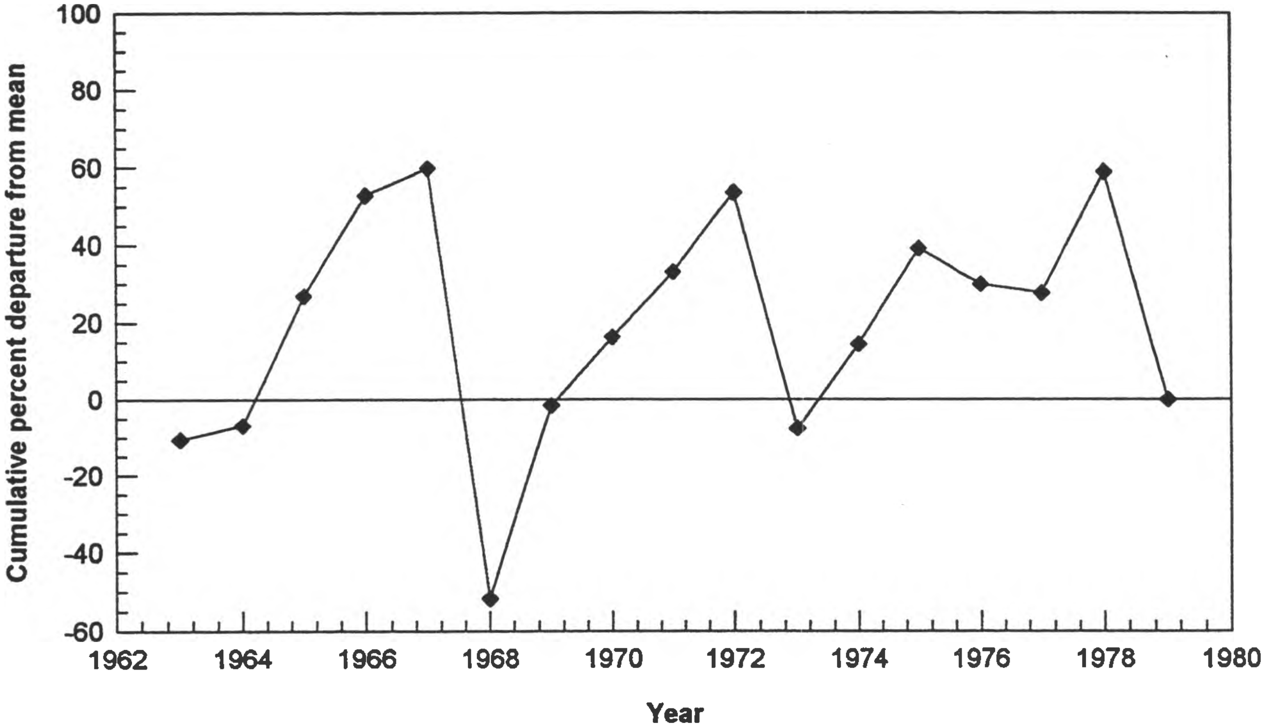

Figure 6.27. Pre-regulation spring hydrographs for selected stations.

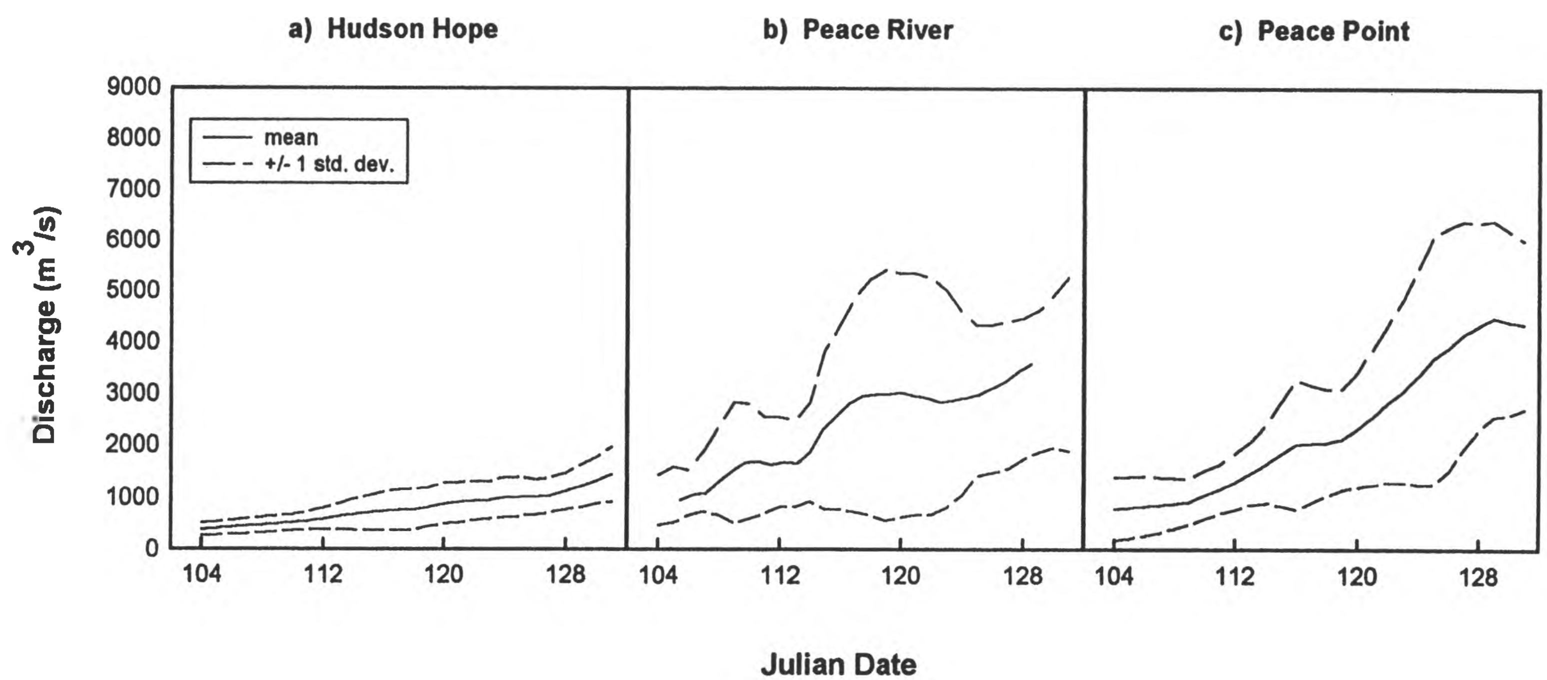

Figure 6.28. Post-regulation spring hydrographs for selected stations.

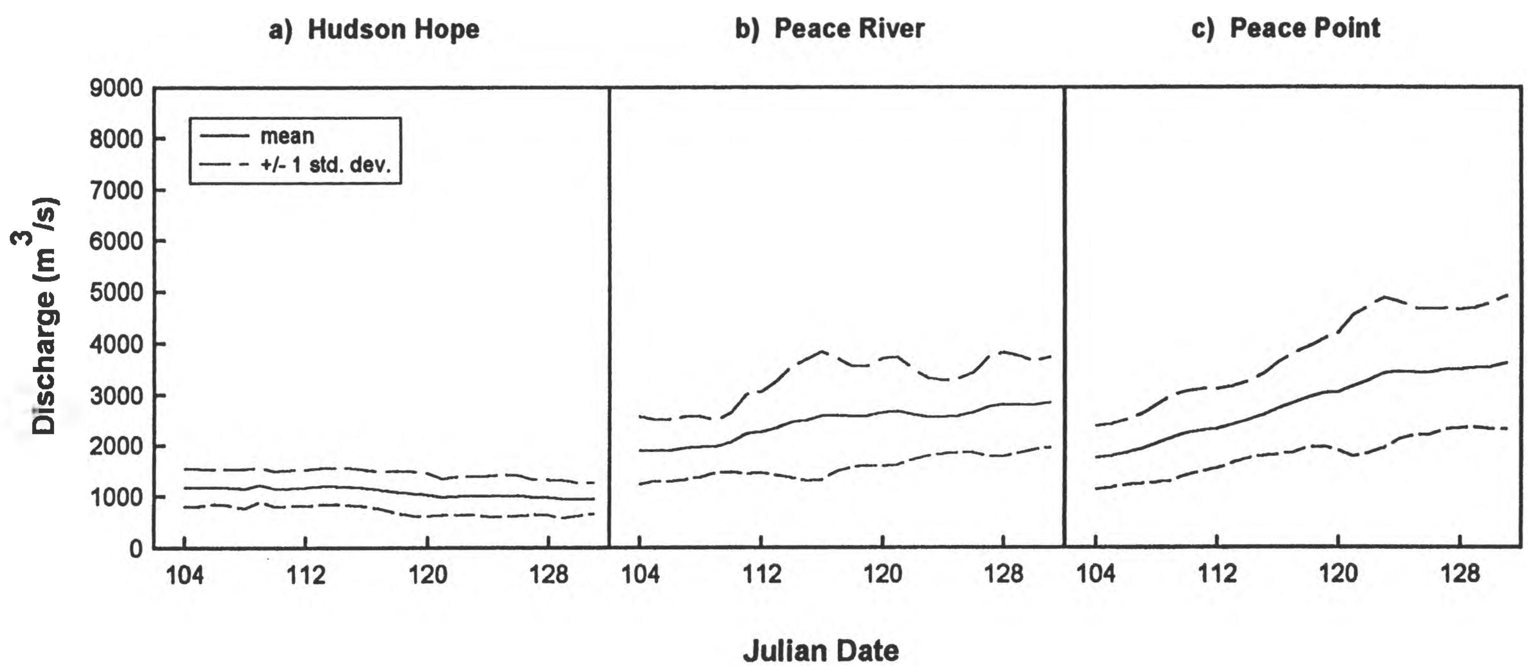

Figure 6.29. Spring hydrographs for selected stations, 1965.

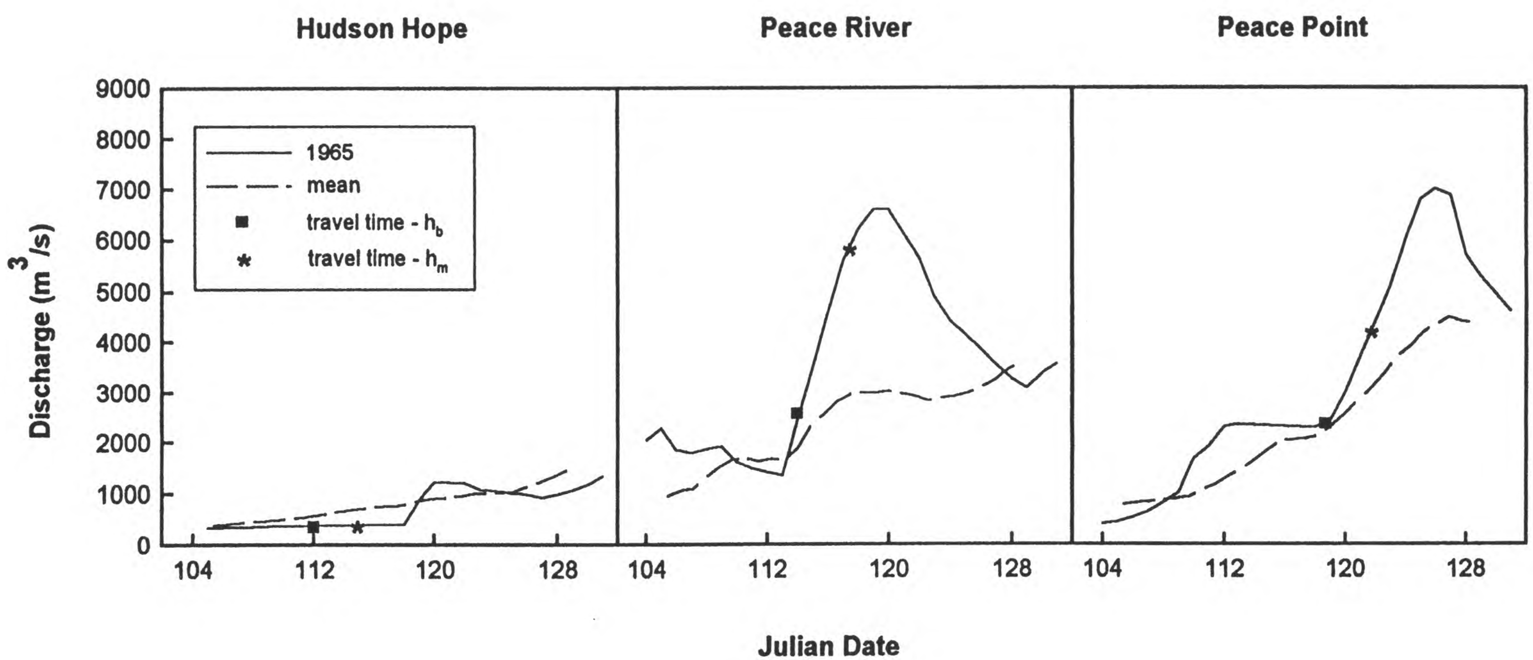

Figure 6.30. Spring hydrographs for selected stations, 1974.

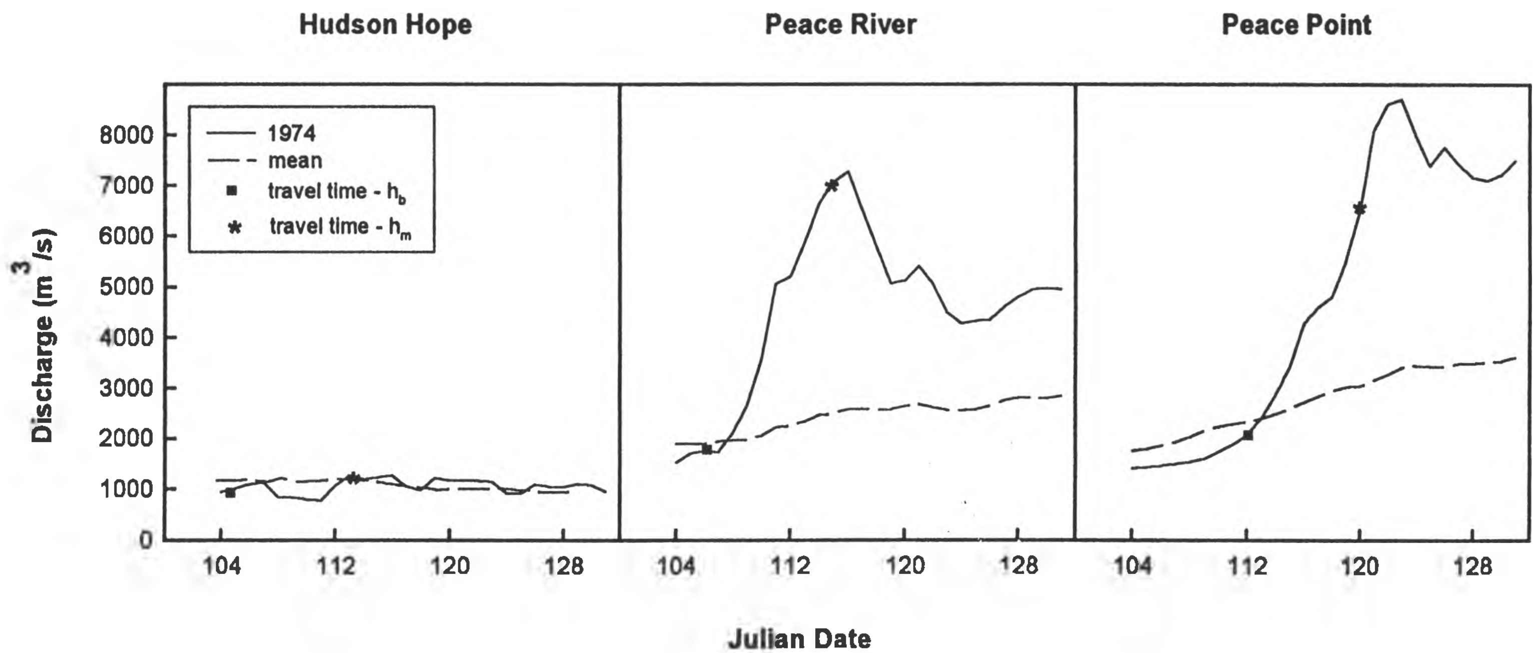

Figure 6.31. Estimated time of travel (+/- 6 to 12 hours) for the Peace River.

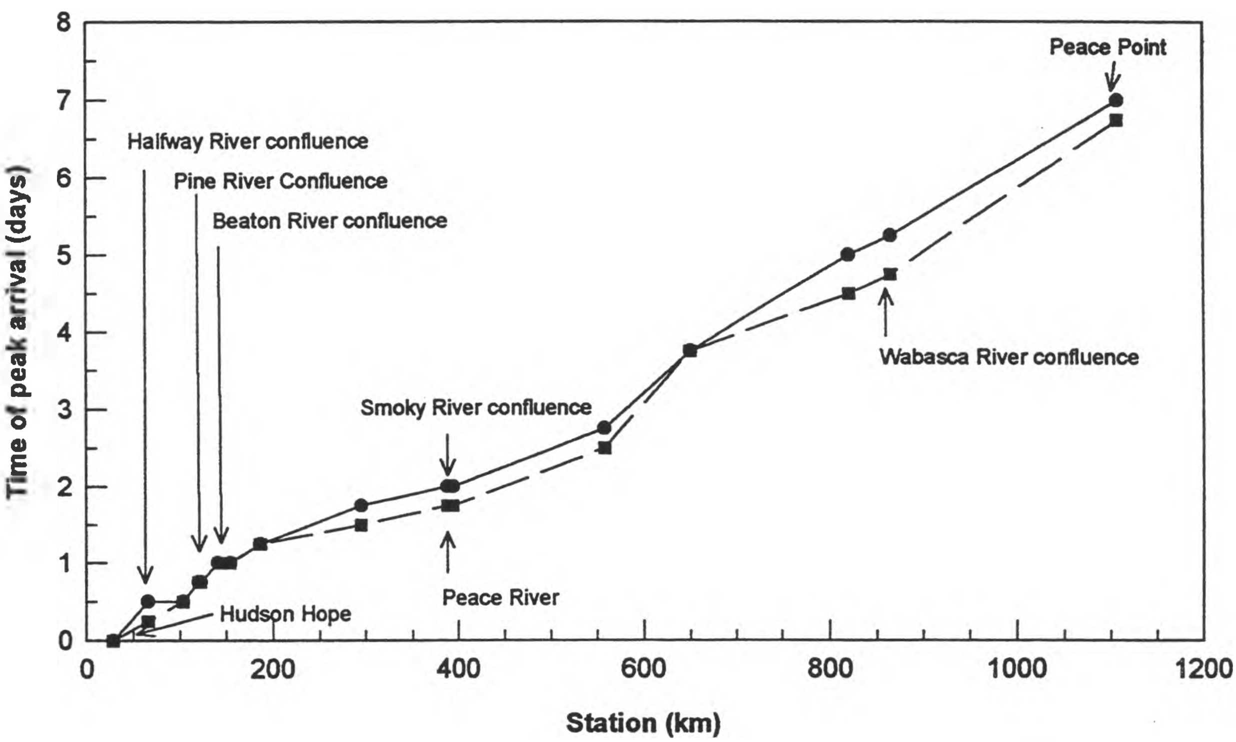

Figure 6.32. Pre-regulation spring hydrographs for selected stations.

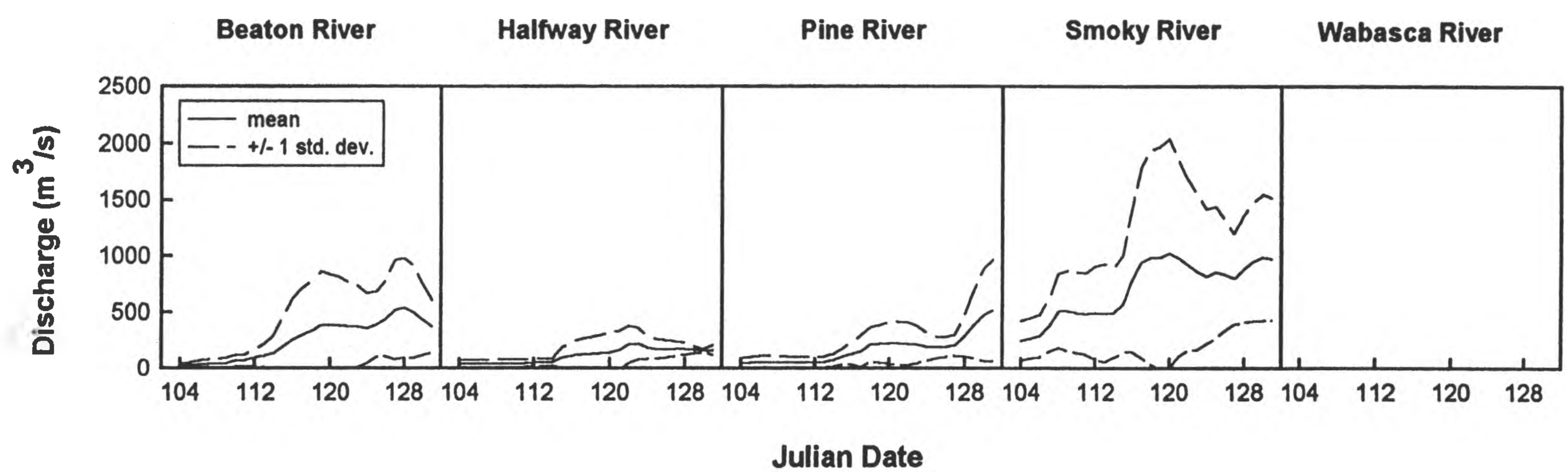

Figure 6.33. Post-regulation spring hydrographs for selected stations.

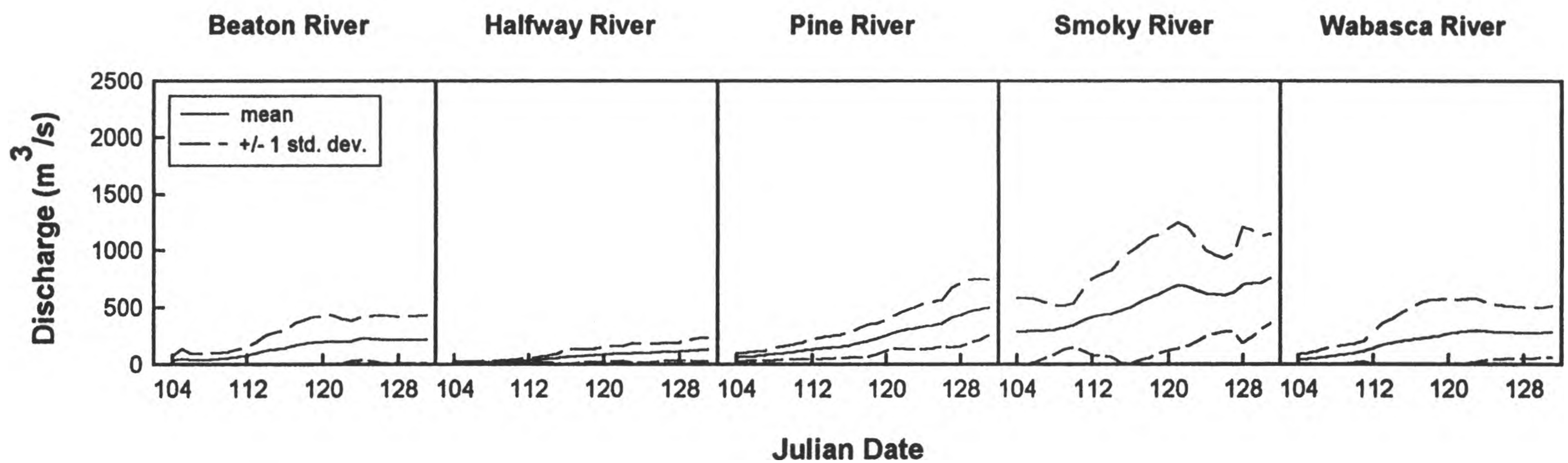

Figure 6.34. Spring hydrographs for selected stations, 1965.

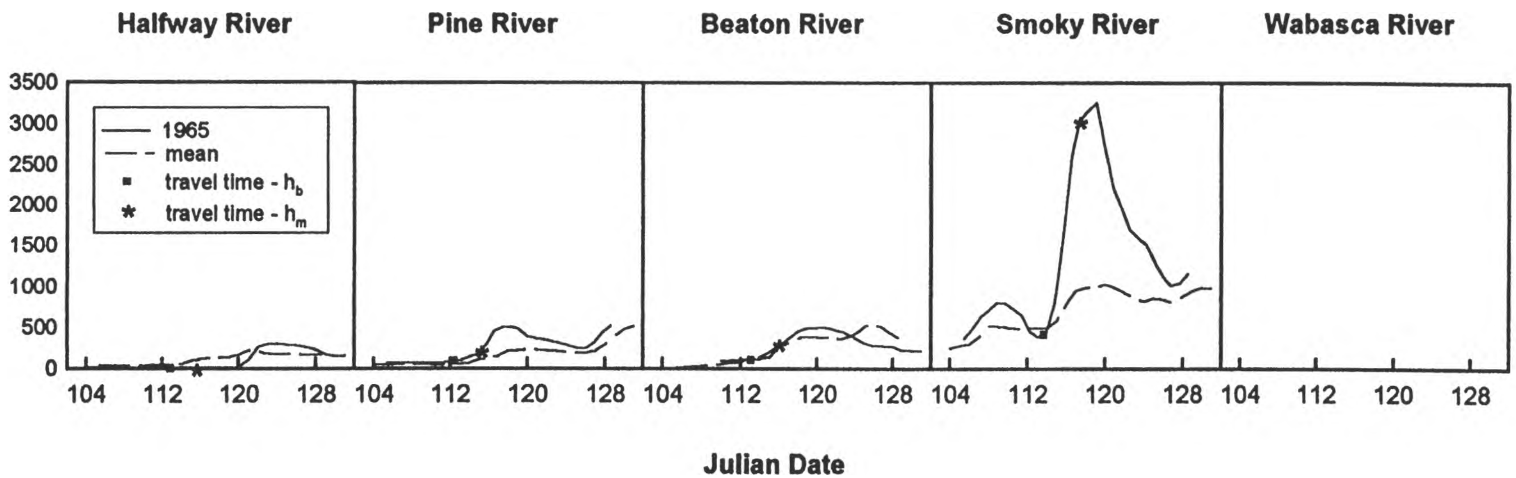

Figure 6.35. Spring hydrographs for selected stations, 1974.

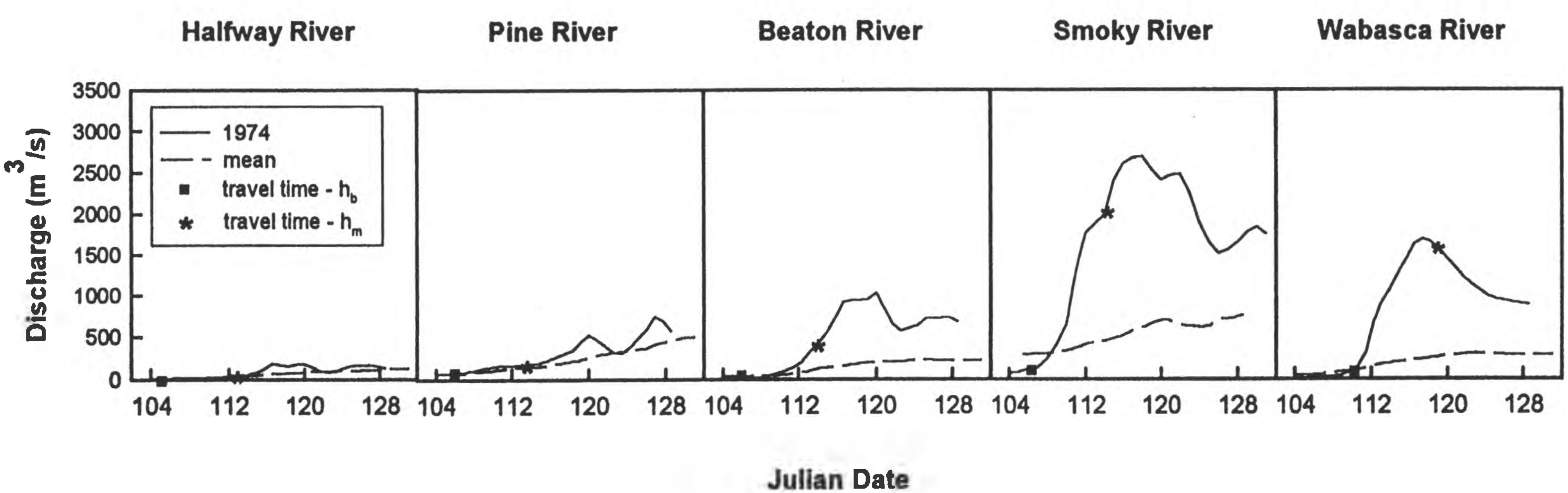

Figure 6.36. Peace River flow at time of break-up 1962-92.

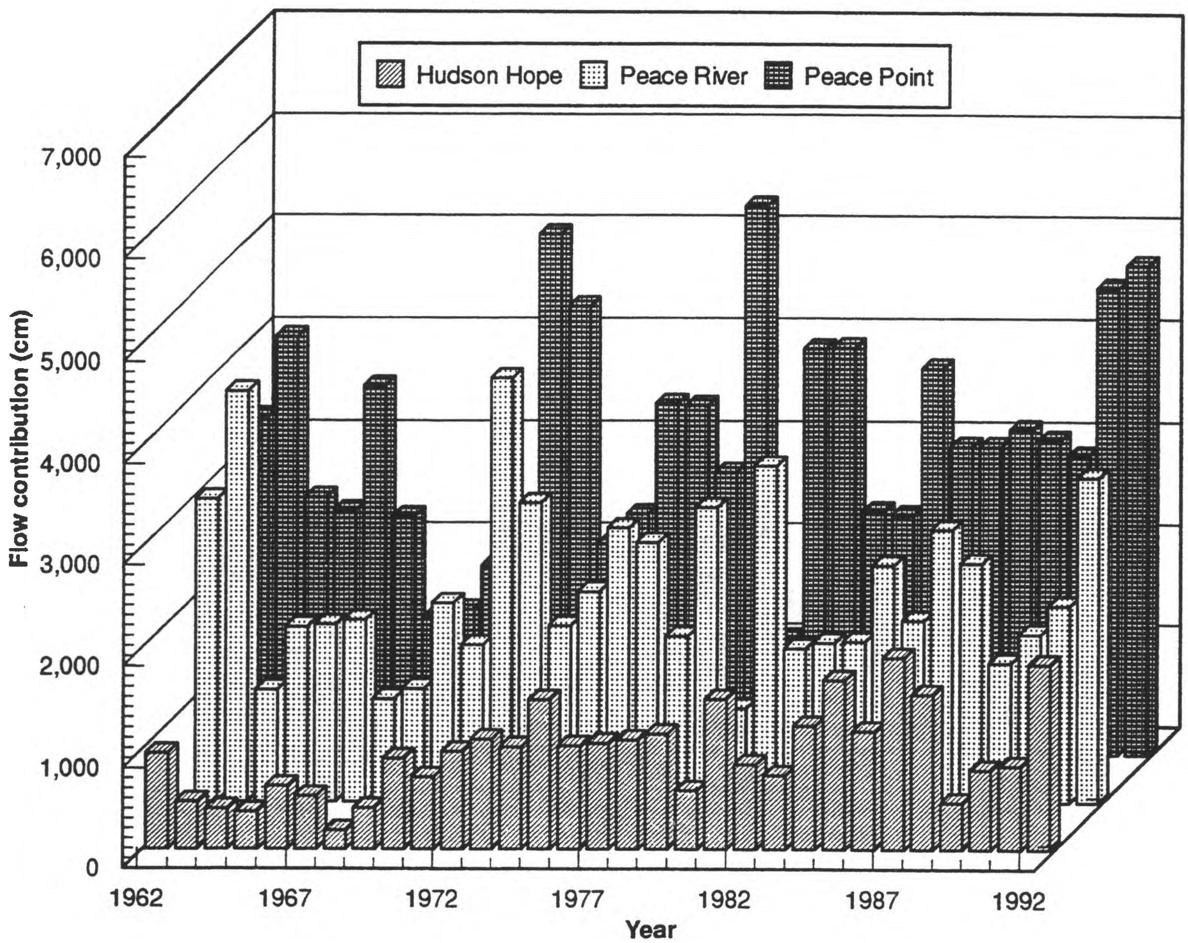

Figure 6.37. Peace River tributary flow contributions at break-up 1962-92.

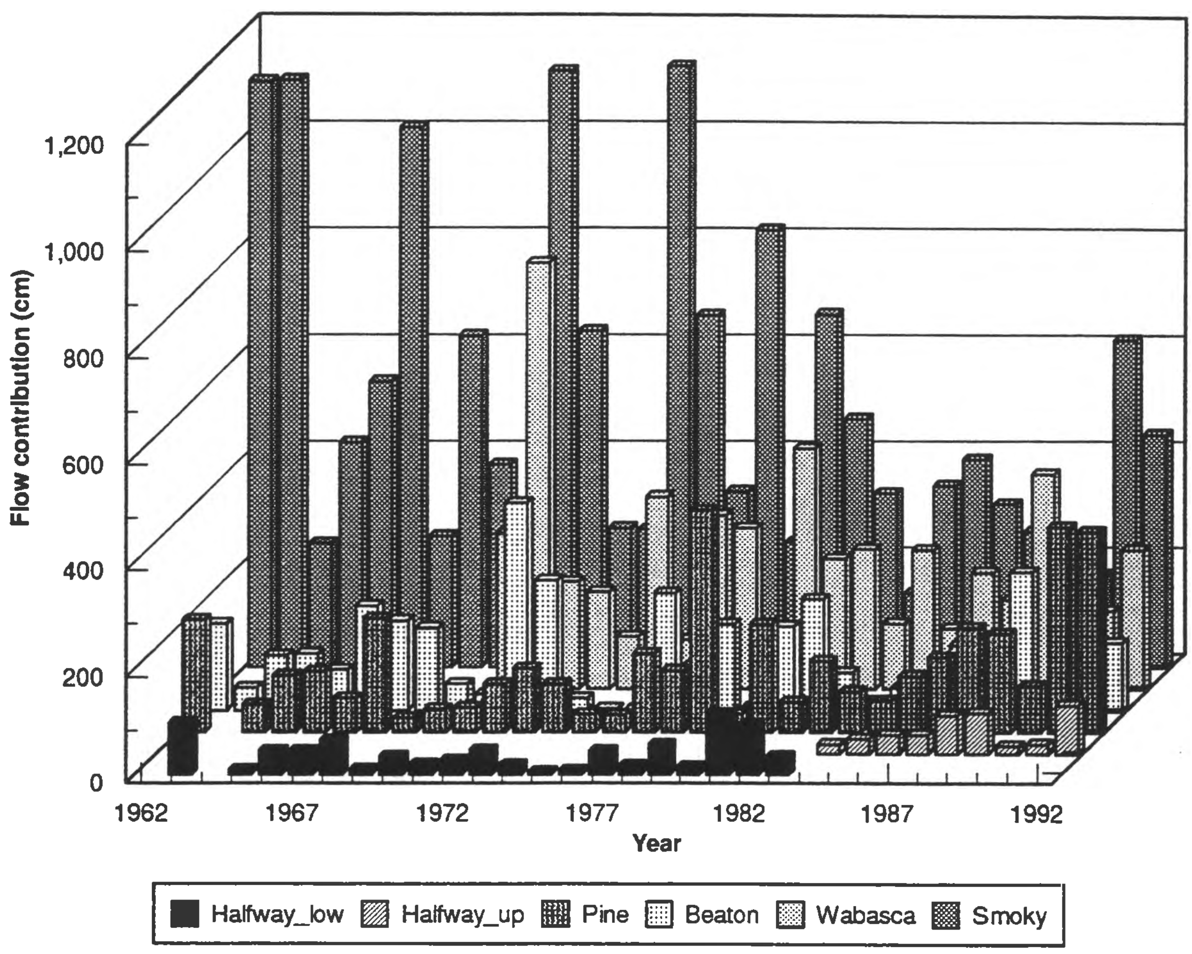

Figure 6.38. Flow contributions relative to Peace Point at time of break-up 1962-92.

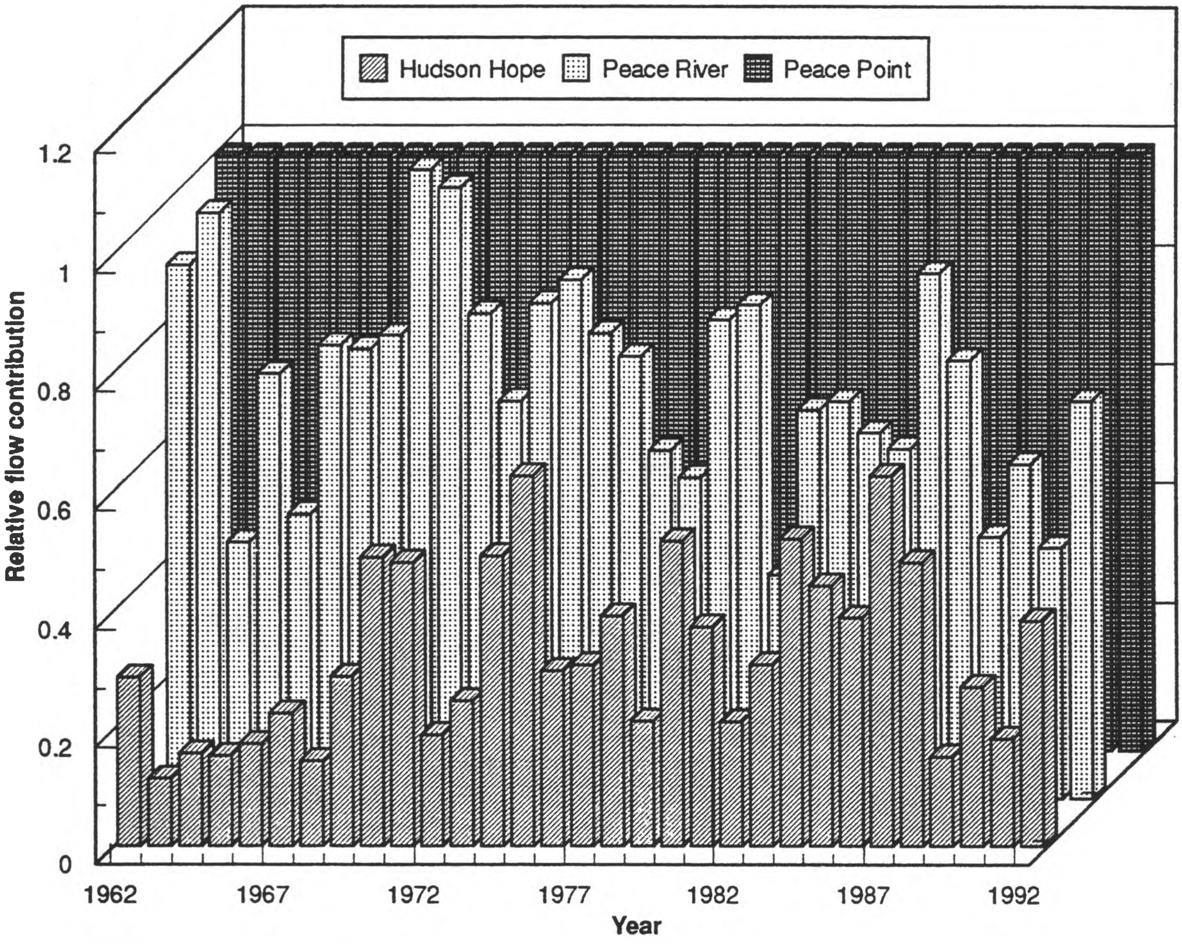

Figure 6.39. Tributary flow contributions relative to Peace Point at time of break-up 1962-92.

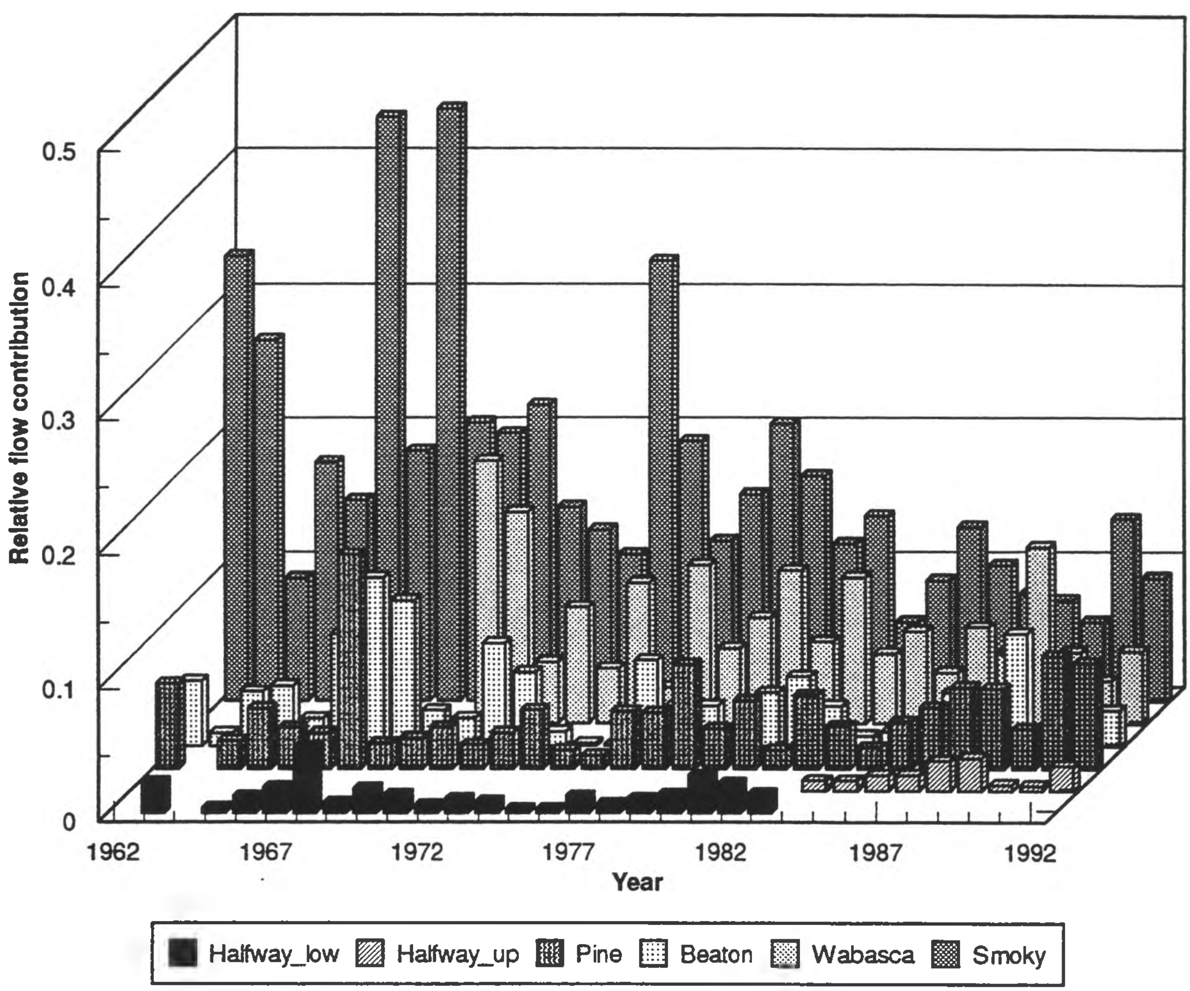

Figure 6.40. Peace River flow at time of h_m at Peace Point 1962-92.

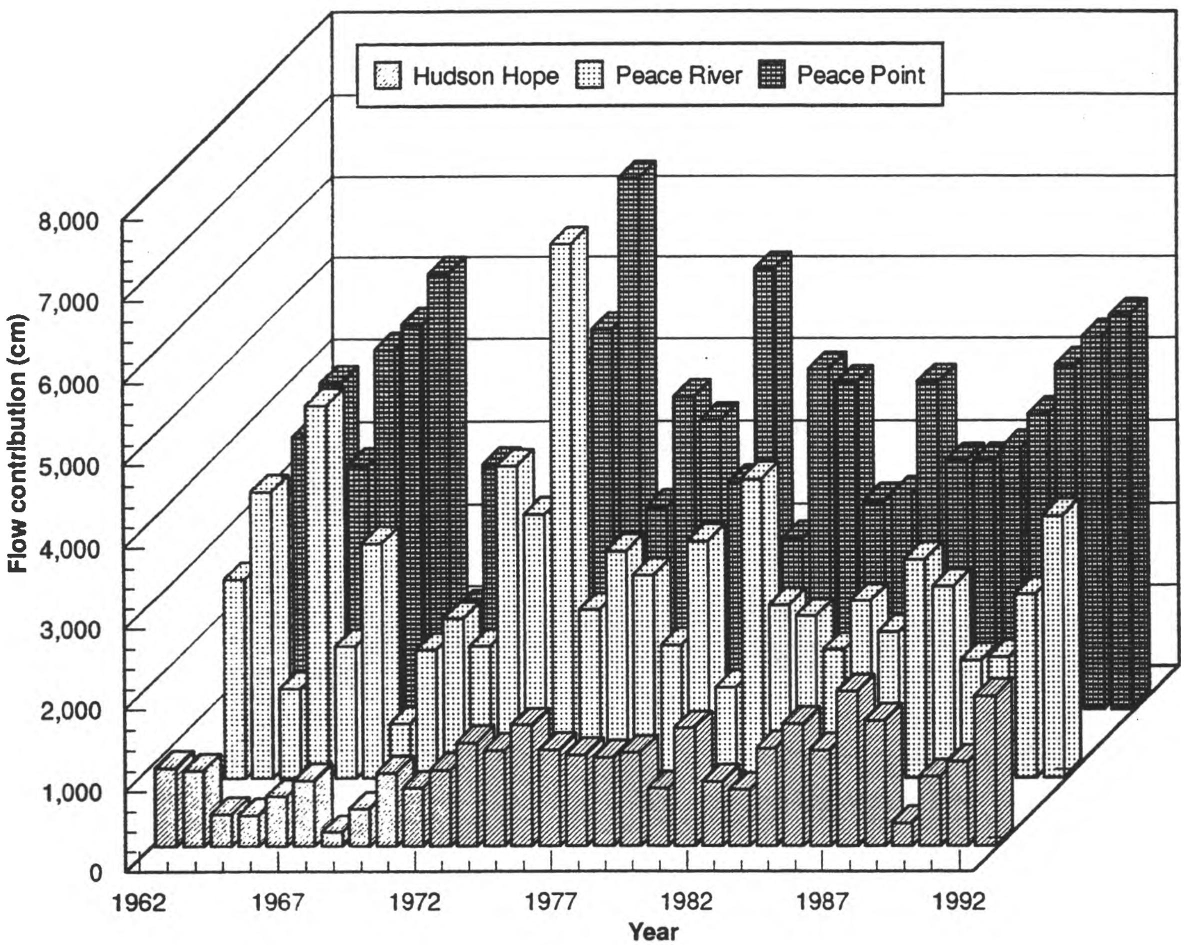

Figure 6.41. Peace River tributary flow contributing to hm at Peace Point 1962-92.

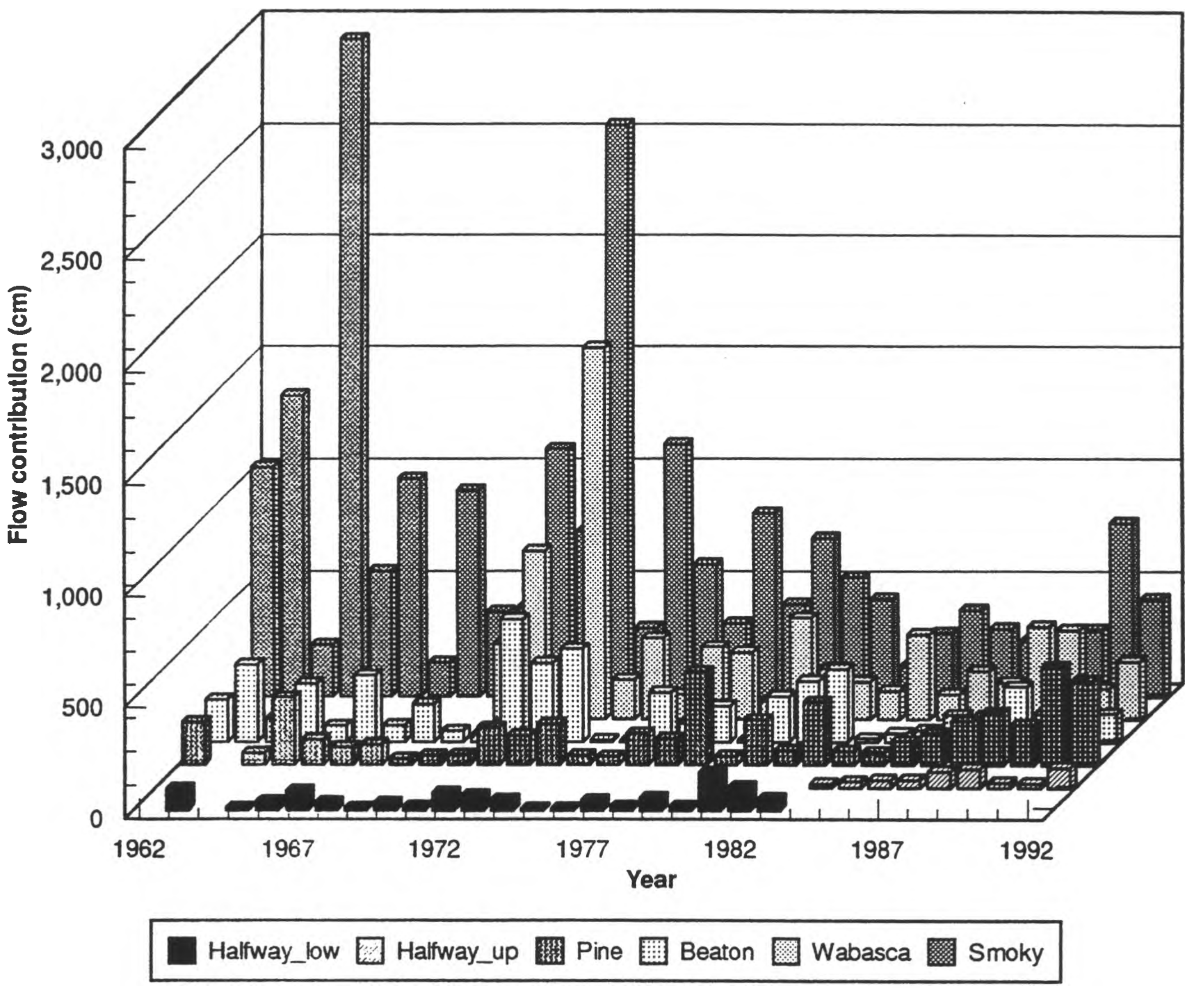

Figure 6.42. Flow contributions relative to Peace Point at time of h_m 1962-92.

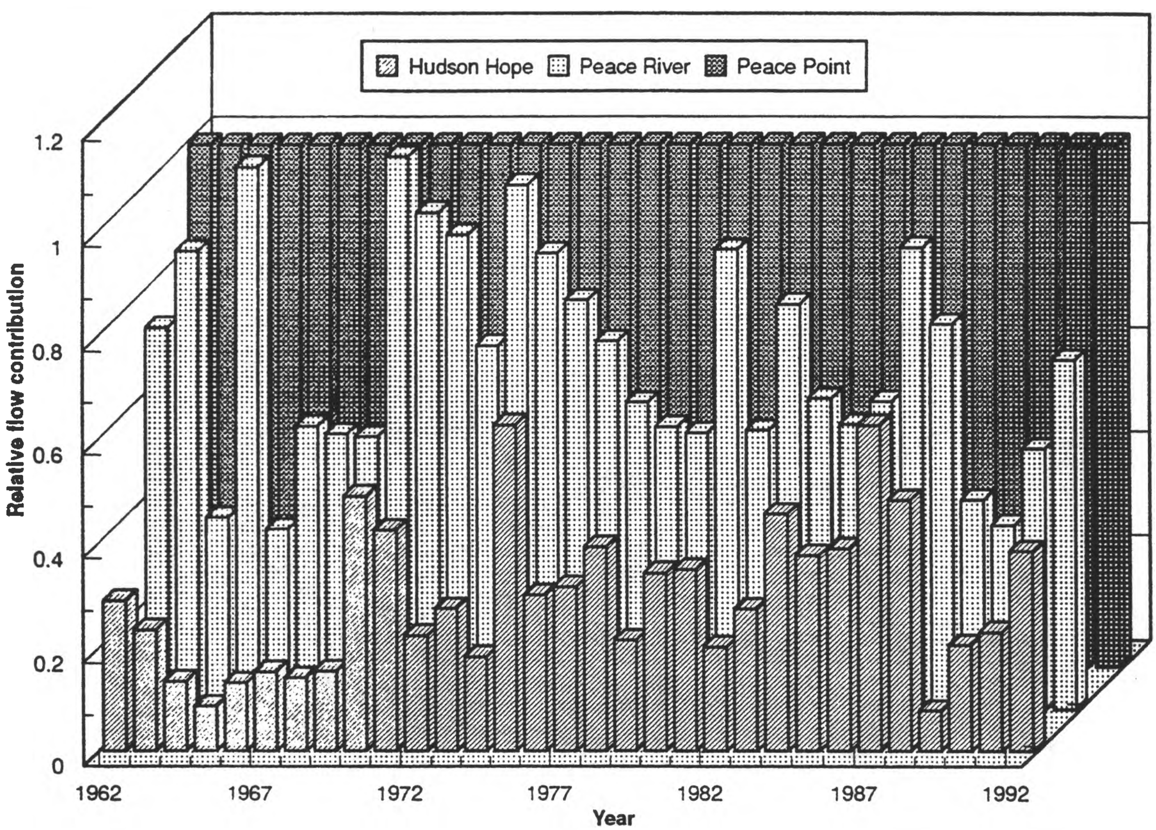

Figure 6.43. Tributary flow contributions relative to Peace Point at time of h_m 1962-92.

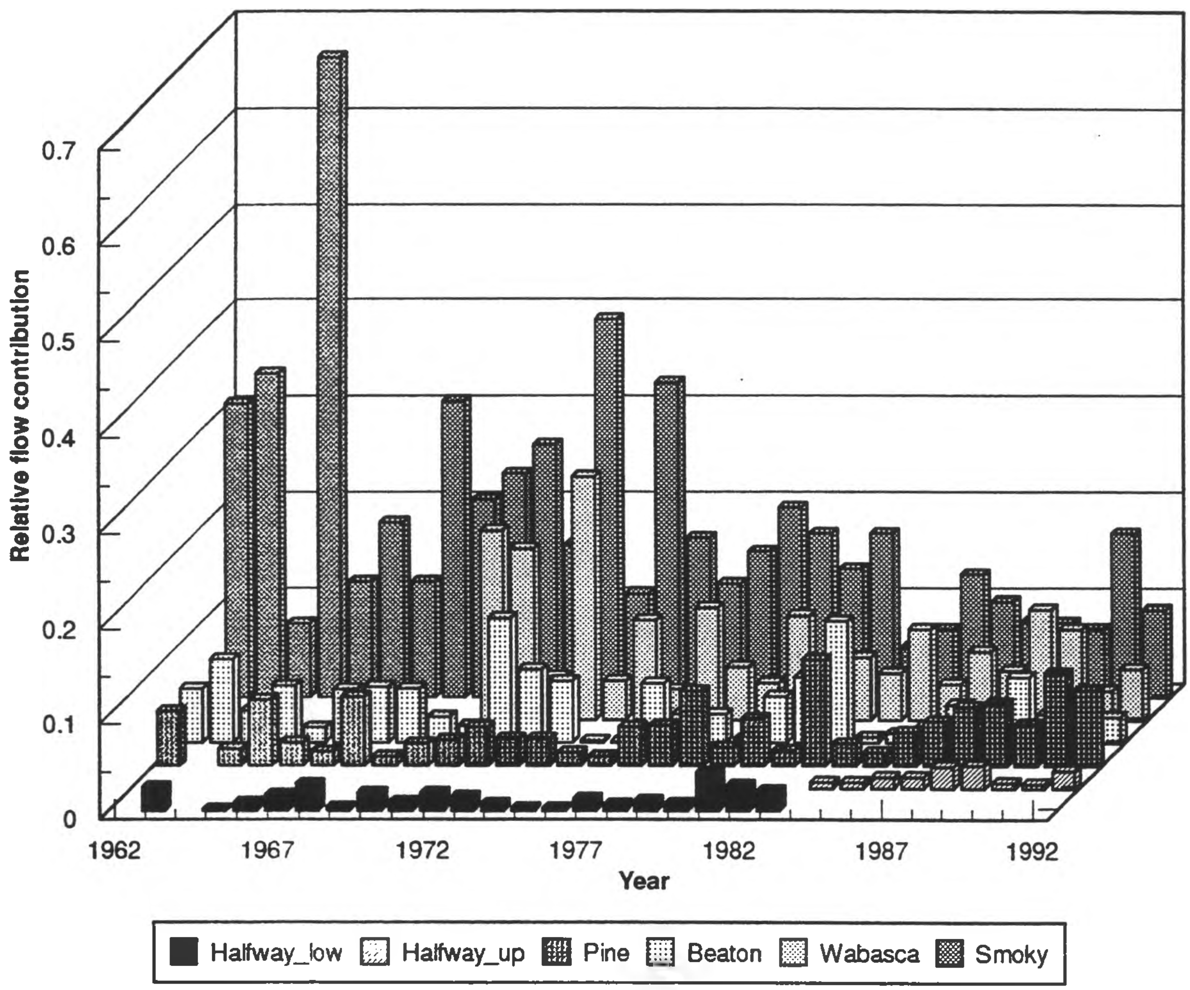

Figure 6.44. Time series of snow water equivalent at selected stations in the Peace River Basin.

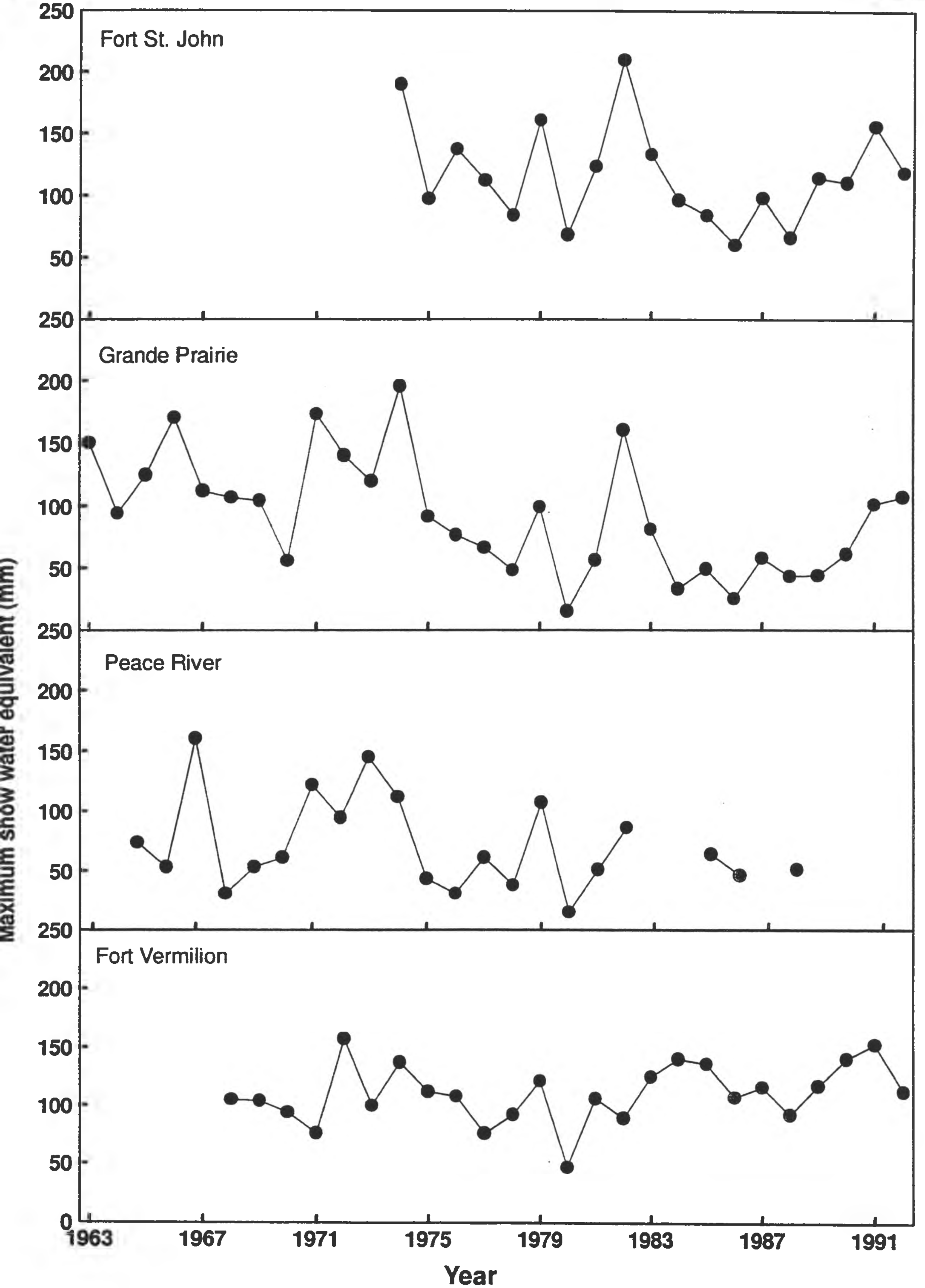

Figure 6.45. Seasonal precipitation at Grande Prairie, November to March 1947-92.

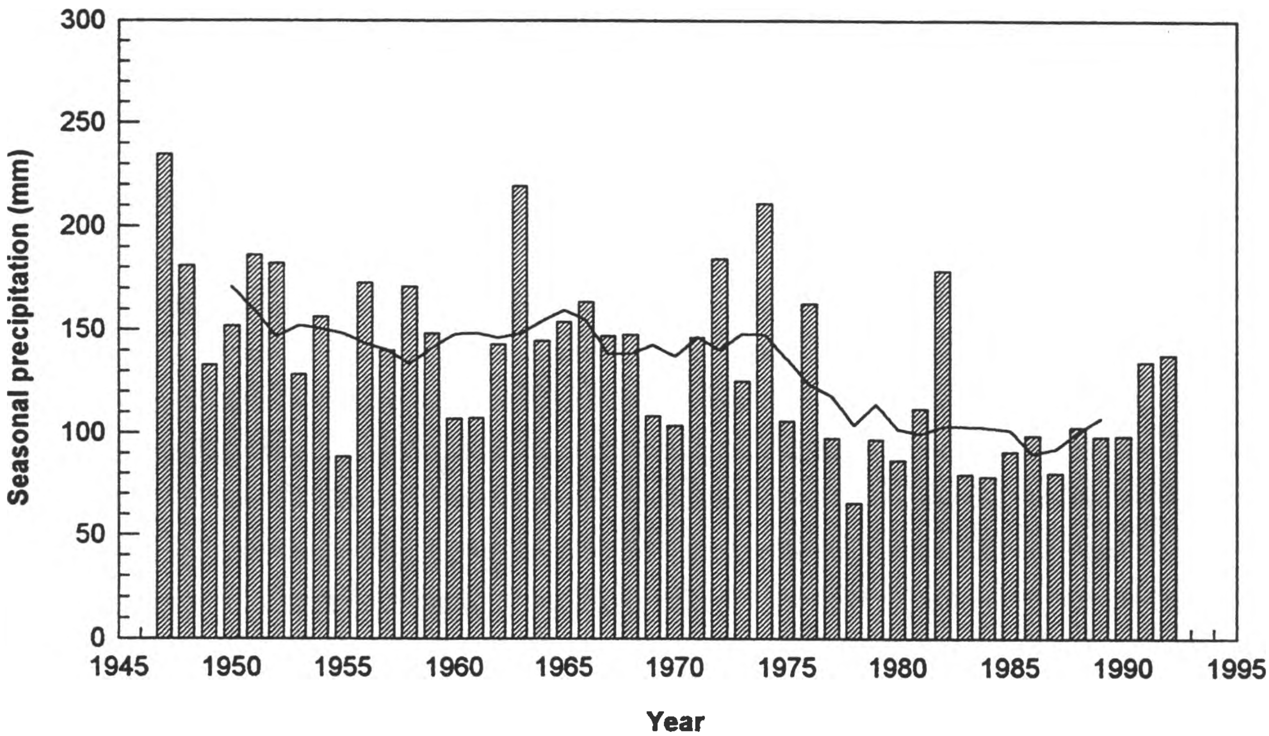

Figure 6.46. Trend in spring snowpacks, snow water equivalent, for Grande Prairie 1947-92.

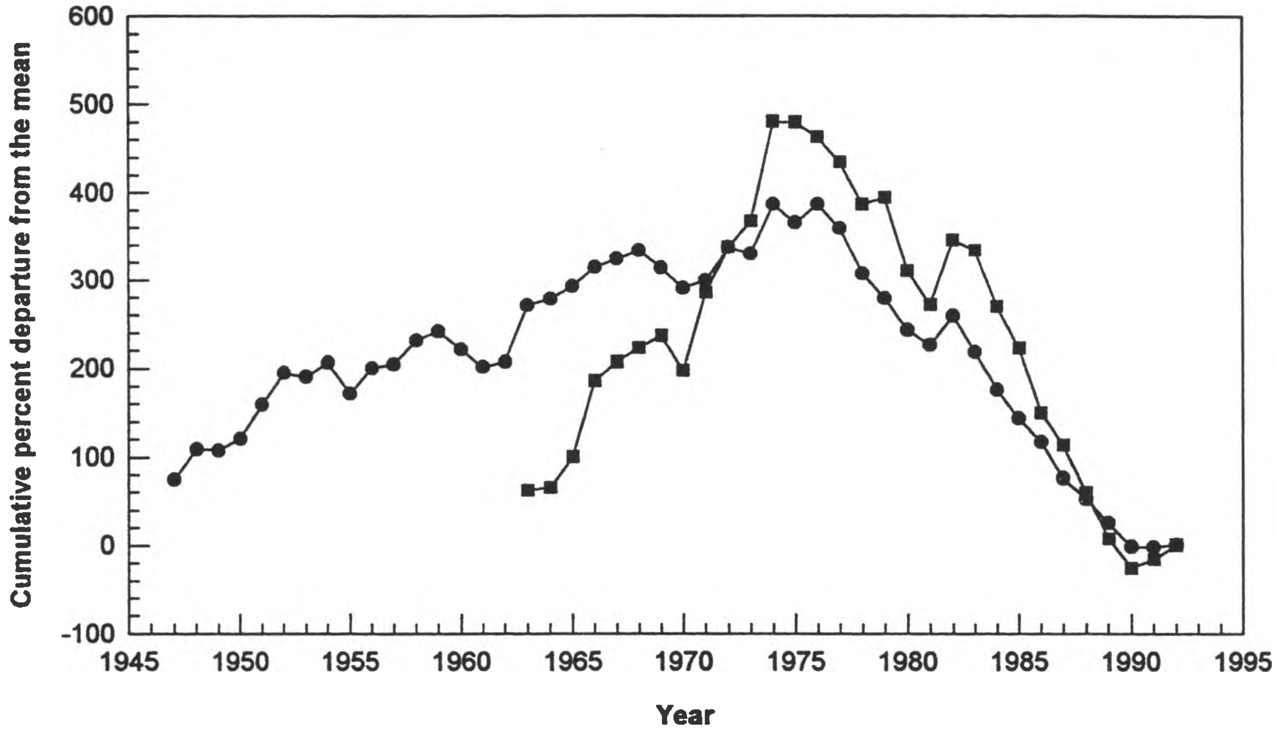

Figure 6.47. Freeze-up stage - break-up stage relationship.

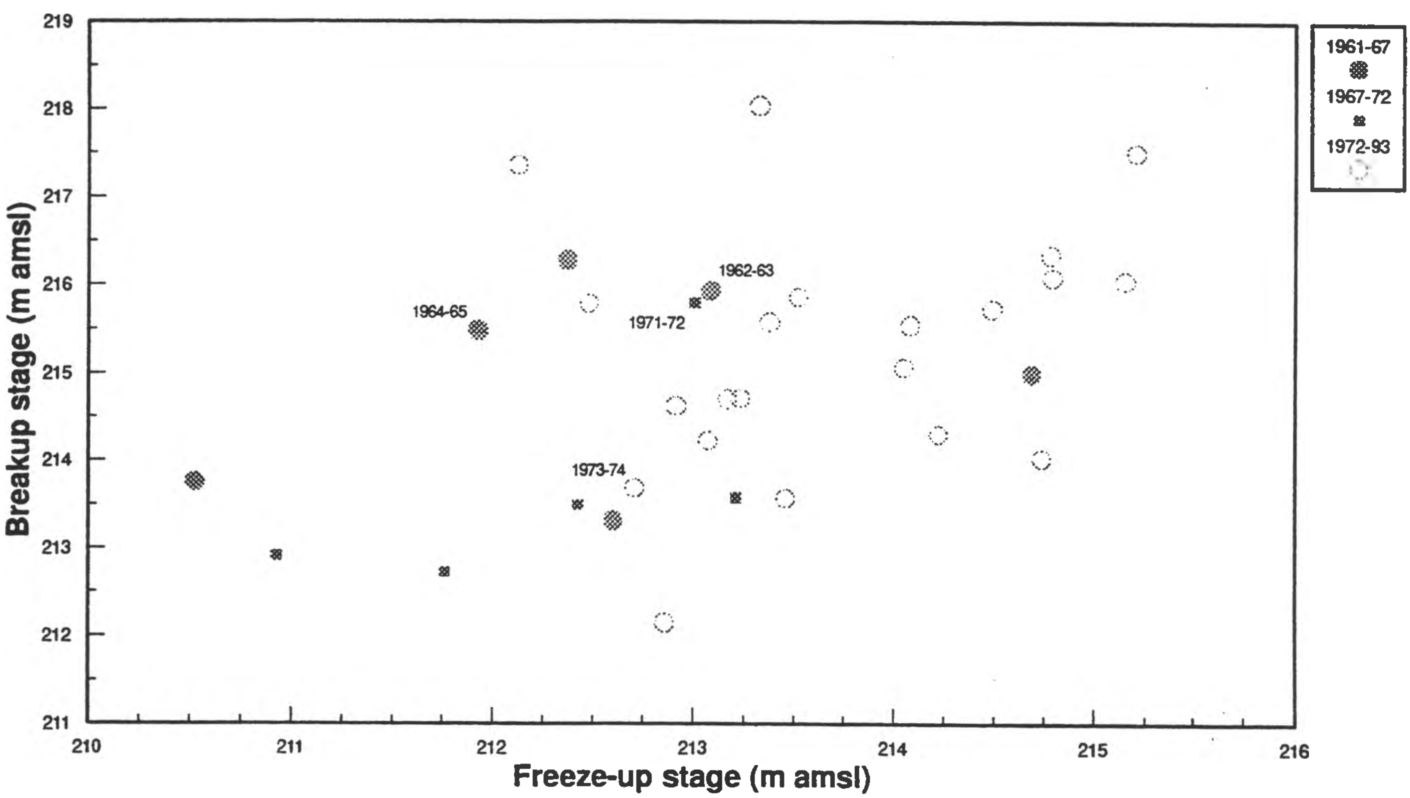

Figure 6.48. Freeze-up levels for the Peace River at Peace Point.

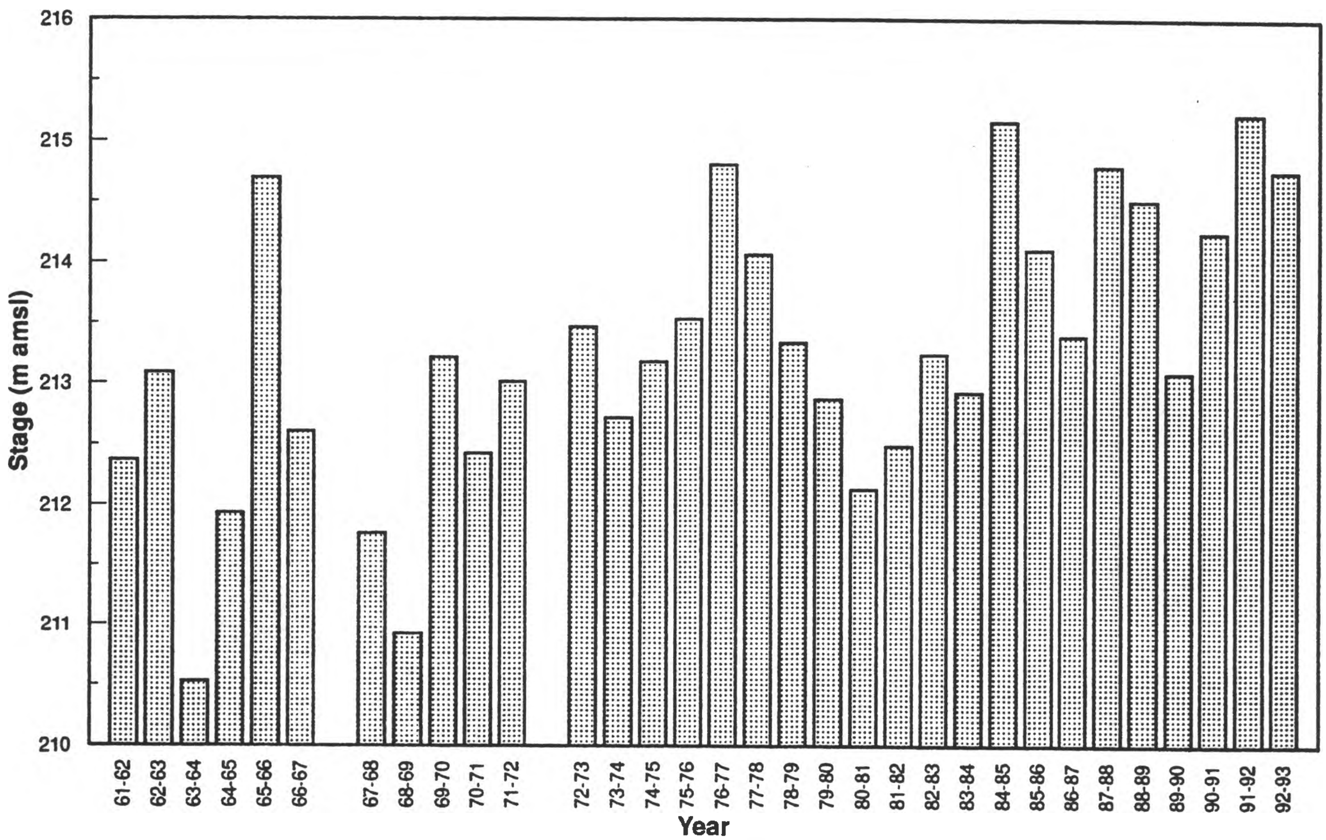

APPENDIX C: TABLES

Table 5.1 List of Water Survey of Canada stations along the Peace River for which some river-ice-related data is available.

Name and Location	Record Count	Years of Record
Peace River at Hudson Hope	50	1917-22; 1949-92
Peace River at Taylor	49	1944-92
Peace River at Dunvegan	29	1960-69; 1974-92
Peace River at Peace River	54	1915-32; 1957-93
Peace River at Fort Vermilion	25 + 14	1915-22; 1961-78 1979-92 (Level)
Peace River at Peace Point	34	1959-92

Table 5.2 Descriptive statistics for the freeze-up, solid ice cover and break-up regimes for hydrometric stations along the Peace River. For stations with sufficient data, significance tests using Student's t-test were conducted to determine if a shift in the pre- and post-regulation mean dates occurred for freeze-up and break-up, and for the duration of the ice cover.

A) FREEZE-UP	F_{avg}	σ_f	n_f	F_{avg}'	σ_f'	n_f'	Shift in Mean α=0.05
Hudson Hope 07EF001	N/A	N/A	N/A	N/F	N/F	N/F	
Taylor 07FD002	N/A	N/A	N/A	N/F	N/F	N/F	
Dunvegan 07FD003	N/A	N/A	N/A	N/A	N/A	N/A	
Peace River 07HA001	Dec 13	7.8	5	Jan 1	16.9	21	Yes
Fort Vermilion 07HF001	Nov 15	7.2	5	N/A	N/A	N/A	
Peace Point 07KC001	Nov 16	7.9	6	Nov 21	9.34	21	No
B) DURATION OF SOLID ICE COVER	D_{avg}	σ_D	n_D	D_{avg}'	σ_D'	n_D'	Shift in Mean α=0.05
Hudson Hope[1] 07EF001	141	58.4	24	No Ice	No Ice	No Ice	
Taylor[2] 07FD002	158	19.3	17				
Dunvegan 07FD003	N/A	N/A	N/A	N/A	N/A	N/A	
Peace River 07HA001	124	18.1	5	97	29	21	Yes
Fort Vermilion 07HF001	168	11.2	5	N/A	N/A	N/A	
Peace Point 07KC001	169	10.9	6	160	11.8	21	No
C) BREAK-UP	B_{avg}	σ_B	n_B	B_{avg}'	σ_B'	n_B'	Shift in Mean α=0.05
Hudson Hope 07EF001	N/A	N/A	N/A	No Ice	No Ice	No Ice	
Taylor 07FD002	N/A	N/A	N/A	No Ice	No Ice	No Ice	
Dunvegan 07FD003	Apr 27	10.6	3	N/A	N/A	N/A	
Peace River 07HA001	Apr 16	9.1	5	Apr 10	13.2	21	No
Fort Vermilion 07HF001	Apr 29	5.0	5	Apr 24	7.6	12	Yes
Peace Point 07KC001	May 2	4.97	6	Apr 28	6.1	21	No

[1] Due to the paucity of pre-regulation data for Hudson Hope, the duration of the ice cover is based on the period of ice effect. Although the statistics for the other stations are based on continuous solid ice cover, using ice effect period for Hudson Hope illustrates the impact of regulation on the ice regime at this location.

[2] Although the Taylor gauge has been affected by ice and temporary lodging of ice has occurred around the gauge, Water Survey of Canada personnel responsible for the gauge state that a permanent solid ice cover has not formed at this gauge since regulation (B. Thoron, pers. comm., 1995).

Table 6.1 Pre- and post-regulation melt effects due to fluid friction.

Month	Discharge (m^3/s)		Friction (w/m^2)		Melt (mm/month)	
	pre	post	pre	post	pre	post
December	555	1620	0.855	2.50	7.47	21.8
January	528	1570	0.814	2.42	7.10	21.1
February	441	1520	0.680	2.34	5.36	18.4
March	393	1440	0.606	2.22	5.29	19.4
Total					25.2	80.8

Table 6.2 Mean peak ice thicknesses for the Peace River at Peace Point. Mean values are derived from Water Survey of Canada field notes. The two periods represent conditions before and after regulation of the Peace River.

Ice Season	Measurement Date	Ice Thickness (m)
1958/59	27-03-59	0.79
1959/60	-	-
1960/61	28-03-61	0.76
1961/62	22-03-62	1.01
1962/63	28-03-63	0.76
1963/64	20-03-64	0.85
1964/65	23-03-65	0.88
1965/66	22-03-66	0.91
1966/67	20-03-67	0.91
1967/68	28-03-68	0.91
Mean		0.86
σ		0.08
n		9
1972/73	27-03-73	0.98
1973/74	14-03-74	0.82
1974/75	26-03-75	0.79
1975/76	05-04-76	0.82
1976/77	29-03-77	0.76
1977/78	13-04-78	0.91
1978/79	17-04-79	0.95
1979/80	02-04-80	0.70
1980/81	14-04-81	0.84
1981/82	06-04-82	0.96
1982/83	13-04-83	0.74
1983/84	-	-
1984/85	13-04-85	0.96
1985/86	08-04-86	1.09
1986/87	-	-
1987/88	-	-
1988/89	-	-
1989/90	-	-
1990/91	-	-
1991/92	08-04-92	0.84
1992/93	16-04-93	1.16
1993/94	-	-
Mean		0.89
σ		0.13
n		15

Table 6.3 Global radiation summary

	Mean Bias Error		Root Mean Square Error		Correlation Coefficient	
Year	Constant	Calculated	Constant	Calculated	Constant	Calculated
1972	2005.524	269.302	3484.069	2611.380	0.913	0.915
1973	1102.750	388.889	2972.029	2575.854	0.913	0.910
1974	1060.336	-921.096	2787.575	2774.347	0.909	0.894
1975	1437.426	-630.035	2199.879	1738.357	0.956	0.964
1976	2735.155	267.214	3534.056	1960.755	0.922	0.942
1977	1381.329	-672.900	3303.228	2669.025	0.823	0.855
1978	877.986	-905.814	2798.342	2681.110	0.896	0.903
Mean	1514.358	-314.920	3011.311	2430.118	0.905	0.912

Table 6.4 Small streams used as index stations for determining melt initiation.

Station Name	Latitude	Longitude	Drainage Area (km^2)	Mean April Flow (m^3/s)
Beaver River (above Syncrude)	56° 56' 29" N	111° 33' 54" W	165	0.686
Bench Mark Creek (near Fort Smith)	59° 48' 50" N	111° 57' 45" W	65.5	0.237
Birch River (below Alice Creek)	58° 19' 20" N	113° 4' 5" W	9860	36.1
Firebag River (near the mouth)	57° 39' 3" N	111° 12' 5" W	5990	28.0
Jackpine Creek (at Wadlin Lake Road)	58° 11' 35" N	115° 45' 00" W	582	3.55
Ponton River (above Boyer River)	58° 27' 53" N	116° 15' 23" W	2440	7.21
Richardson River (near the mouth)	58° 21' 48" N	111° 14' 14" W	2700	18.8

Table 6.5 Julian dates of melt initiation, breakup and peak water levels for the Peace River at Peace Point.

Year	Melt Initiation	Breakup Date	Duration of Melt	Date of Peak
1963	105	115	11	119
1964	115	126	12	127
1965	113	119	7	122
1966	122	127	6	128
1967	120	127	8	129
1968	100	124	25	124
1969	102	109	8	112
1970	100	109	10	109
1971	109	116	8	117
1972	118	124	7	129
1973	98	116	19	118
1974	105	112	8	120
1975	108	116	9	119
1976	97	109	13	111
1977	99	111	13	112
1978	115	122	8	122
1979	117	131	15	131
1980	91	113	23	116
1981	113	121	9	122
1982	115	128	14	129
1983	108	118	11	122
1984	98	112	15	112
1985	108	124	17	127
1986	109	125	17	125
1987	104	117	14	117
1988	105	120	16	120
1989	109	125	17	126
1990	107	114	8	117
1991	104	119	16	120
1992	108	118	11	118

Table 6.6 Positive and net heat flux versus stage increase for Peace Point.

Year	Stage increase	Net MJ/m^2	Positive MJ/m^2	MDD from April 1	MDD from first melt
1962	3.58				
1963	5.99	26.45	69.5	139.9	100.1
1964	1.59	89.35	102.4	187.8	134.1
1965	4.10	46.6	54.7	194.5	103.4
1966	2.36	65.49	76.6	146	83.8
1967	3.60	37.34	77.1	132.5	64.2
1968	2.64	32.08	123.9	146.7	122.7
1969	3.69	24.10	34.5	157.7	105.8
1970	2.11	33.90	43.1	88.7	83.7
1971	4.26	65.55	71.3	180.9	106.4
1972	5.78	60.66	66.2	176.2	120.8
1973	2.39	33.48	89.6	146.8	127.7
1974	4.03	38.06	45.3	181.4	131.1
1975	2.67	35.40	52.1	144.9	82.7
1976	3.22	37.30	69.1	140.8	115.3
1977	2.31	51.81	65.8	130.5	111.4
1978	3.37	67.38	69.8	160.9	91.1
1979	3.54	35.59	104.2	153.7	92.7
1980	1.41			250.6	250.6
1981	3.61			136.7	89.3
1982	2.36			200.3	131.1
1983	4.13			181.1	105.7
1984	2.96			185.1	155
1985	2.24			268.6	196.3
1986	2.78			215	145.1
1987	2.65			186.4	145.1
1988	3.27			126.5	90.8
1989	4.15			185.2	148.6
1990	1.96			116.5	85
1991	2.45			186.5	90.7
1992	3.67			168.9	112.5

Table 6.7 Basin characteristics of the Peace River and its major tributaries.

	Drainage Area (km^2)	Percent of Drainage Area	Distance from Peace Point (km)	Estimated Flood Travel Time (days)
Peace Point	293,000	100%	0	0
Fort Vermilion	223,000	76%	299	2
Peace River	186,000	64%	712	5
Hudson Hope	69,990	24%	1079	7
Smoky River	50,300	17%	719	5
Wabasca River	35,800	12%	242	1.5
Beaton River	15,600	5.3%	966	6
Pine River	12,100	4.1%	987	6.25
Halfway River	9,350	3.2%	1042	6.75